

Exploring the phase structure and dynamics of QCD

Jan M. Pawłowski

Universität Heidelberg & ExtreMe Matter Institute

Beijing, May 22th & June 1st 2015



Outline

- Vacuum QCD & the hadron spectrum

- Phase structure of QCD

Part I

- Spectral Functions & Transport Coefficients

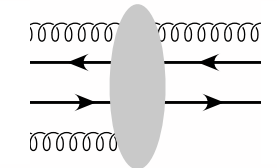
Part II

- Outlook

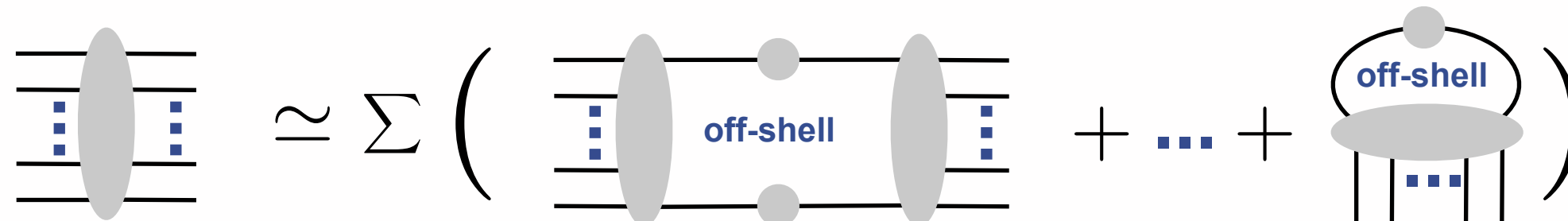
Continuum Methods for QCD

quark-gluon correlations

$$\langle q(x_1) \cdots \bar{q}(x_{2n}) A_\mu(y_1) \cdots A_\mu(y_m) \rangle$$



functional relations

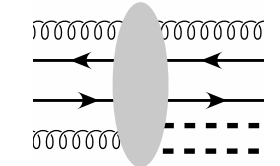


scattering amplitude/
vertex functions

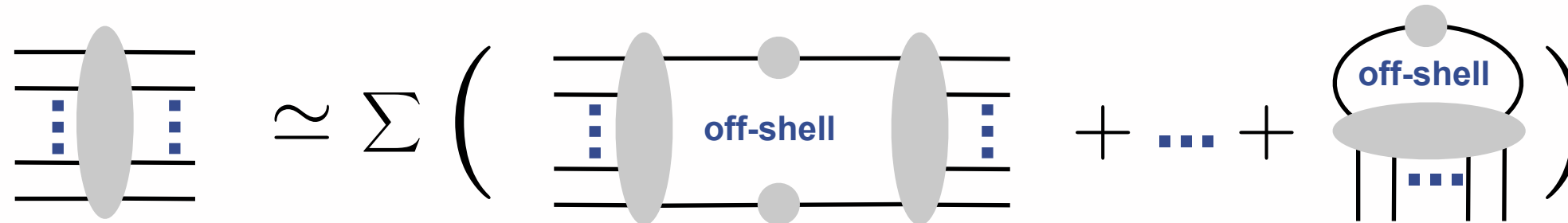
Continuum Methods for QCD

quark-gluon-hadron correlations

$$\langle q(x_1) \cdots \bar{q}(x_{2n}) A_\mu(y_1) \cdots A_\mu(y_m) h(z_1) \cdots h(z_l) \rangle$$



functional relations



scattering amplitude/
vertex functions

Functional renormalisation group equations

Dyson-Schwinger equations

2PI/nPI hierarchies

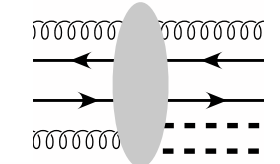
Bethe-Salpeter equations

⋮

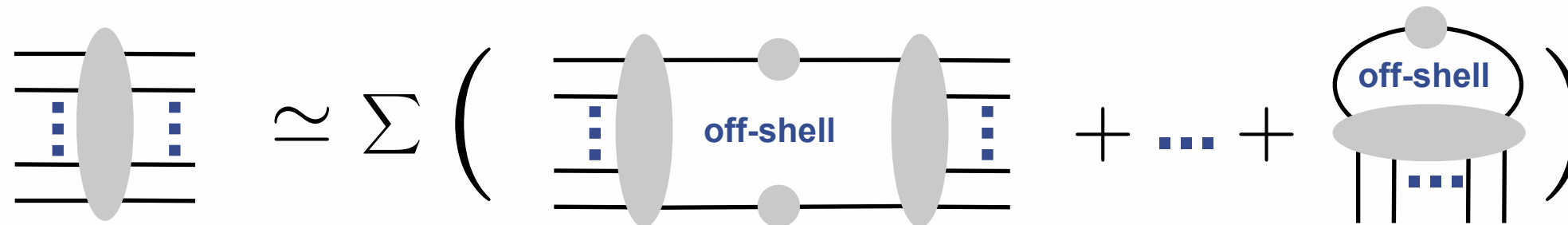
Continuum Methods for QCD

quark-gluon-hadron correlations

$$\langle q(x_1) \cdots \bar{q}(x_{2n}) A_\mu(y_1) \cdots A_\mu(y_m) h(z_1) \cdots h(z_l) \rangle$$



functional relations



scattering amplitude/
vertex functions

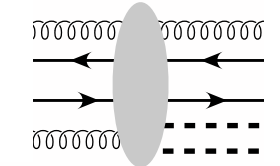
properties

- access to physics mechanisms 
- numerically tractable
no sign problem
systematic error control via closed form
- low energy models naturally incorporated

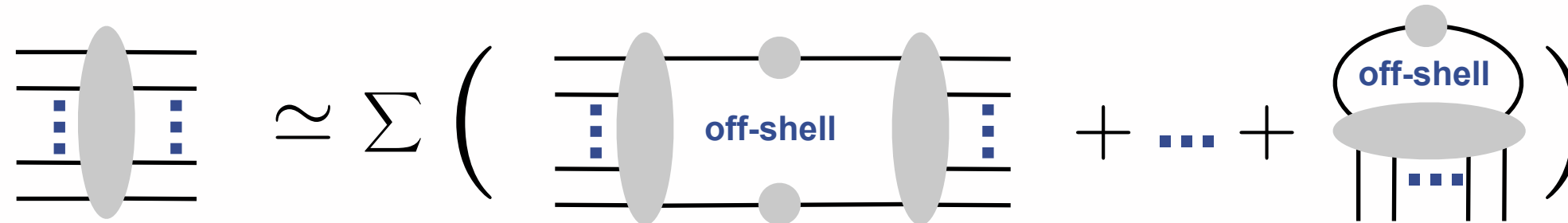
Continuum Methods for QCD

quark-gluon-hadron correlations

$$\langle q(x_1) \cdots \bar{q}(x_{2n}) A_\mu(y_1) \cdots A_\mu(y_m) h(z_1) \cdots h(z_l) \rangle$$



functional relations



scattering amplitude/
vertex functions

properties

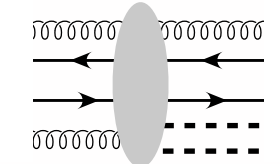
- access to physics mechanisms 
- numerically tractable
no sign problem
systematic error control via closed form
- low energy models naturally incorporated



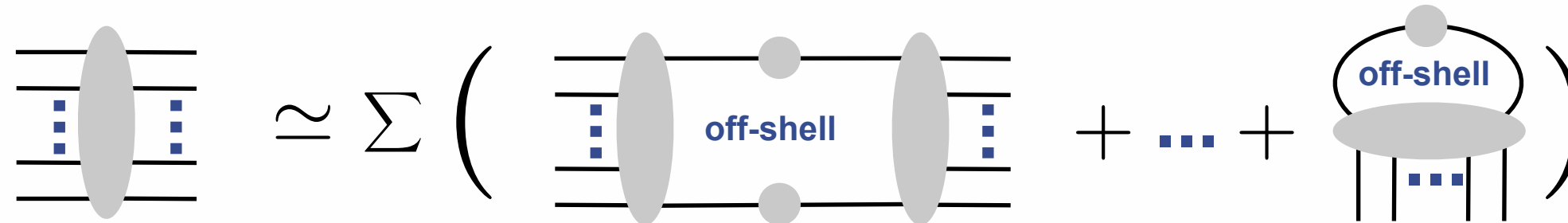
Continuum Methods for QCD

quark-gluon-hadron correlations

$$\langle q(x_1) \cdots \bar{q}(x_{2n}) A_\mu(y_1) \cdots A_\mu(y_m) h(z_1) \cdots h(z_l) \rangle$$



functional relations



scattering amplitude/
vertex functions

e.g. lattice input on rhs

e.g. volume flucs., finite density,
dynamics, ...

properties

- access to physics mechanisms 
- numerically tractable
no sign problem
systematic error control via closed form
- low energy models naturally incorporated

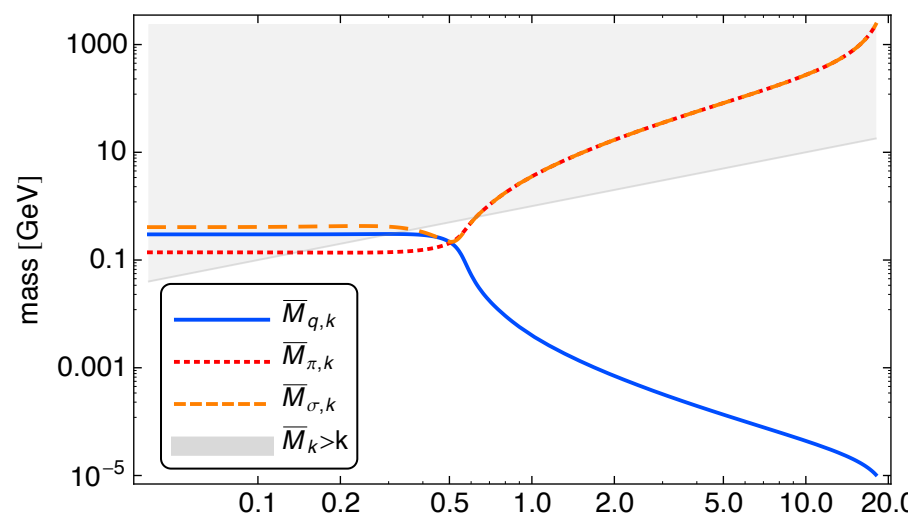
FunMethods complementary to lattice



Functional Methods for QCD

Scales

- **intrinsic scale of QCD:** $\Lambda_{\text{QCD}} \approx 200 \text{ MeV}$
 - **glue mass gap (Landau gauge: mass gap of glue propagator)** $\Delta m_{\text{glue}} \approx \Lambda_{\text{QCD}}$
 - **chiral symmetry breaking scale:** $\Delta m_\chi \approx m_{q,\text{constit.}} - m_{q,\text{current}}$ $\Delta m_\chi \approx 300 \text{ MeV}$
 - **chiral/confinement critical temperatures:** $T_\chi \approx T_{\text{conf}} \approx 150 \text{ MeV}$
- scales = $c(N_f, N_c) \Lambda_{\text{QCD}}$**
- **explicit mass scales of QCD:**
 - **current quark masses:** $\frac{m_{q,\text{current}}}{\Lambda_{\text{QCD}}} \Big|_{\text{light quarks}} \approx 10^{-2}$ $m_\pi \approx 140 \text{ MeV}$
 - **meson masses**
 - **higher resonances:** $\frac{m_{\text{res}}}{\Lambda_{\text{QCD}}} \lesssim 10^{-1}$



Functional Methods for QCD

Scales

- **intrinsic scale of QCD:** $\Lambda_{\text{QCD}} \approx 200 \text{ MeV}$
 - **glue mass gap (Landau gauge: mass gap of glue propagator)** $\Delta m_{\text{glue}} \approx \Lambda_{\text{QCD}}$
 - **chiral symmetry breaking scale:** $\Delta m_\chi \approx m_{q,\text{constit.}} - m_{q,\text{current}}$ $\Delta m_\chi \approx 300 \text{ MeV}$
 - **chiral/confinement critical temperatures:** $T_\chi \approx T_{\text{conf}} \approx 150 \text{ MeV}$

scales = $c(N_f, N_c)\Lambda_{\text{QCD}}$

 - **explicit mass scales of QCD:**
 - **current quark masses:**
$$\frac{m_{q,\text{current}}}{\Lambda_{\text{QCD}}} \Big|_{\text{light quarks}} \approx 10^{-2} \quad m_\pi \approx 140 \text{ MeV}$$
 - **higher resonances:**
$$\frac{m_{\text{res}}}{\Lambda_{\text{QCD}}} \lesssim 10^{-1}$$
 - **nuclear binding energy** $\approx 16 \text{ MeV}$

best done with a combination of imaginary and real time flows



Functional RG for QCD

JMP, AIP Conf. Proc. 1343 (2011)
 Nucl.Phys. A931 (2014) 113

free energy at momentum scale k



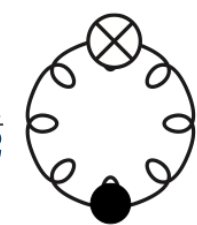
Phase diagram survey

JMP, Schladming '13

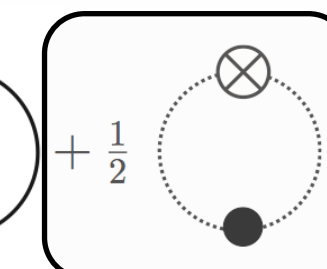
ab initio

glue quantum fluctuations

**free energy/
grand potential**

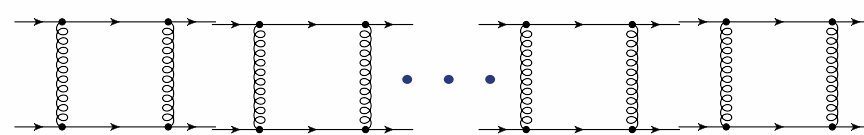


hadronic quantum fluctuations



quark quantum fluctuations

RG-scale k : $t = \ln k$



Dynamical hadronisation

dynamical

Gies, Wetterich '01

JMP '05

Flörchinger, Wetterich '09

Functional RG for QCD

fQCD collaboration: J. Braun, A. Cyrol, L. Fister, W.-j. Fu, T.K. Herbst, M. Mitter, N. Mueller, JMP, S. Rechenberger, F. Rennecke, N. Strodthoff

TARDIS, ERGE, DoFun2.0

DoFun

Huber, Braun, Comput.Phys.Commun. 183 (2012) 1290-1320

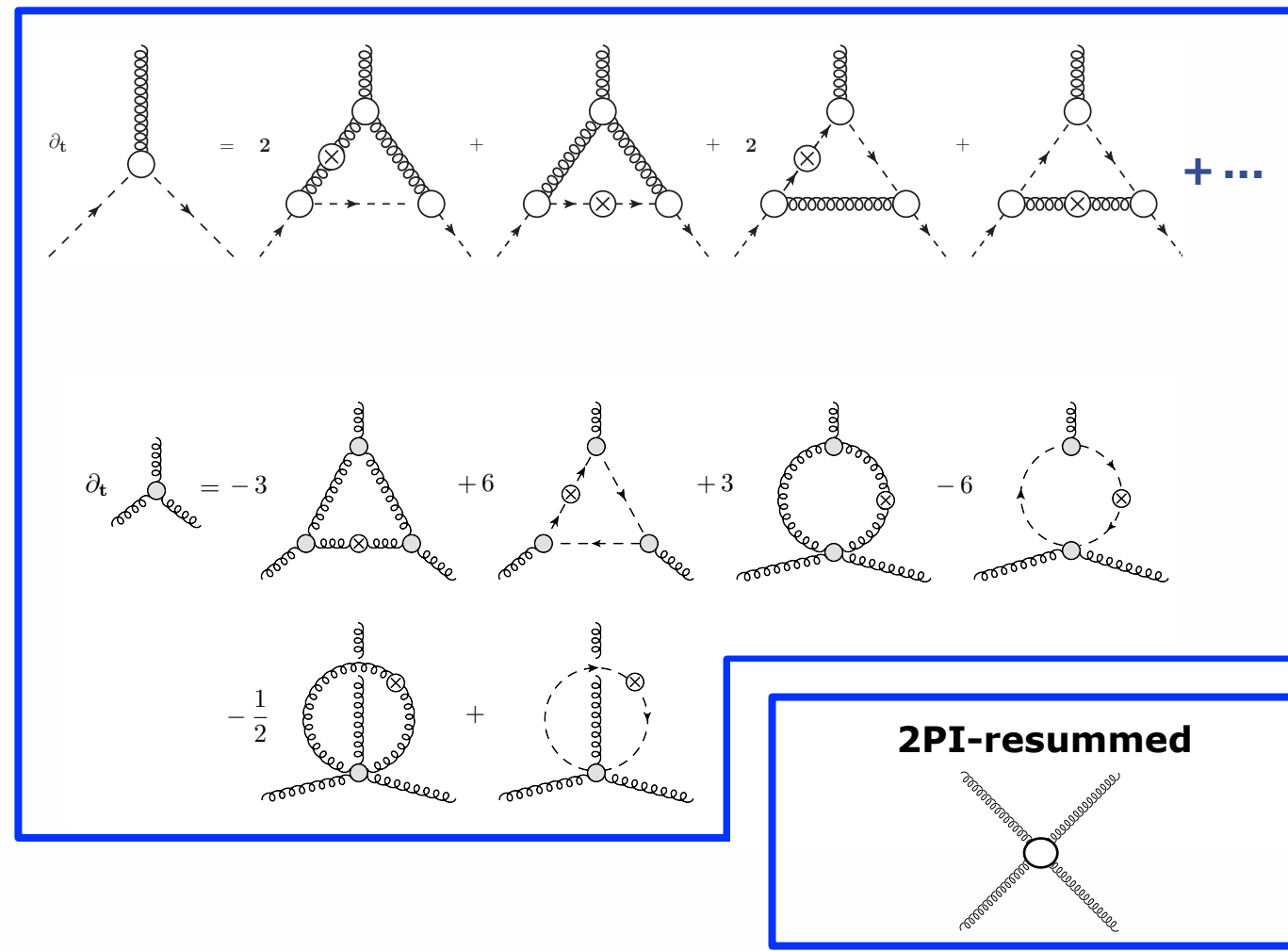
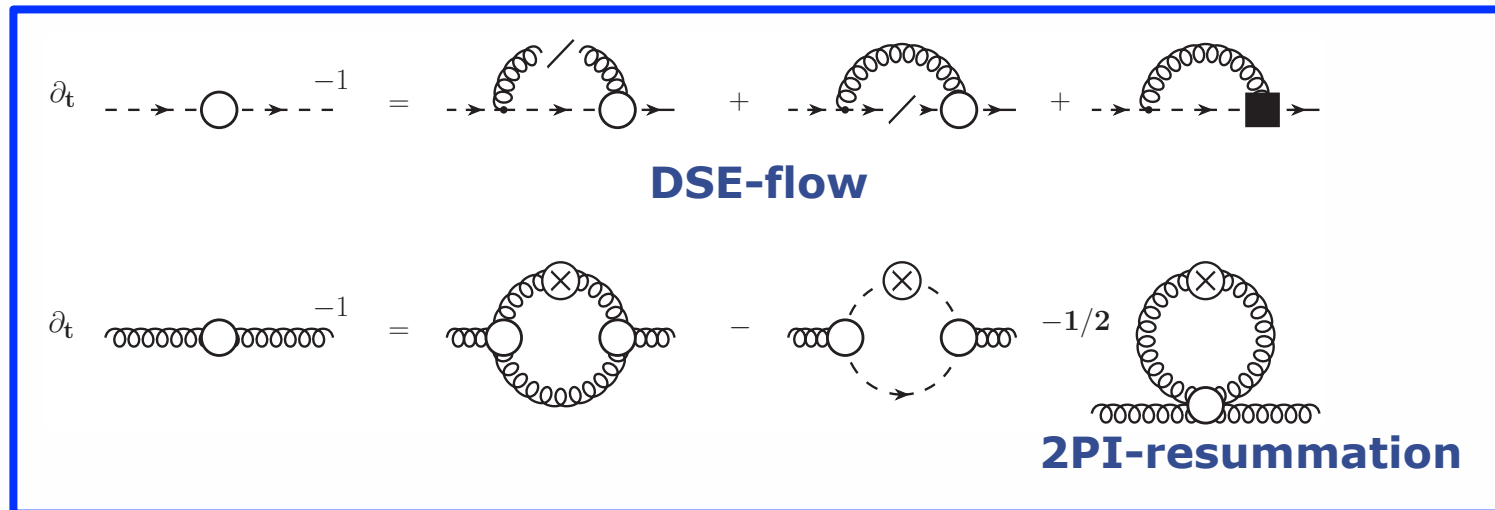
Mitter, JMP, Strodthoff, PRD 91 (2015) 054035

Braun, Fister, Haas, JMP, Rennecke, arXiv:1412.1045

Outline

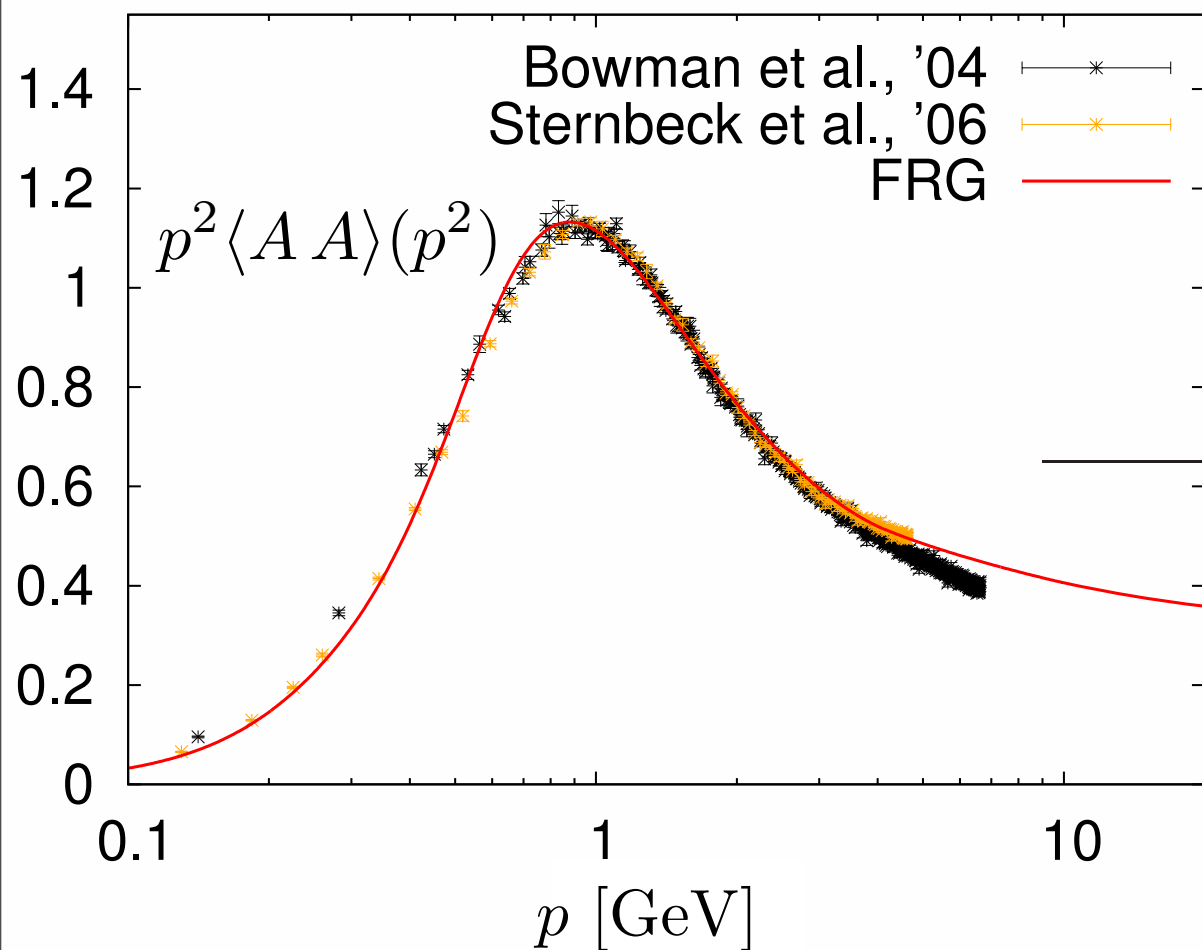
- Vacuum QCD & the hadron spectrum
- Phase structure of QCD
- Spectral Functions & Transport Coefficients
- Outlook

Glue sector

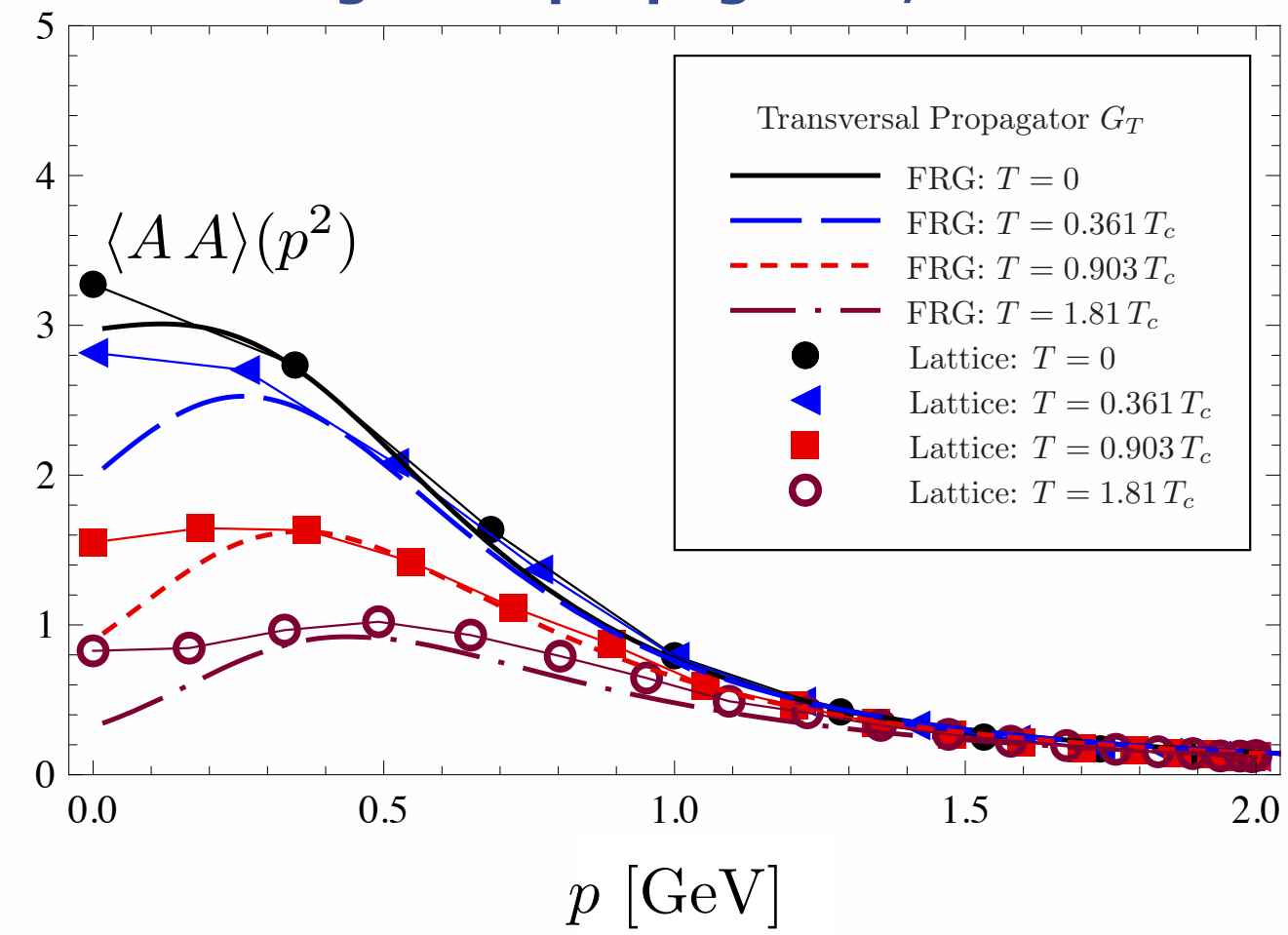


Glue sector

Yang-Mills propagators, T=0



Yang-Mills propagators, finite T



Fischer, Maas, JMP, Annals Phys. 324 (2009) 2408

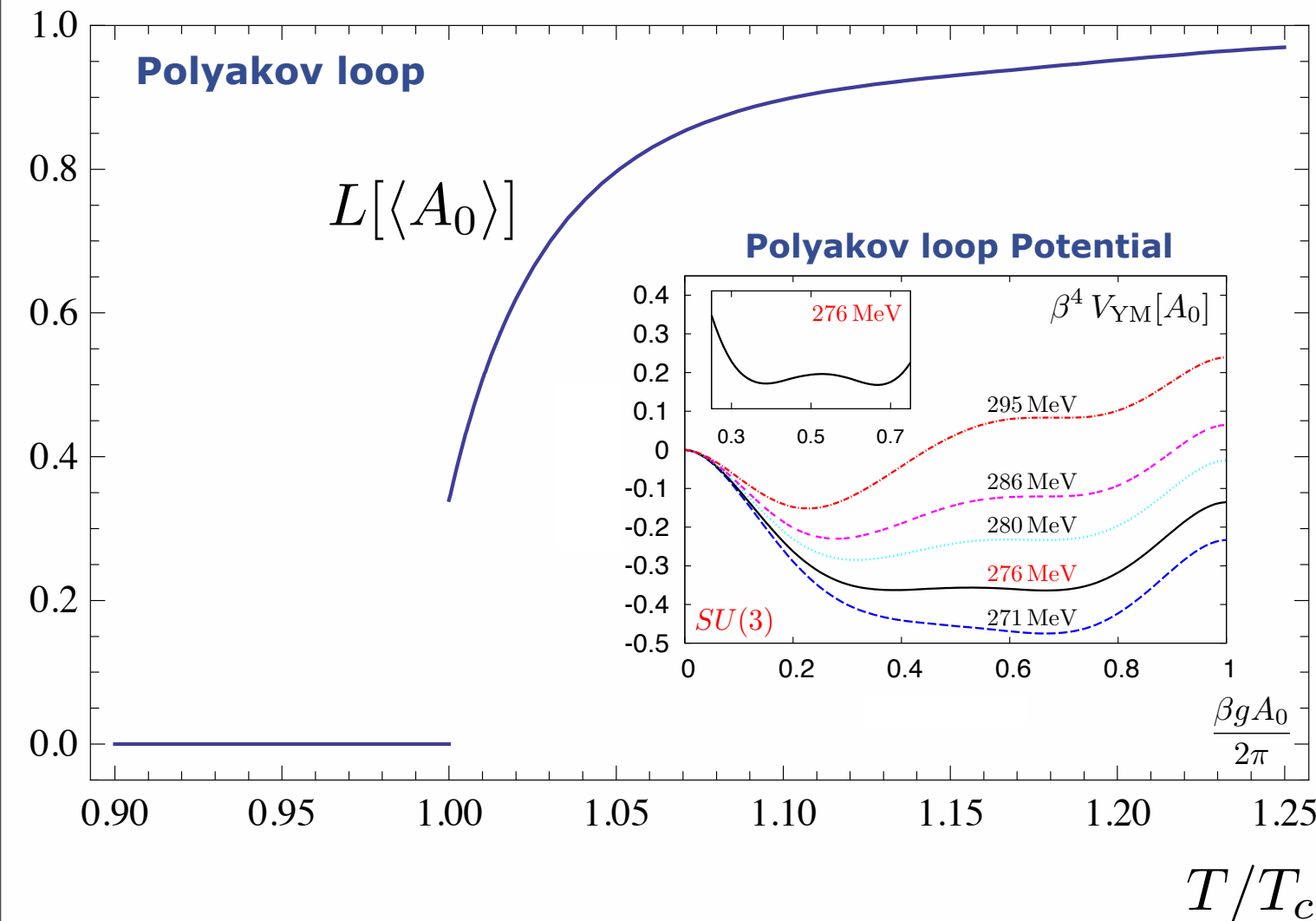
Fister, JMP '14

Fister, JMP, arXiv:1112.5440

Confinement

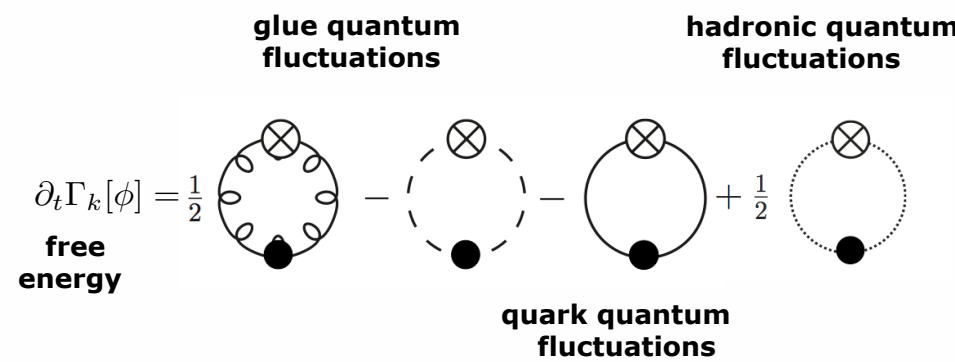
FRG: Braun, Gies, JMP, PLB 684 (2010) 262

FRG, DSE, 2PI: Fister, JMP, PRD 88 (2013) 045010



$$T_c/\sqrt{\sigma} = 0.658 \pm 0.023$$

$$\text{lattice : } T_c/\sqrt{\sigma} = 0.646$$



confinement

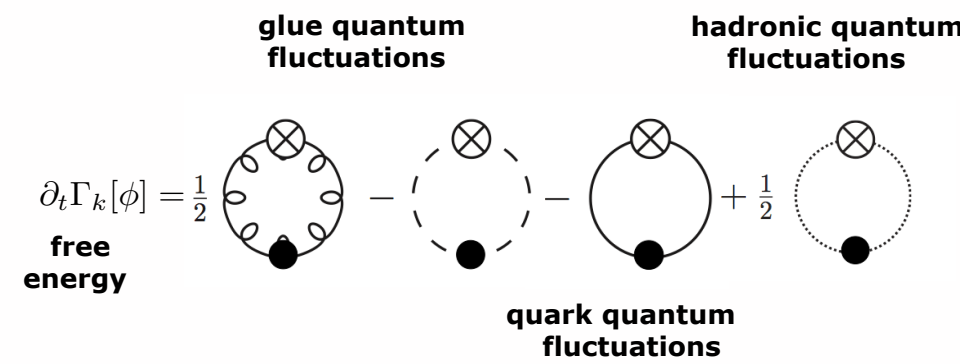
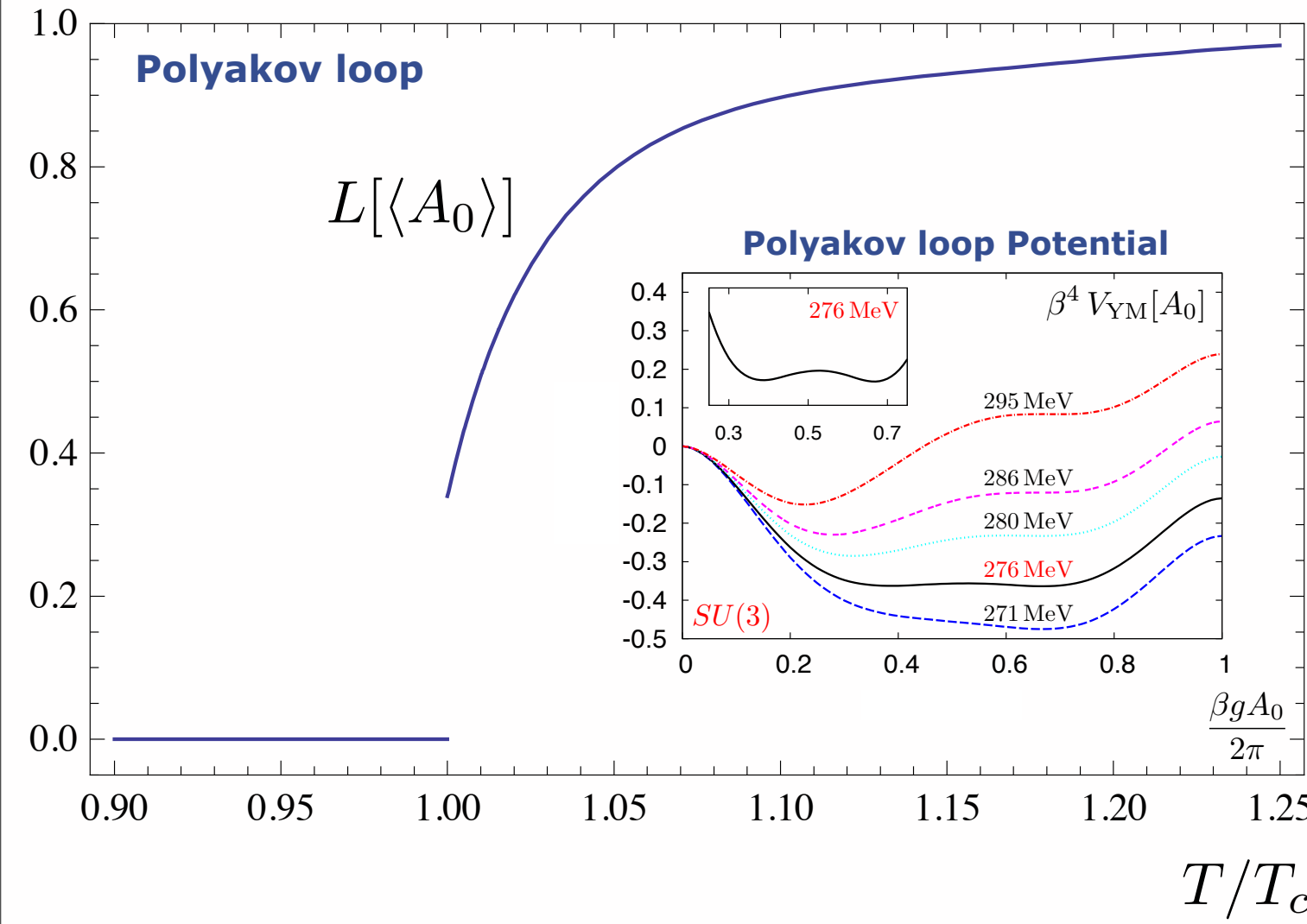
gluon propagator
gapped relative to
ghost propagator

Braun, Gies, JMP '07
Marhauser, JMP '08
Fister, JMP '13

Confinement

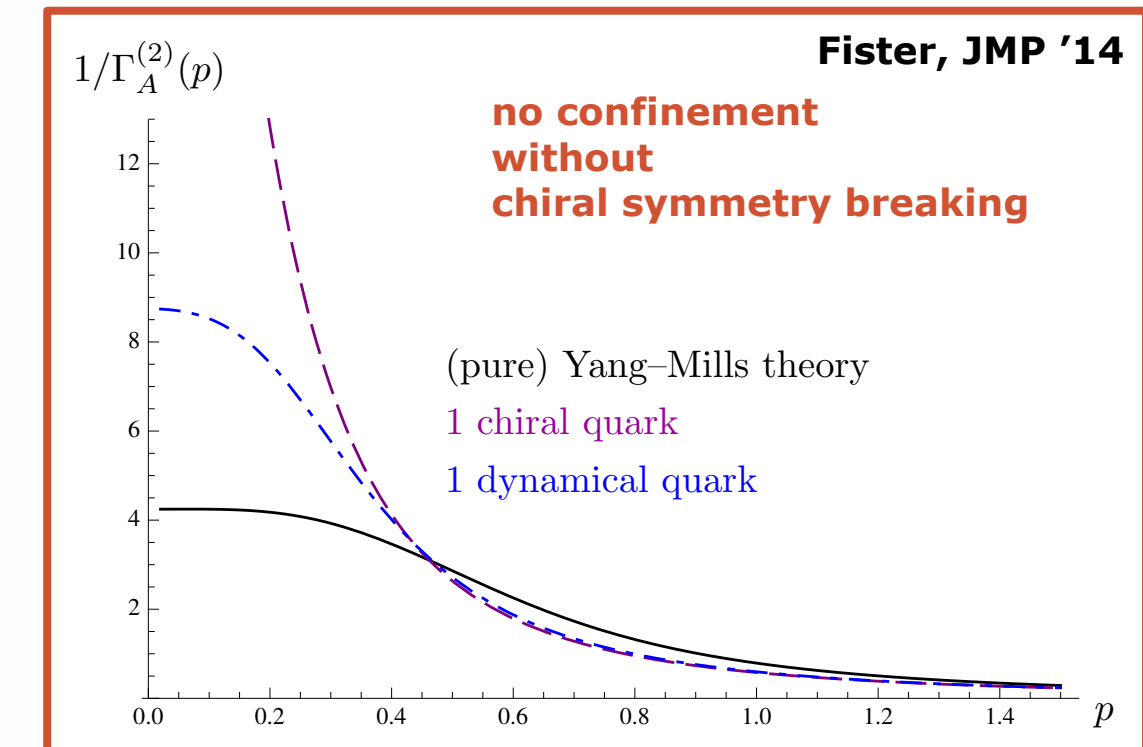
FRG: Braun, Gies, JMP, PLB 684 (2010) 262

FRG, DSE, 2PI: Fister, JMP, PRD 88 (2013) 045010

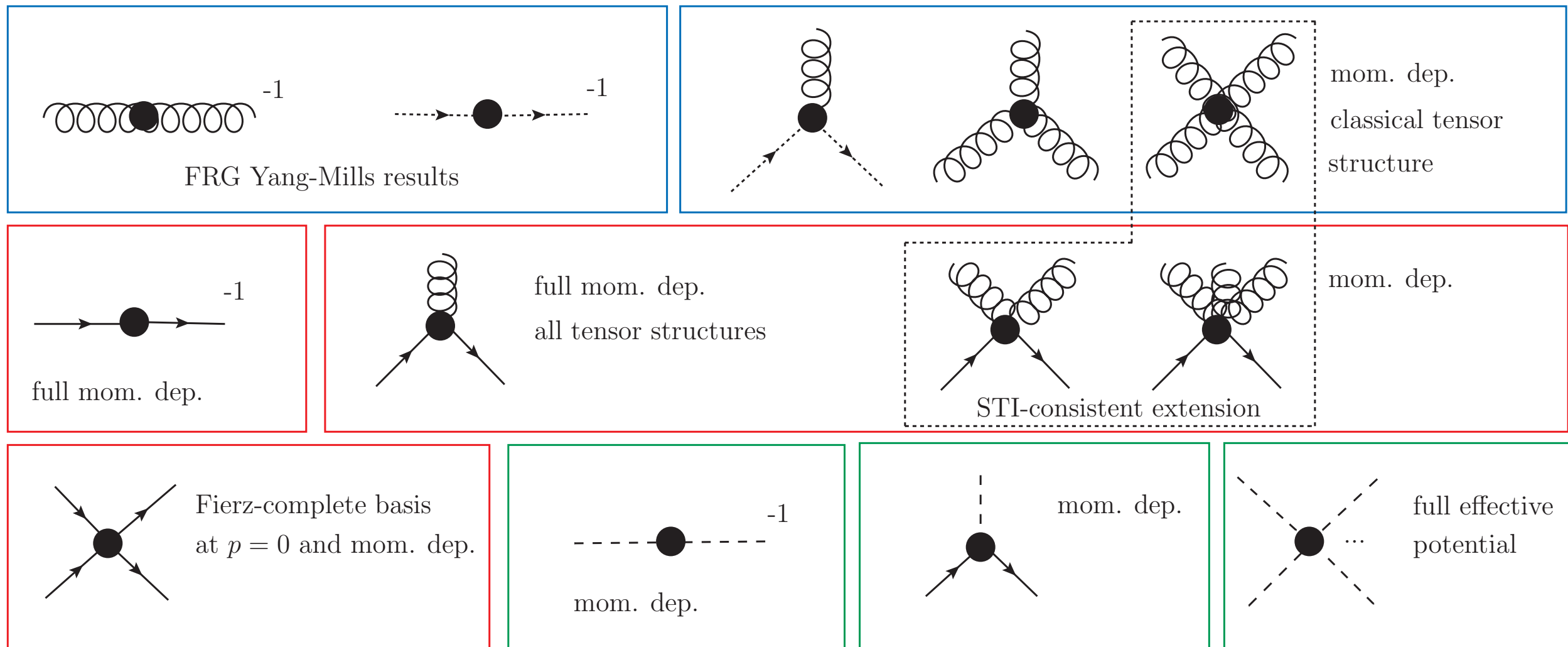


$$T_c/\sqrt{\sigma} = 0.658 \pm 0.023$$

$$\text{lattice : } T_c/\sqrt{\sigma} = 0.646$$



Chiral symmetry breaking



fQCD

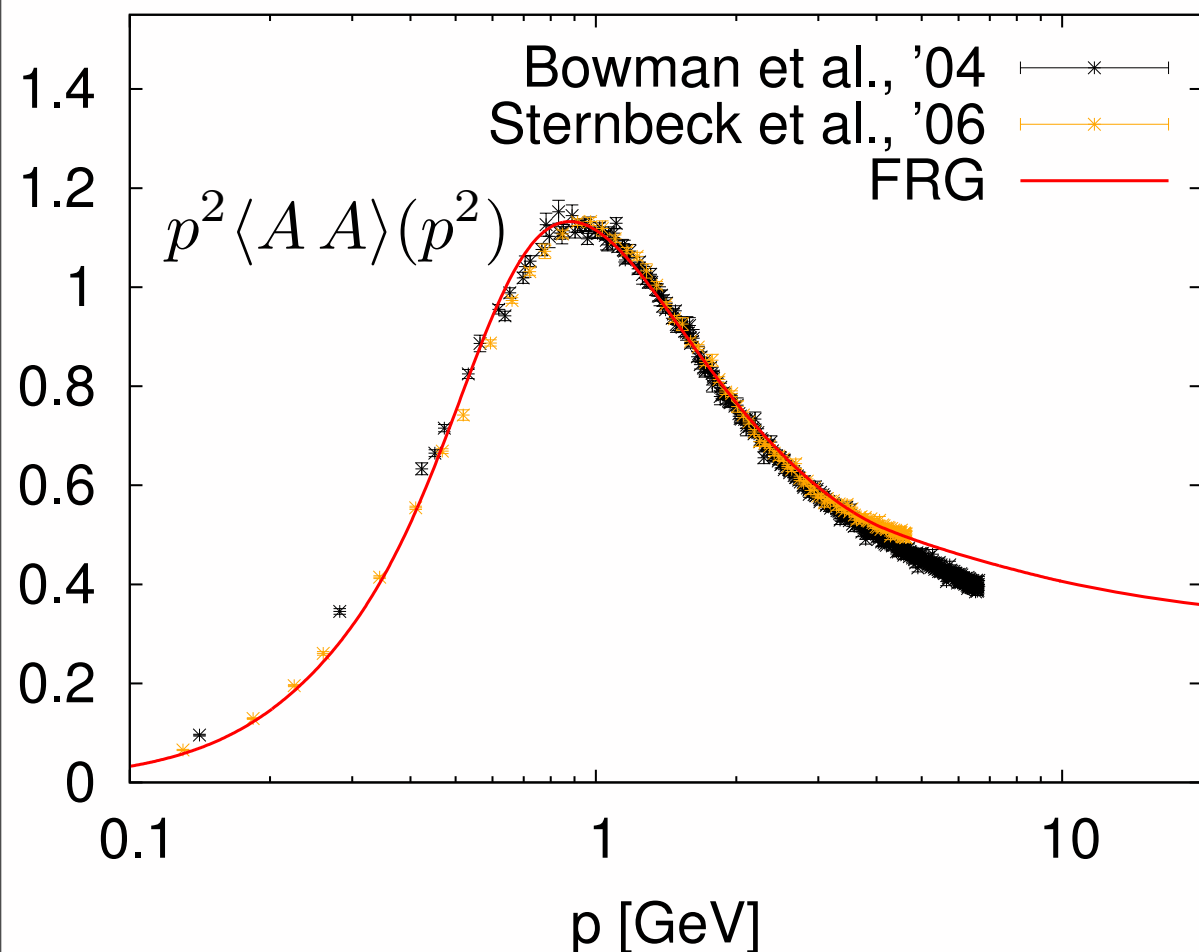
Mitter, JMP, Strodthoff, PRD 91 (2015) 054035

see also Williams, Eur.Phys.J. A51 (2015) 5, 57

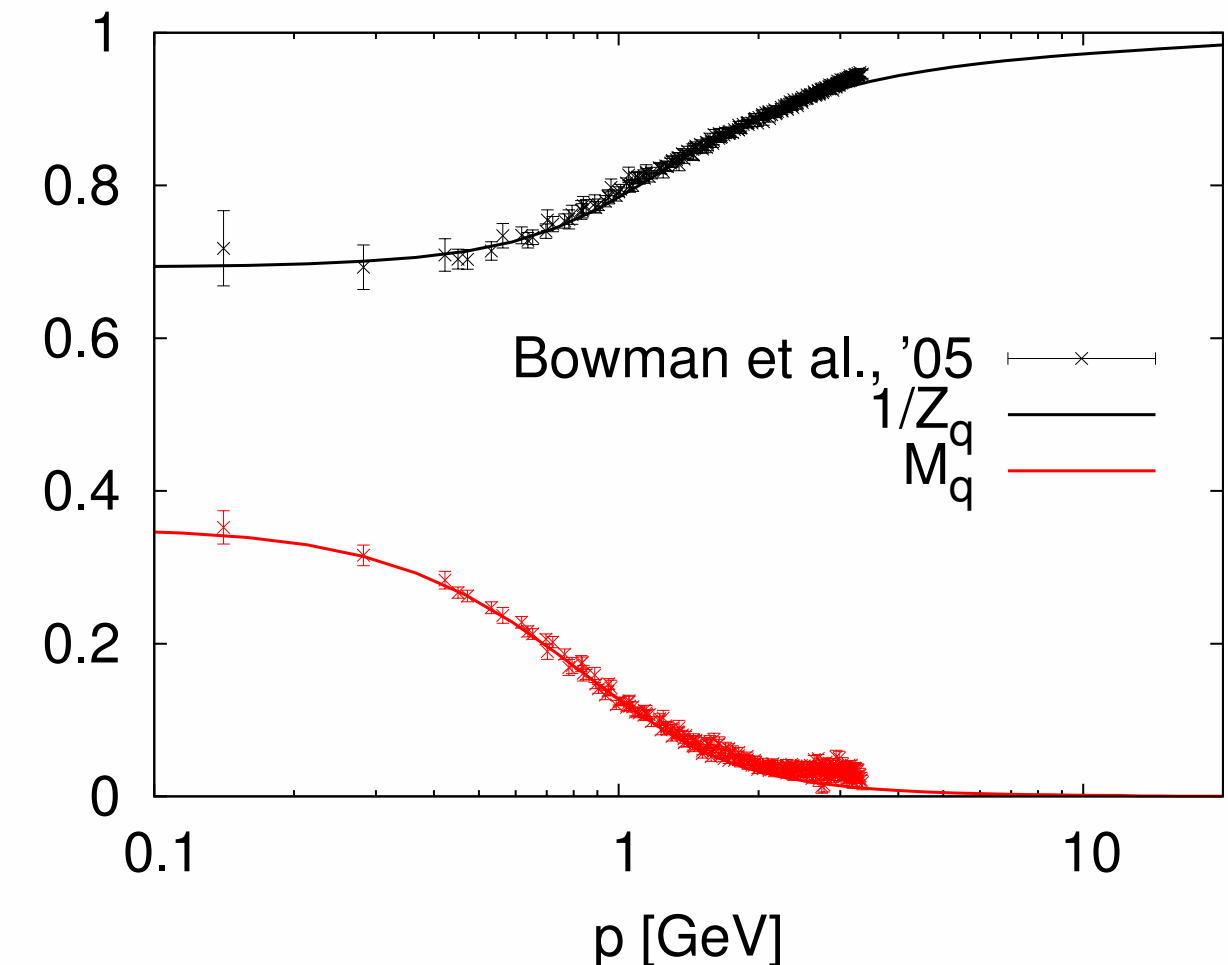
Chiral symmetry breaking

FRG-quenched QCD vs lattice-quenced QCD

quenched gluon dressing



quark propagator



JMP, Rennecke, PRD 90, 076002

Helmboldt, JMP, Strodthoff, PRD 91 (2015) 5, 054010

Braun, Fister, Haas, JMP, Rennecke, arXiv:1412.1045

$N_f = 2$

systematic error estimate: ~10%

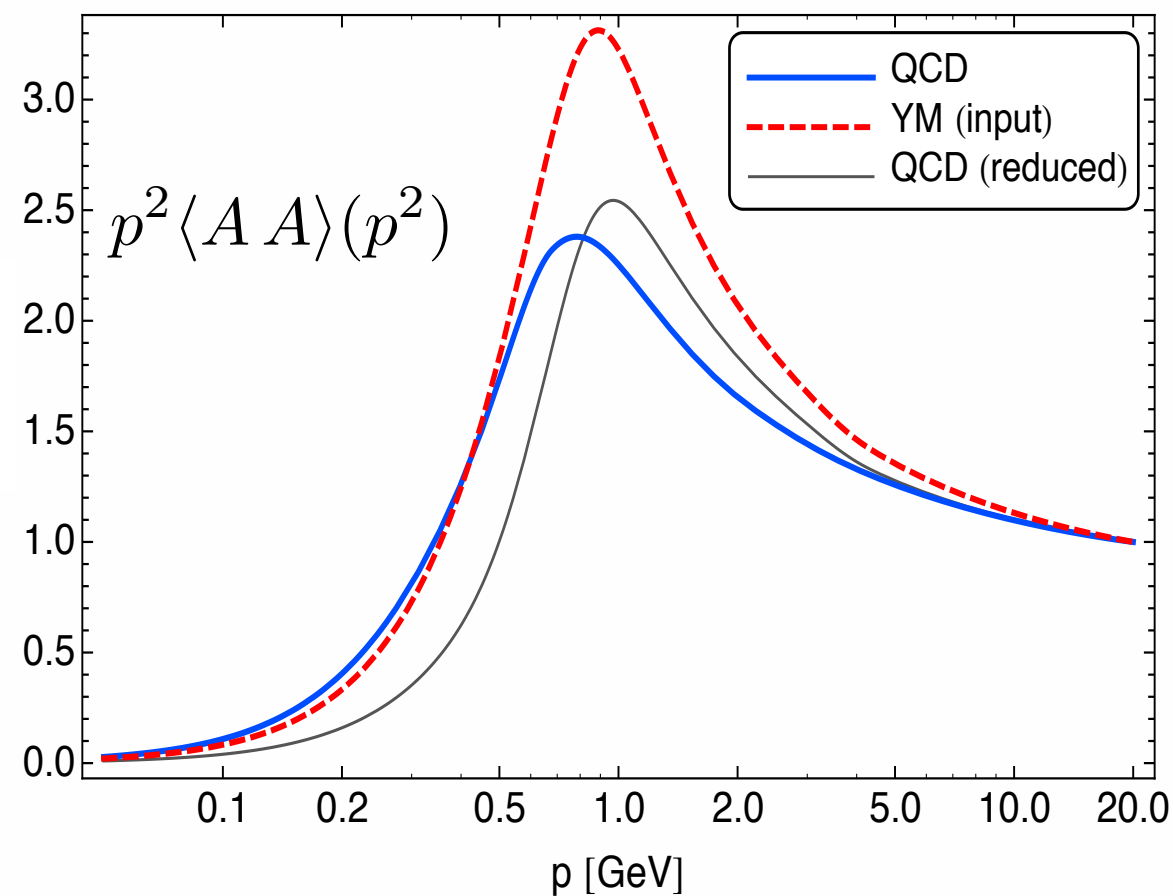
JMP

Mitter, JMP, Strodthoff, PRD 91 (2015) 054035

Chiral symmetry breaking

FRG-quenched QCD vs lattice-quenced QCD

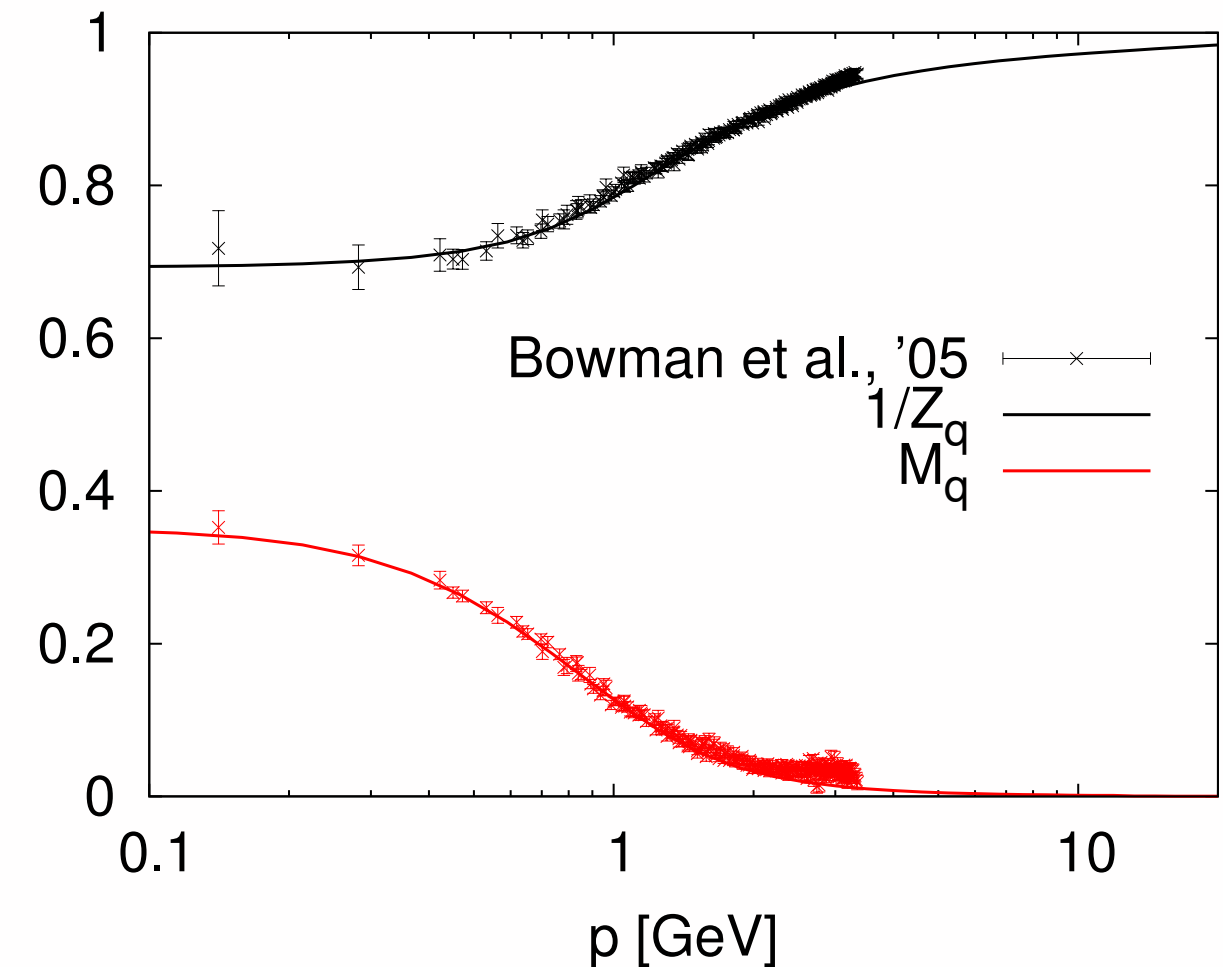
unquenched gluon dressing



Braun, Fister, Haas, JMP, Rennecke, arXiv:1412.1045

Rennecke, arXive:1504.03585

quark propagator

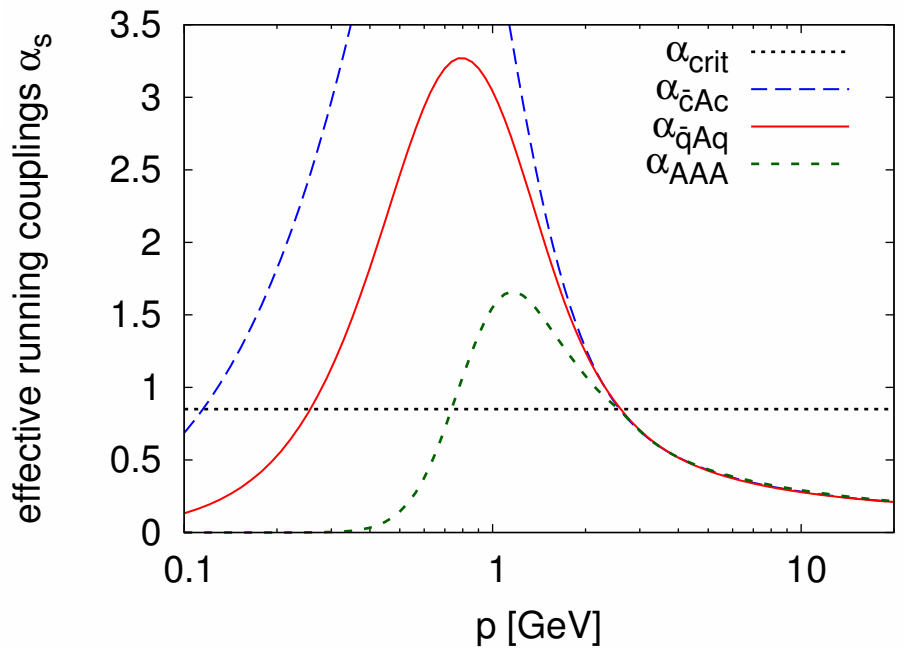
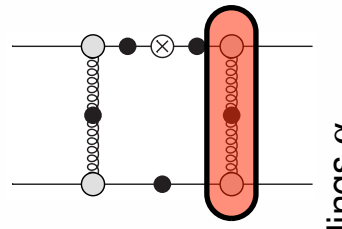
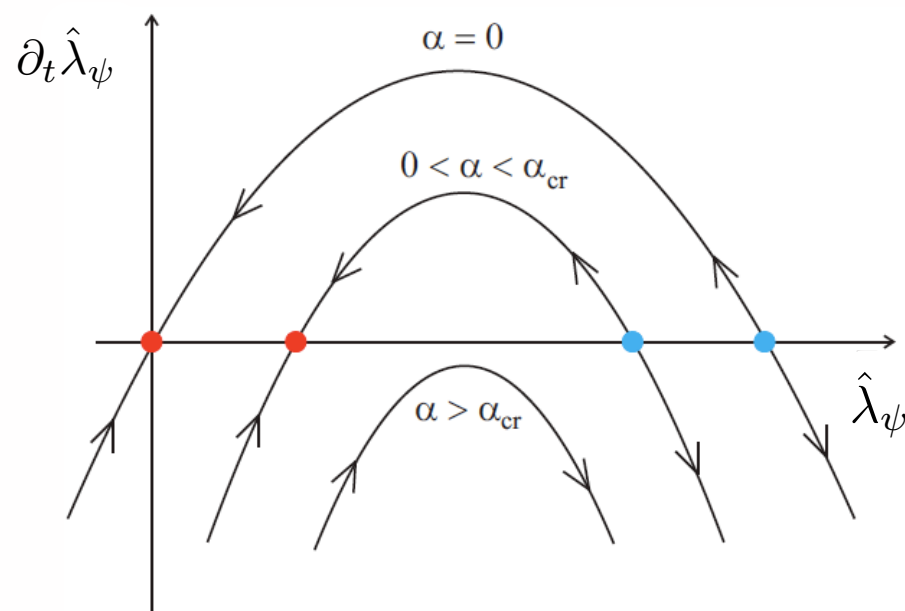


$N_f = 2$

systematic error estimate: ~10%

Mitter, JMP, Strodthoff, PRD 91 (2015) 054035

Confinement & symmetry breaking

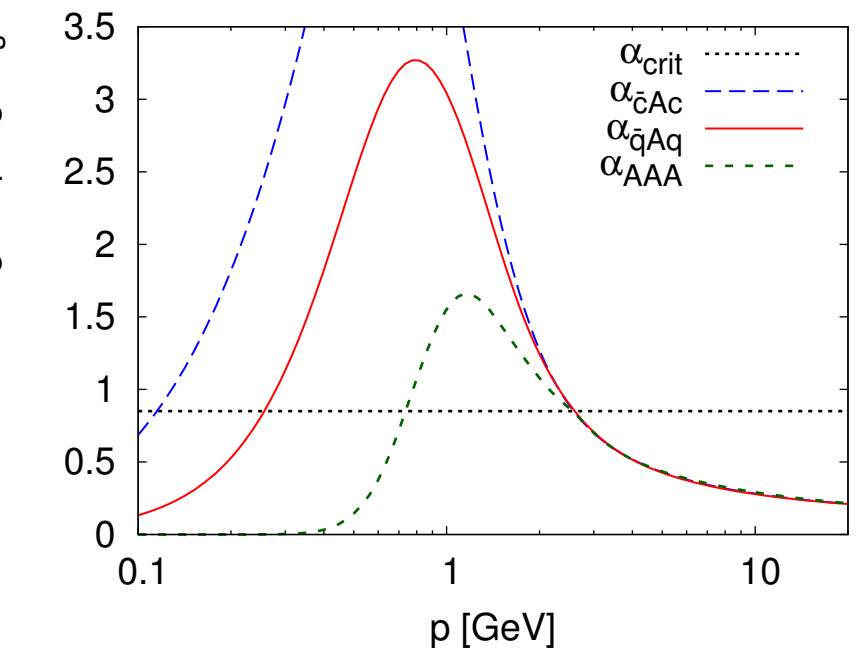
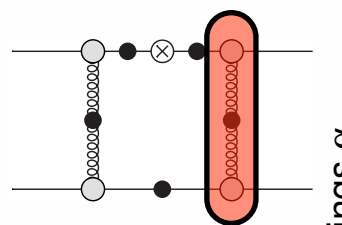
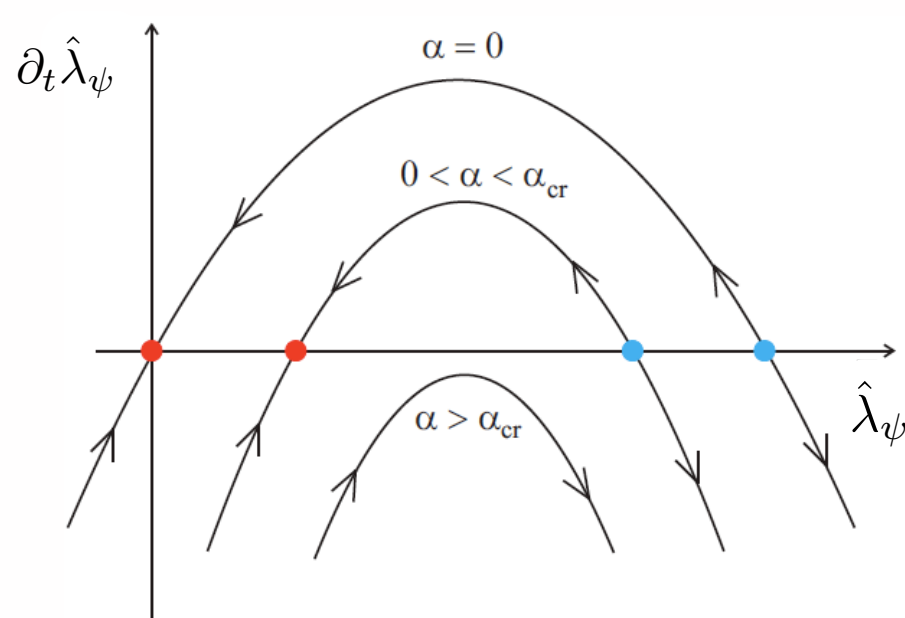


Mitter, JMP, Strodthoff '14

Braun, Fister, Haas, JMP, Rennecke '14

$$k \partial_k \hat{\lambda}_\psi = 2 \hat{\lambda}_\psi + \text{[Feynman diagram with a circle and a cross]} + \text{[Feynman diagram with a loop and a cross]} + \text{[Feynman diagram with two vertical gluons and a cross]} + \text{[Feynman diagram with a loop and a gluon line]} + \dots$$

Confinement & symmetry breaking



Mitter, JMP, Strodthoff '14

Braun, Fister, Haas, JMP, Rennecke '14

**dynamical correlation of confinement
and
chiral symmetry breaking**

confinement

**gluon propagator
gapped relative to
ghost propagator**

chiral symmetry breaking

**gluon propagator
not gapped too much**

Fister, Mitter, JMP, Strodthoff '14

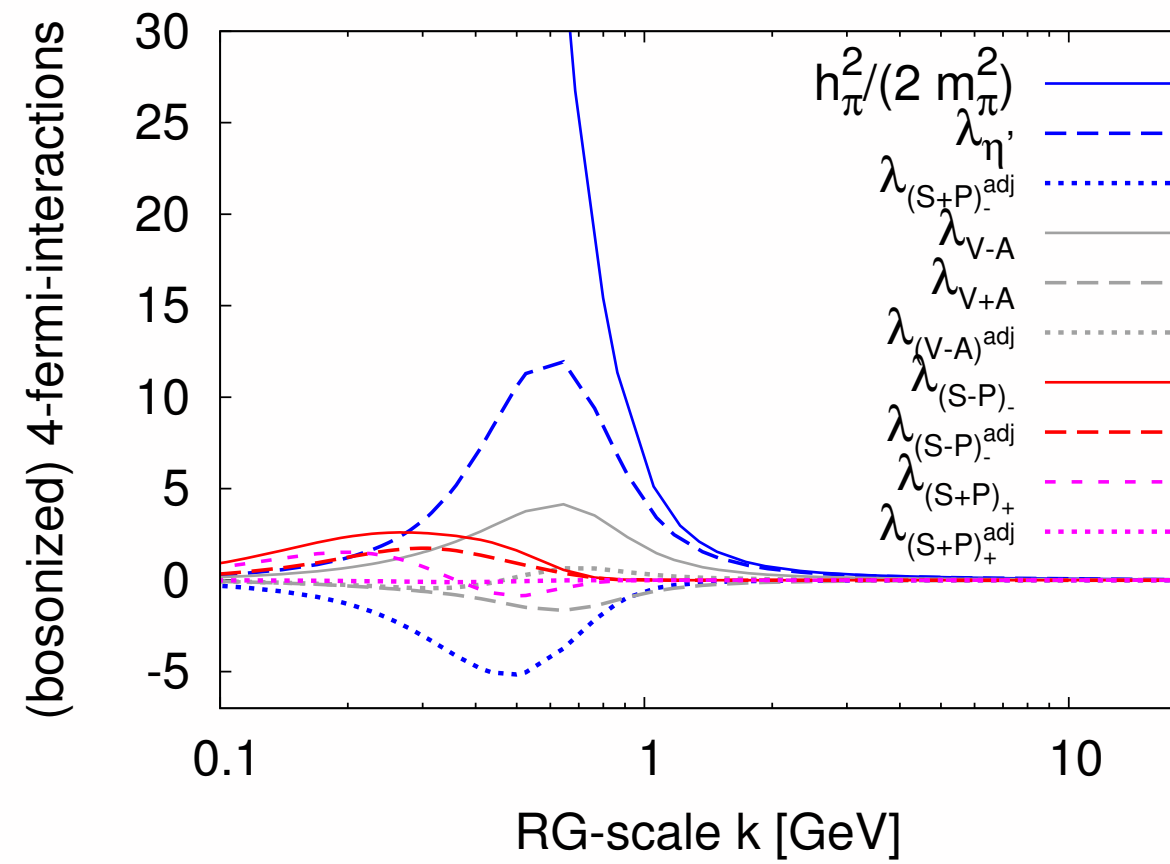
A glimpse at the hadron spectrum

preliminary

four-fermi scattering amplitude at pion pole

$$\langle \bar{q} \vec{\sigma} \gamma_5 q(p) \bar{q} \vec{\sigma} \gamma_5 q(-p) \rangle \rightarrow \frac{\chi_{\bar{q}\pi q} \bar{\chi}_{\bar{q}\pi q}}{p^2 - m_\pi^2} + \text{finite terms}$$

$$\Gamma^{(4)}(p_1, p_2, p_3, p_4)$$



A glimpse at the hadron spectrum

preliminary

four-fermi scattering amplitude at pion pole

$$\langle \bar{q} \vec{\sigma} \gamma_5 q(p) \bar{q} \vec{\sigma} \gamma_5 q(-p) \rangle \rightarrow \frac{\chi_{\bar{q}\pi q} \bar{\chi}_{\bar{q}\pi q}}{p^2 - m_\pi^2} + \text{finite terms}$$

↓

$$\Gamma_{(\bar{q}\gamma_5 \vec{\sigma} q)^2}^{(4)}(p, p, -p, -p)$$

↓

$$\frac{\Gamma_{\bar{q}\pi q}^{(3)} \Gamma_{\bar{q}\pi q}^{(3)}}{p^2 - m_\pi^2}$$

pion decay constant f_π via normalisation of $\Gamma_{\bar{q}\pi q}^{(3)}$

aka BSE wave function

recent mini-review on DSE-BSE
Sanchis-Alepuz, Williams, arXiv:1503.05896

A glimpse at the hadron spectrum

preliminary

four-fermi scattering amplitude at pion pole

$$\langle \bar{q} \vec{\sigma} \gamma_5 q(p) \bar{q} \vec{\sigma} \gamma_5 q(-p) \rangle$$

↓

$$\Gamma_{(\bar{q} \gamma_5 \vec{\sigma} q)^2}^{(4)}(p, p, -p, -p)$$

$$\rightarrow \frac{\chi_{\bar{q}\pi q} \bar{\chi}_{\bar{q}\pi q}}{p^2 - m_\pi^2} + \text{finite terms}$$

↓

$$\frac{\Gamma_{\bar{q}\pi q}^{(3)} \Gamma_{\bar{q}\pi q}^{(3)}}{p^2 - m_\pi^2}$$

pion decay constant f_π via normalisation of $\Gamma_{\bar{q}\pi q}^{(3)}$

real-time:

- Spectral Fcts & Transport Coeffs

A glimpse at the hadron spectrum

preliminary

four-fermi scattering amplitude at pion pole

$$\langle \bar{q} \vec{\sigma} \gamma_5 q(p) \bar{q} \vec{\sigma} \gamma_5 q(-p) \rangle \rightarrow \frac{\chi_{\bar{q}\pi q} \bar{\chi}_{\bar{q}\pi q}}{p^2 - m_\pi^2} + \text{finite terms}$$

↓

$$\Gamma_{(\bar{q}\gamma_5 \vec{\sigma} q)^2}^{(4)}(p, p, -p, -p)$$

↓

$$\frac{\Gamma_{\bar{q}\pi q}^{(3)} \Gamma_{\bar{q}\pi q}^{(3)}}{p^2 - m_\pi^2}$$

pion decay constant f_π via normalisation of $\Gamma_{\bar{q}\pi q}^{(3)}$

$f_\pi \simeq 99 \text{ MeV}$
quenched QCD

$f_\pi \simeq 89 \text{ MeV}$
unquenched QCD

lattice Davies et al., PRL 92 (2004) 022001 $\frac{f_\pi^{\text{quenched}}}{f_\pi^{\text{unquenched}}} \simeq 1.1$

Mitter, JMP, Strodthoff, in preparation

A glimpse at the hadron spectrum

preliminary

four-fermi scattering amplitude at pion pole

$$\langle \bar{q} \vec{\sigma} \gamma_5 q(p) \bar{q} \vec{\sigma} \gamma_5 q(-p) \rangle \rightarrow \frac{\chi_{\bar{q}\pi q} \bar{\chi}_{\bar{q}\pi q}}{p^2 - m_\pi^2} + \text{finite terms}$$

↓

$$\Gamma_{(\bar{q}\gamma_5 \vec{\sigma} q)^2}^{(4)}(p, p, -p, -p)$$

↓

$$\frac{\Gamma_{\bar{q}\pi q}^{(3)} \Gamma_{\bar{q}\pi q}^{(3)}}{p^2 - m_\pi^2}$$

pion decay constant f_π via normalisation of $\Gamma_{\bar{q}\pi q}^{(3)}$

$f_\pi \simeq 99 \text{ MeV}$
quenched QCD

$f_\pi \simeq 89 \text{ MeV}$
unquenched QCD

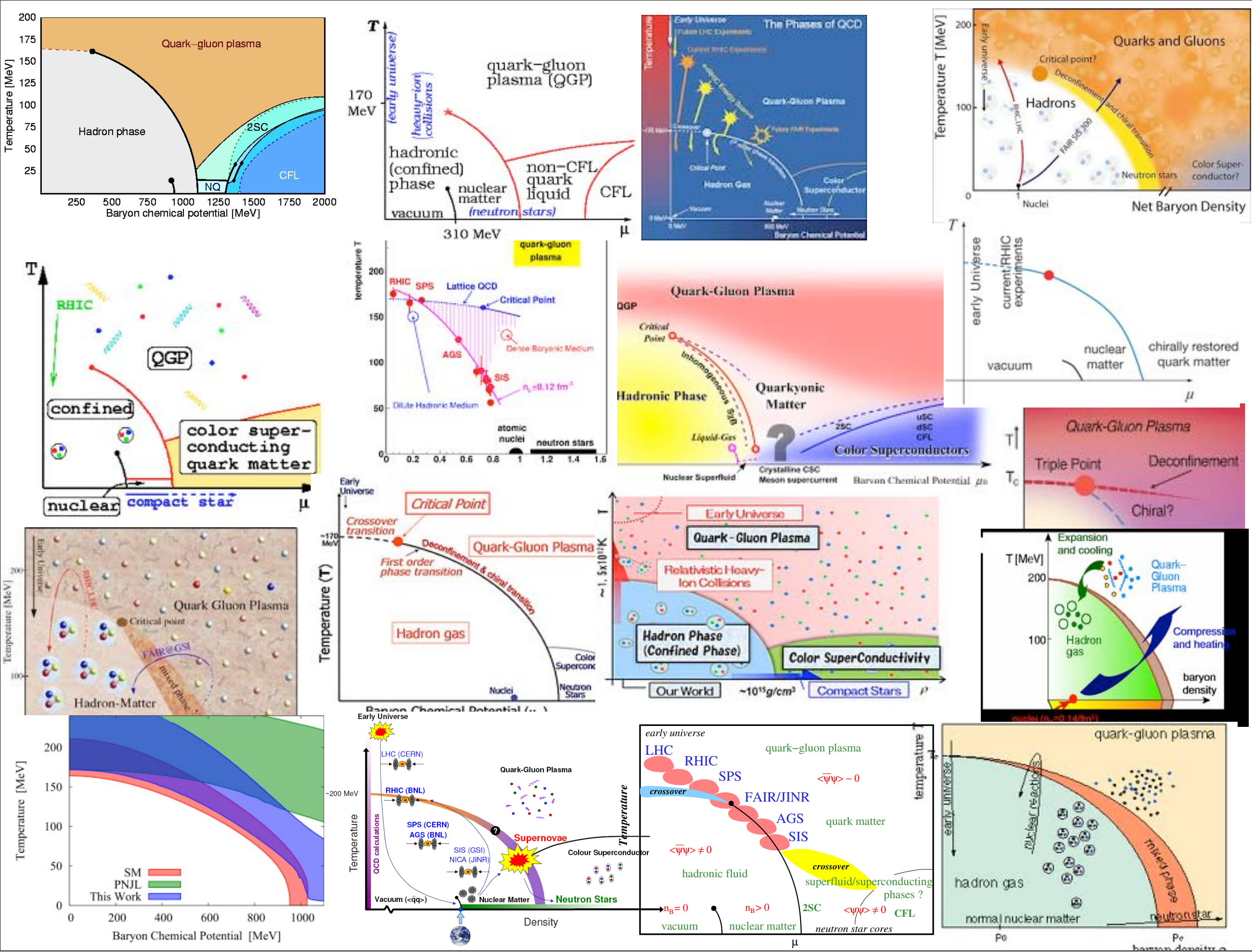
lattice Davies et al., PRL 92 (2004) 022001

unquenched e.g. Horsley et al., PLB 732, 41 (2014) $f_\pi^{\text{lattice}} \simeq 89 \text{ MeV}$

Mitter, JMP, Strodthoff, in preparation

Outline

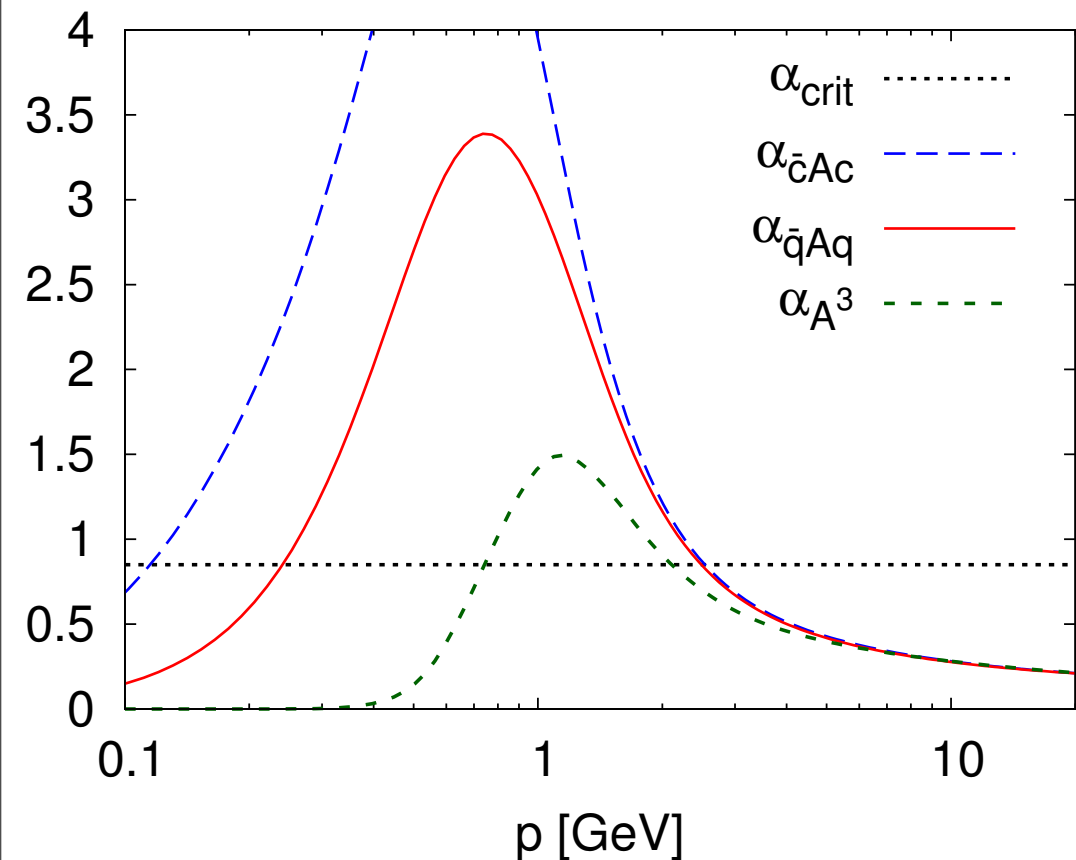
- Vacuum QCD & the hadron spectrum
- Phase structure of QCD
- Spectral Functions & Transport Coefficients
- Outlook



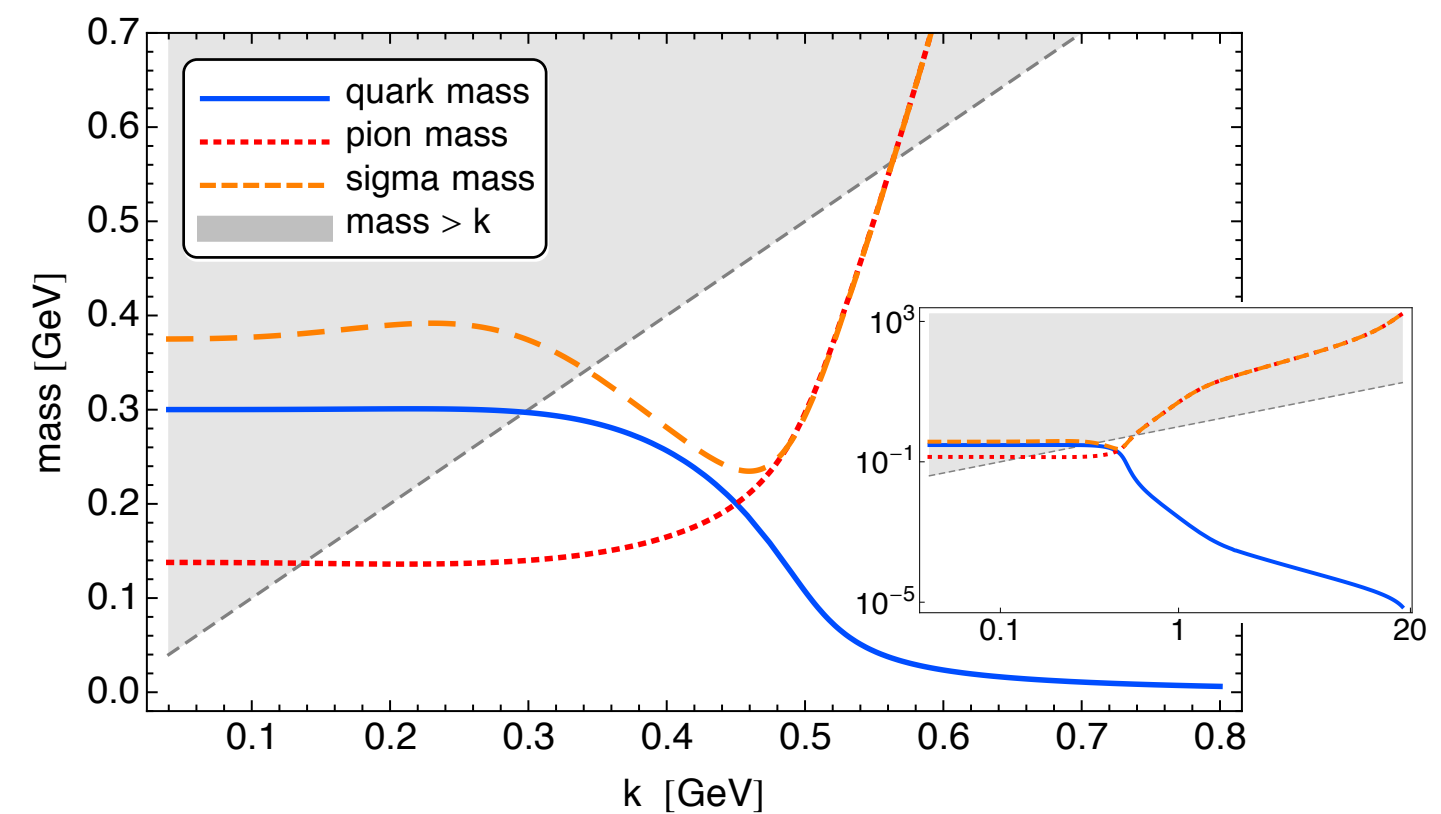
QCD

$$\partial_t \Gamma_k[\phi] = \frac{1}{2} \left(\text{Diagram 1} - \text{Diagram 2} - \text{Diagram 3} + \frac{1}{2} \text{Diagram 4} \right)$$

Sequential decoupling of gluon, quark, sigma, pion fluctuations



Mitter, JMP, Strodthoff, PRD 91 (2015) 054035

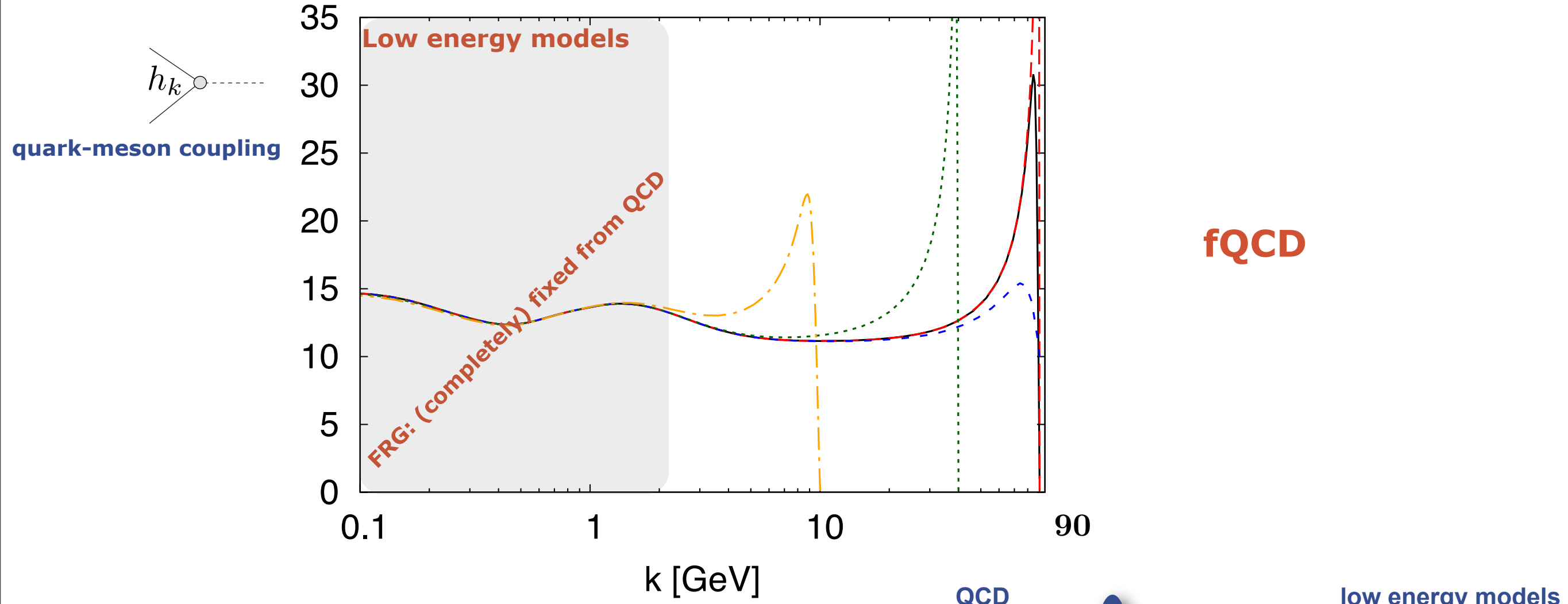


Braun, Fister, Haas, JMP, Rennecke, arXiv:1412.1045

Rennecke, arXiv:1504.03585

QCD

$$\partial_t \Gamma_k[\phi] = \frac{1}{2} \left(\text{Diagram 1} - \text{Diagram 2} - \text{Diagram 3} + \frac{1}{2} \text{Diagram 4} \right)$$



PQM-model

PNJL-model

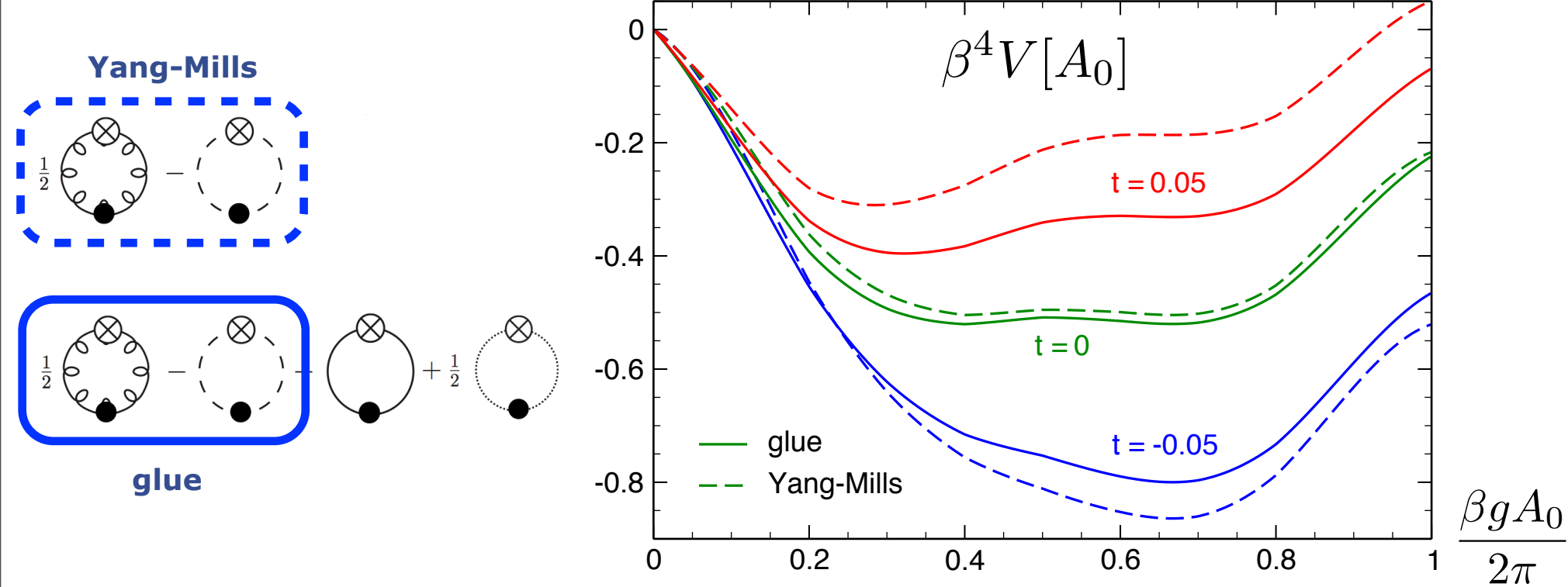
QM-model

NJL-model

QCD

$$\partial_t \Gamma_k[\phi] = \frac{1}{2} \left(\text{Diagram 1} - \text{Diagram 2} - \text{Diagram 3} + \frac{1}{2} \text{Diagram 4} \right)$$

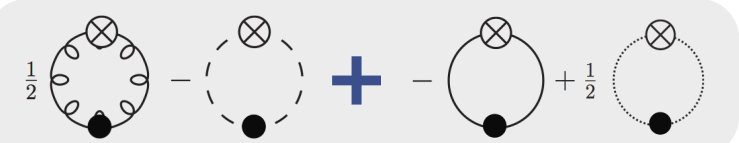
Polyakov loop potential in full QCD



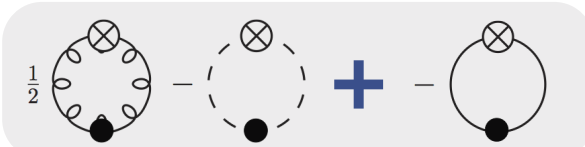
JMP, AIP Conf. Proc. 1343 (2011)

Haas, Stiele et al, PRD 87 (2013) 076004

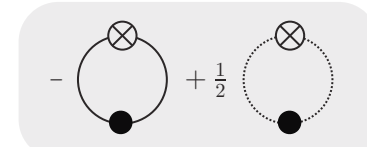
PQM-model



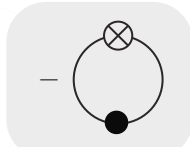
PNJL-model



QM-model



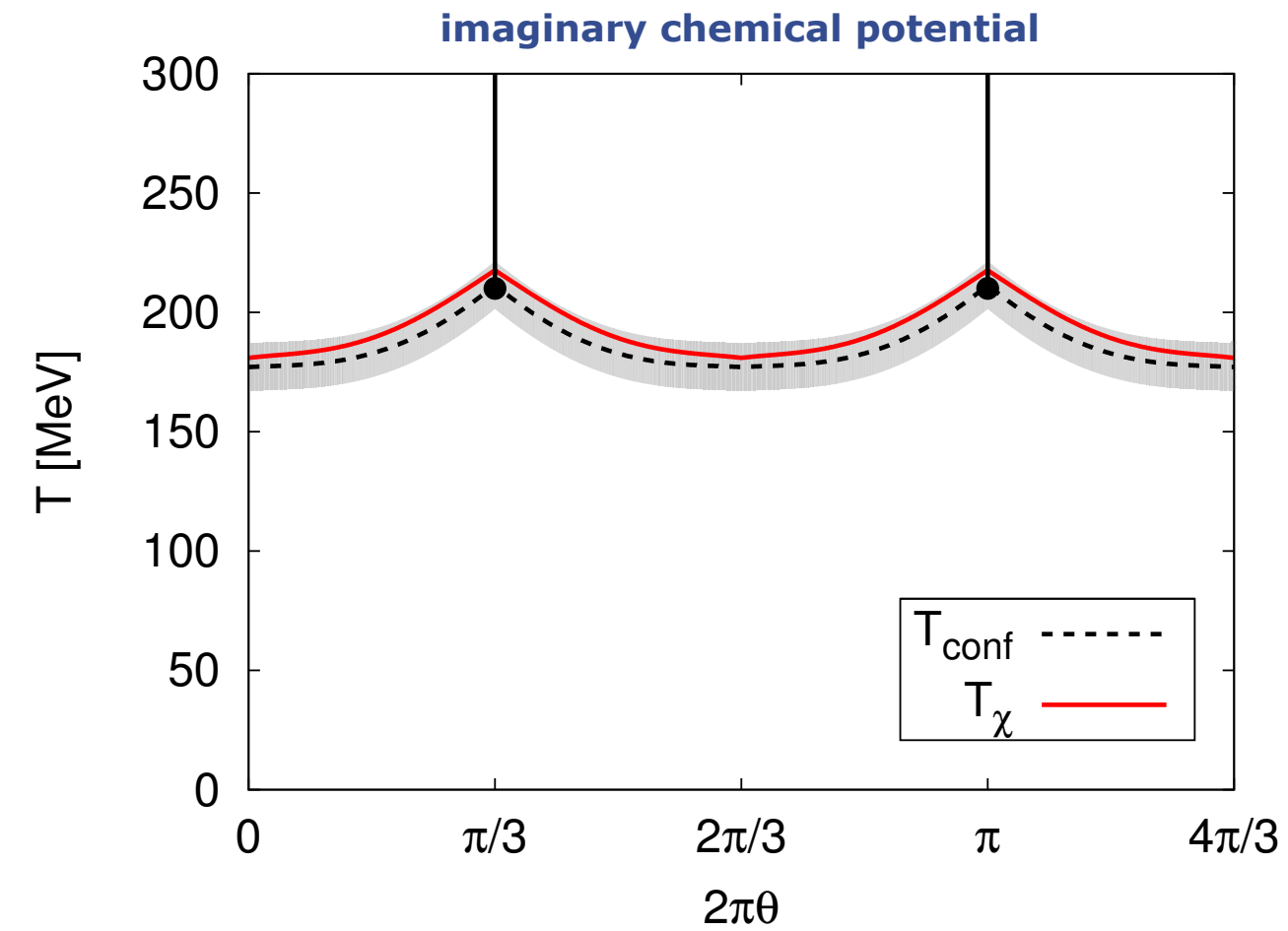
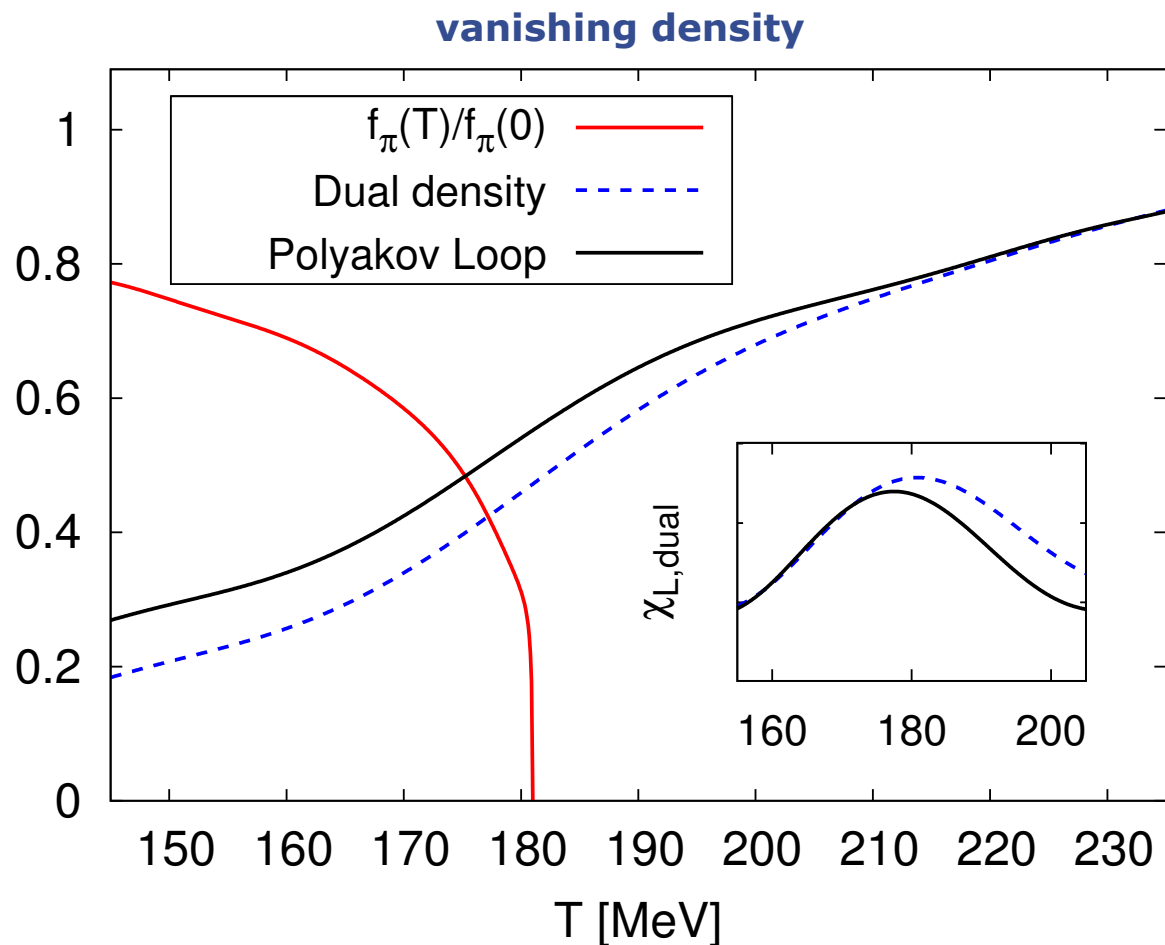
NJL-model



QCD

$$\partial_t \Gamma_k[\phi] = \frac{1}{2} \left(\text{Diagram 1} - \text{Diagram 2} - \text{Diagram 3} + \frac{1}{2} \text{Diagram 4} \right)$$

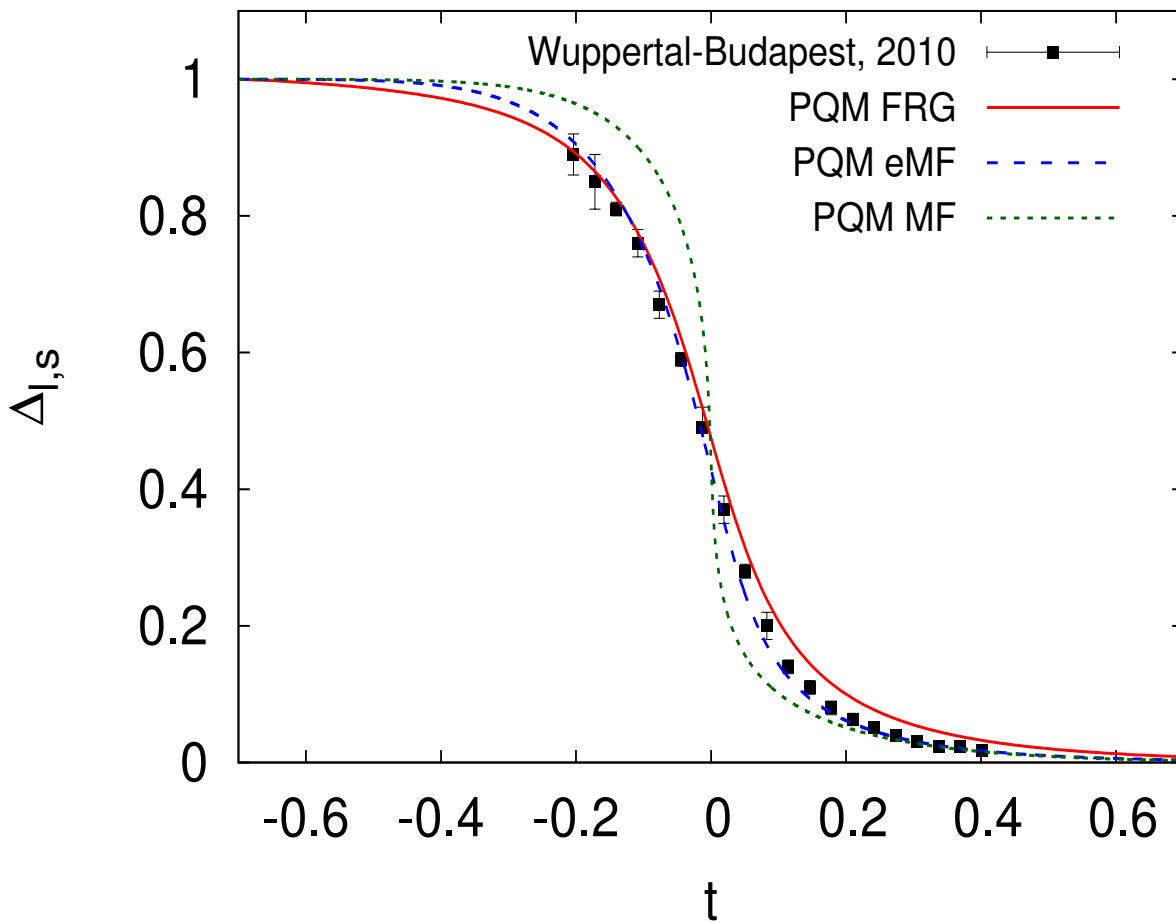
2 flavors & chiral limit



Braun, Haas, Marhauser, JMP, PRL 106 (2011) 022002

Thermodynamics

reduced chiral condensate

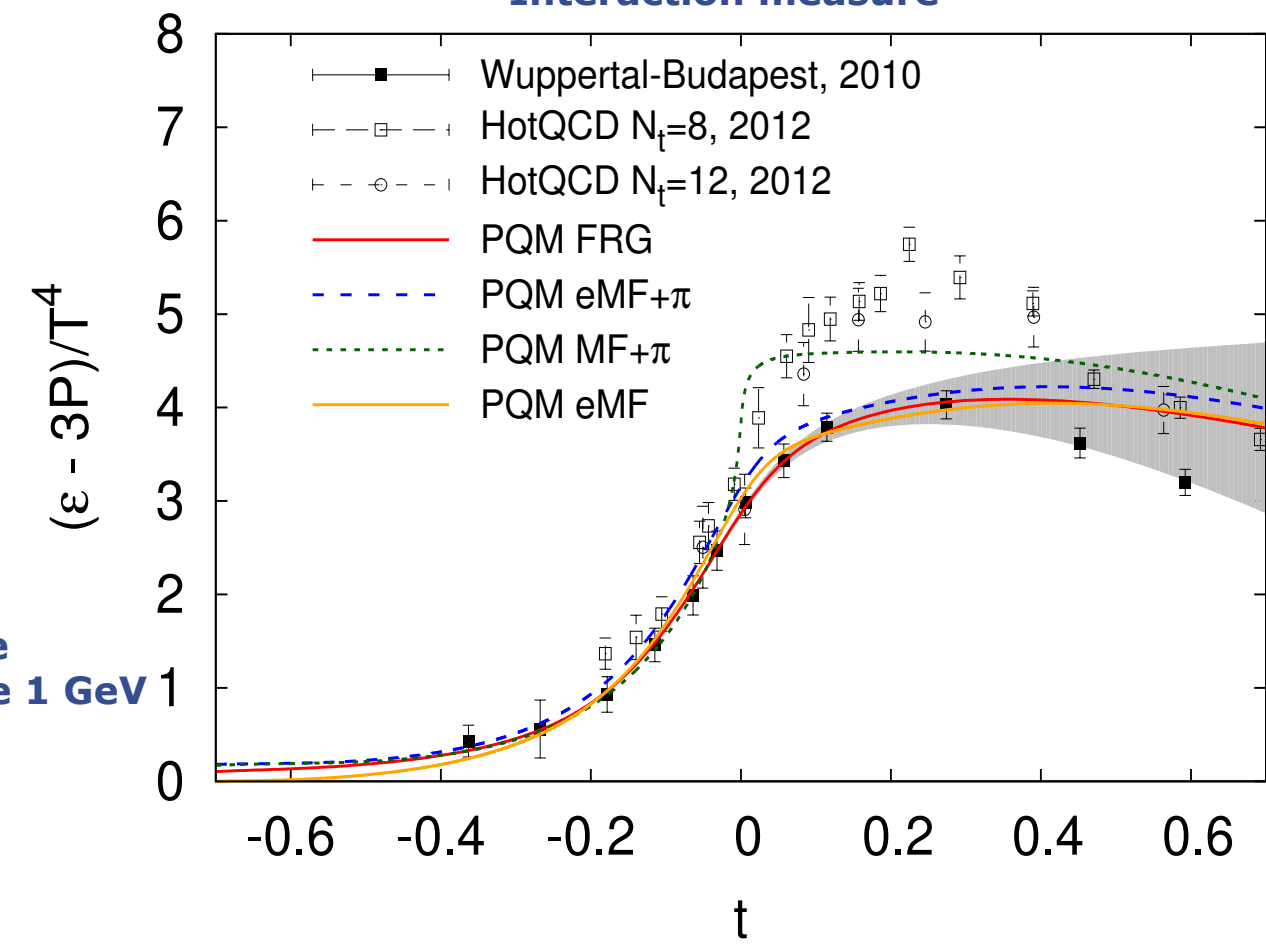


see talk of B.-J. Schaefer

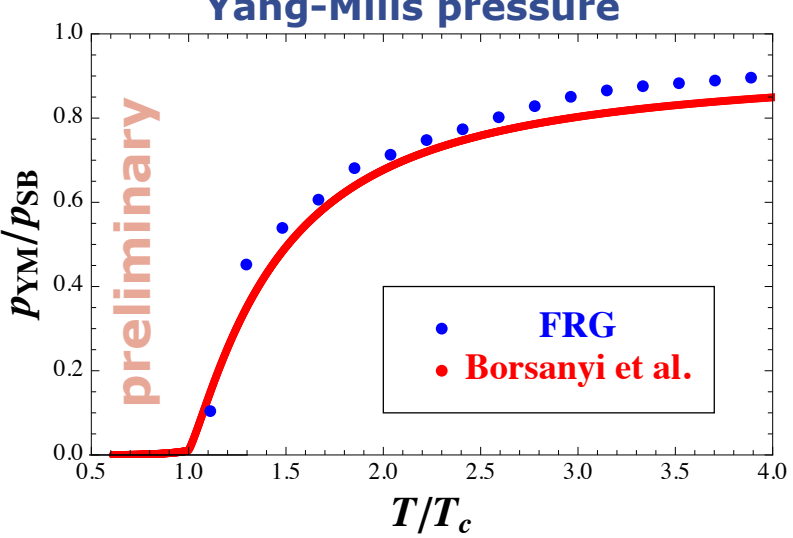
2+1 flavor QCD - enhanced PQM-model

Kurtosis: Fu, JMP, in preparation

Interaction measure



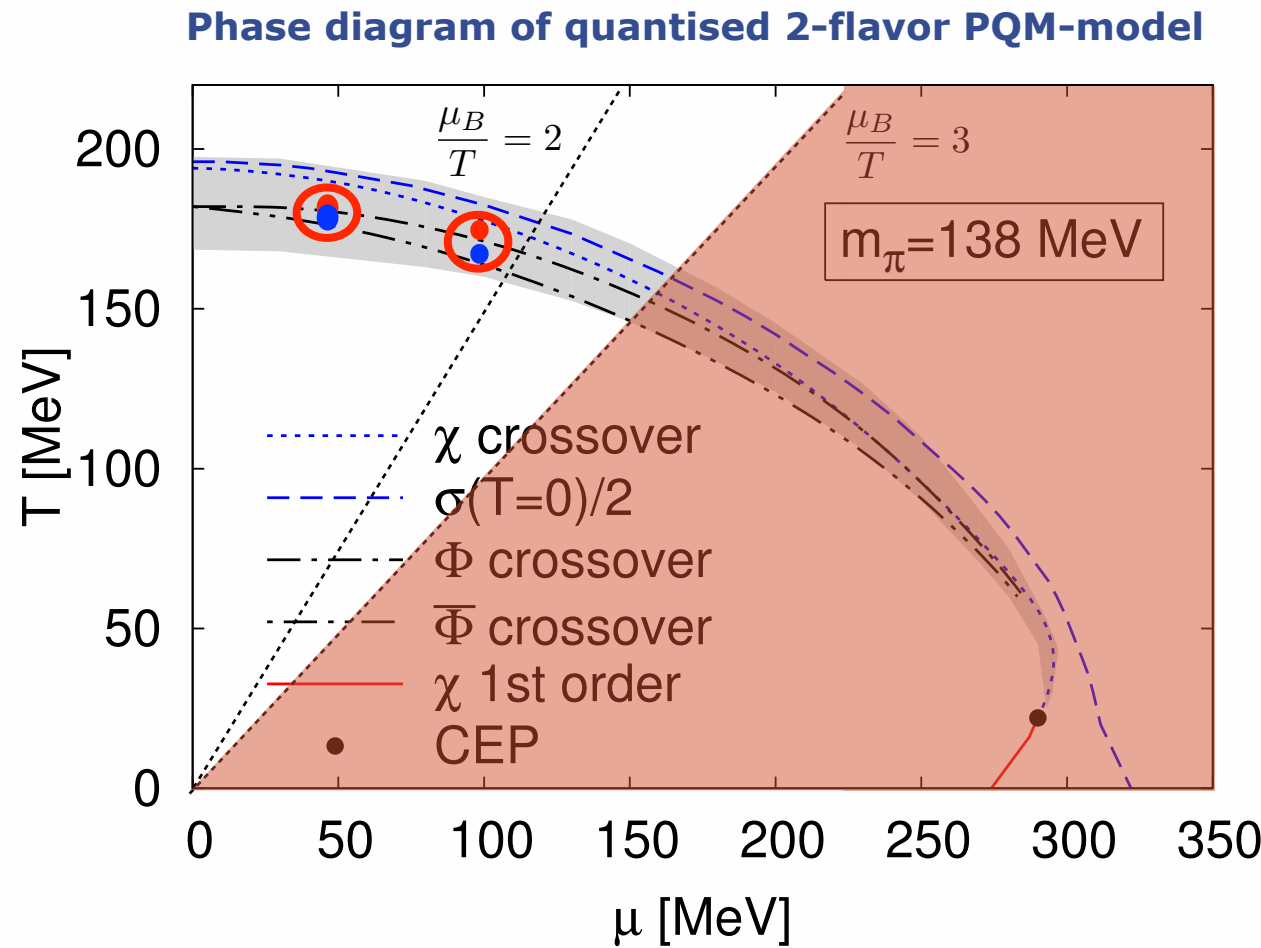
Shaded area:
systematic error estimate
due to low initial UV scale 1 GeV



Fister, JMP '11

Herbst, Mitter et al, PLB 731 (2014) 248-256

Phase structure at finite density



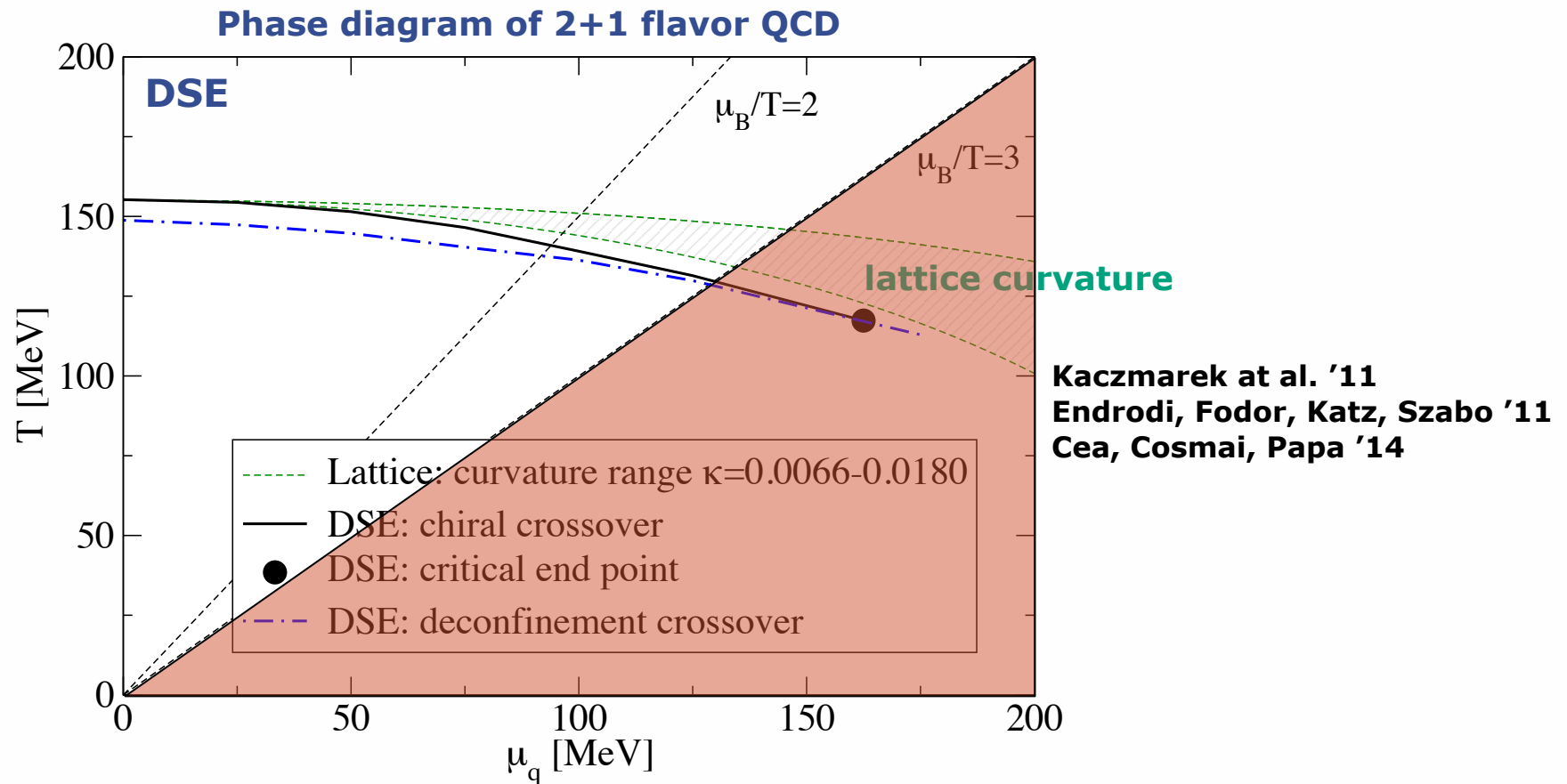
Herbst, JMP, Schaefer, PLB 696 (2011) 58-67
PRD 88 (2013) 1, 014007



FRG QCD results at finite density

Haas, Braun, JMP '09, unpublished

Phase structure at finite density

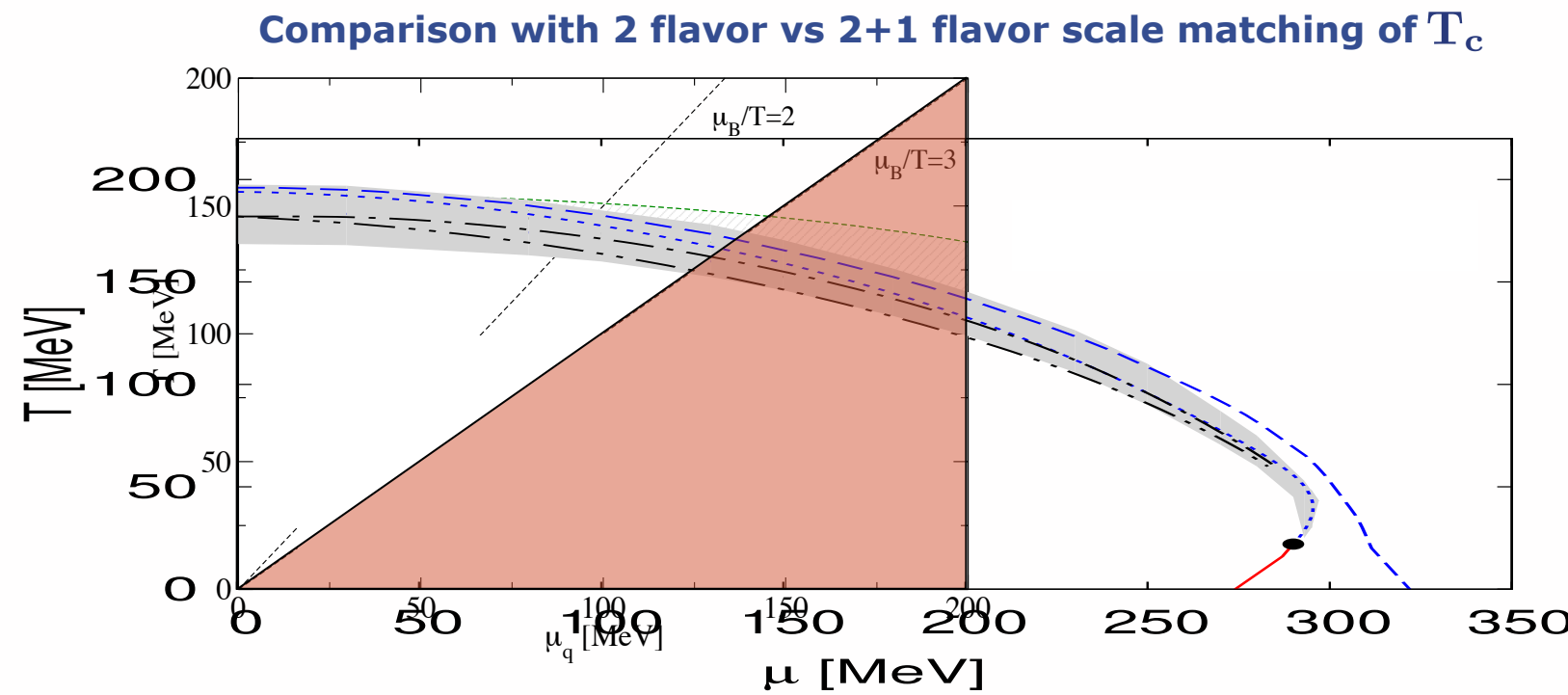
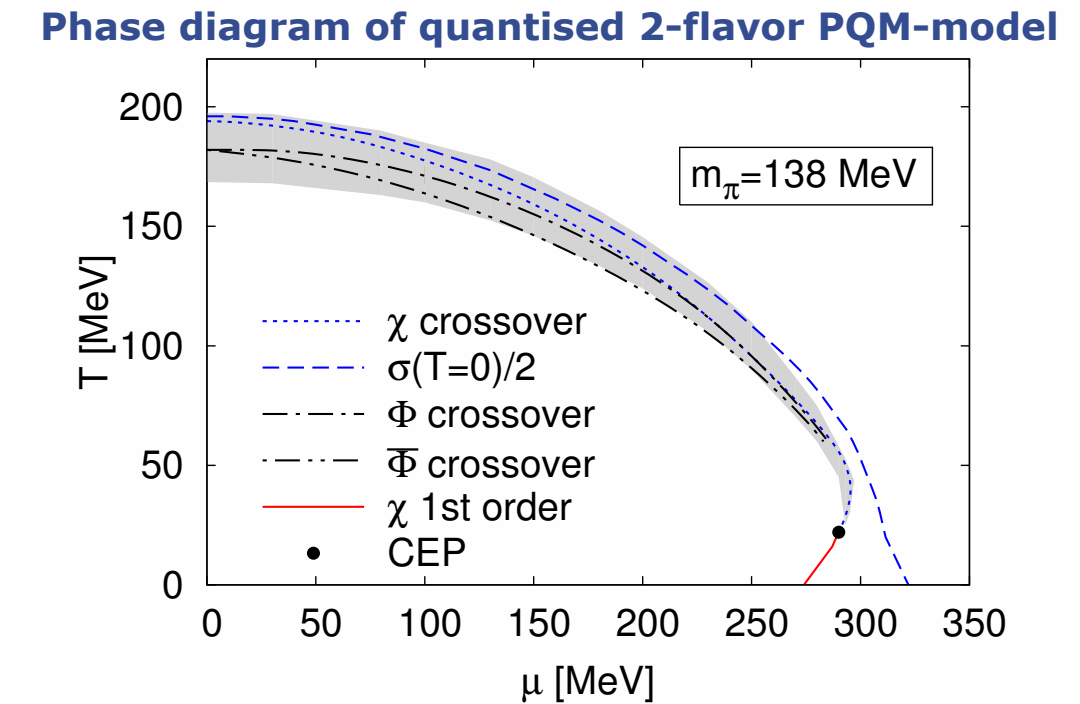
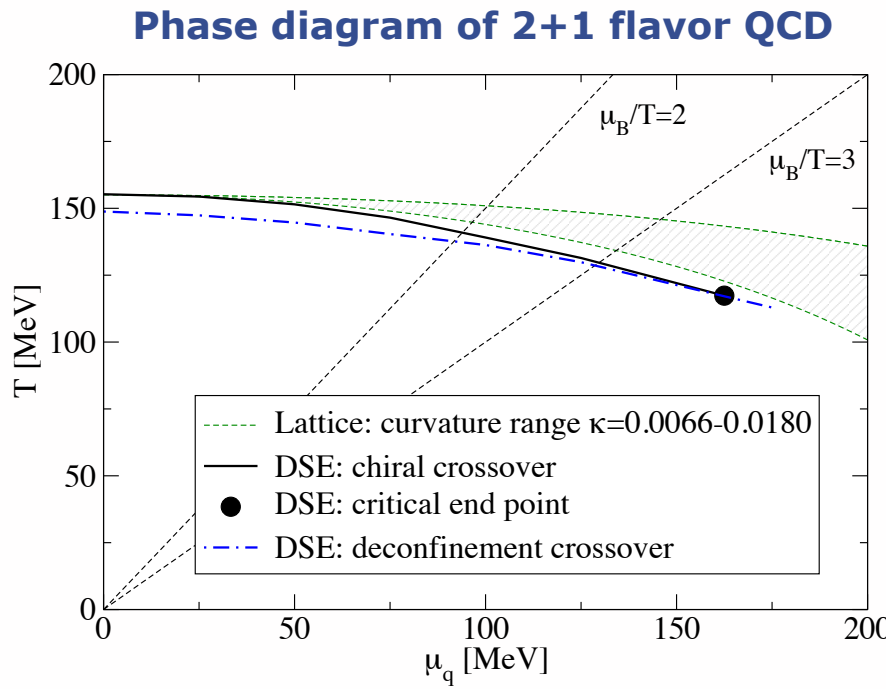


Fischer, Fister, Luecker, JMP, PLB732 (2014) 248
 Fischer, Luecker, Welzbacher, PRD 90 (2014) 034022

$$\frac{\delta(\Gamma - S)}{\delta A_0} = \frac{1}{2} \text{ (loop diagram)} - \text{ (loop diagram)} - \text{ (loop diagram)} - \frac{1}{6} \text{ (loop diagram)} + \text{ (loop diagram)}$$

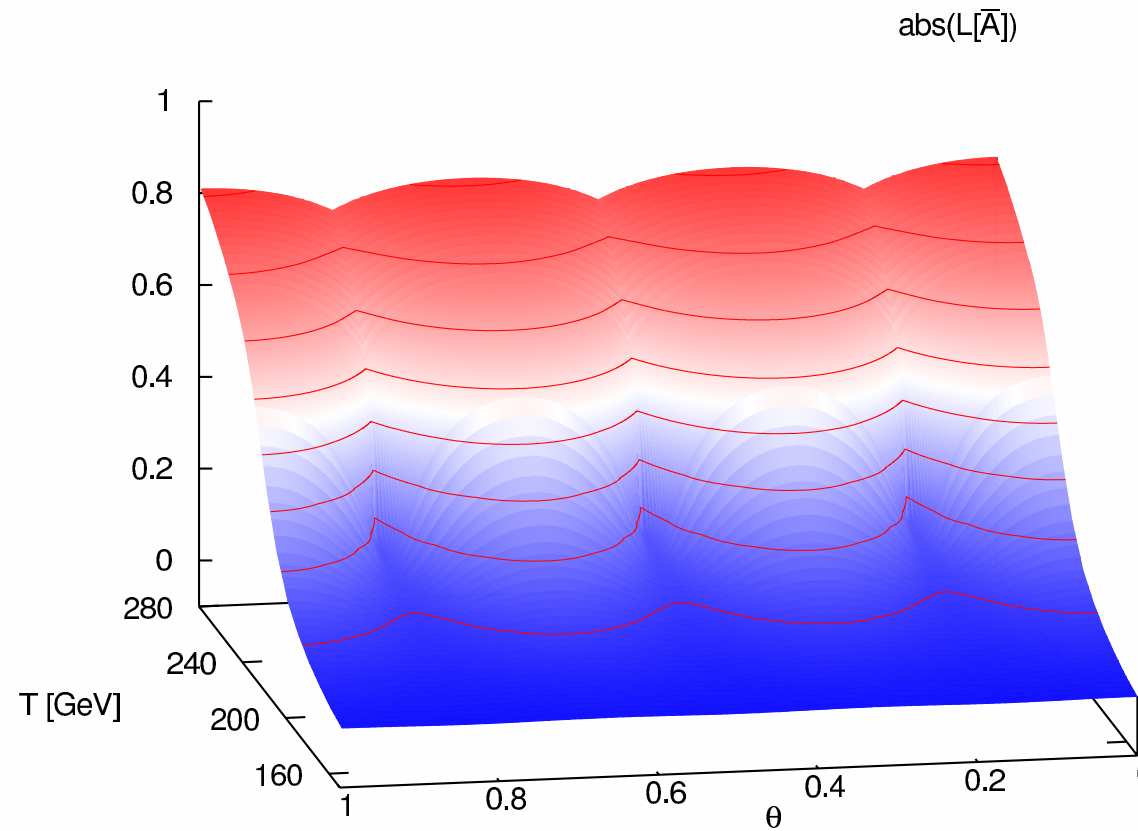
Fister, JMP, PRD 88 (2013) 045010

Phase structure at finite density

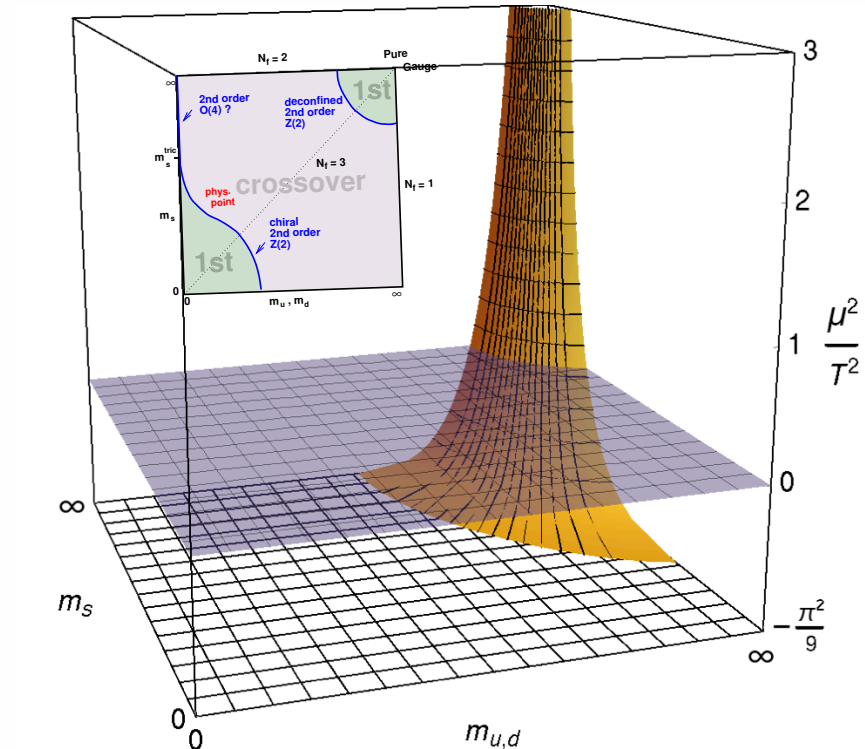


Phase structure at finite density for heavy quarks

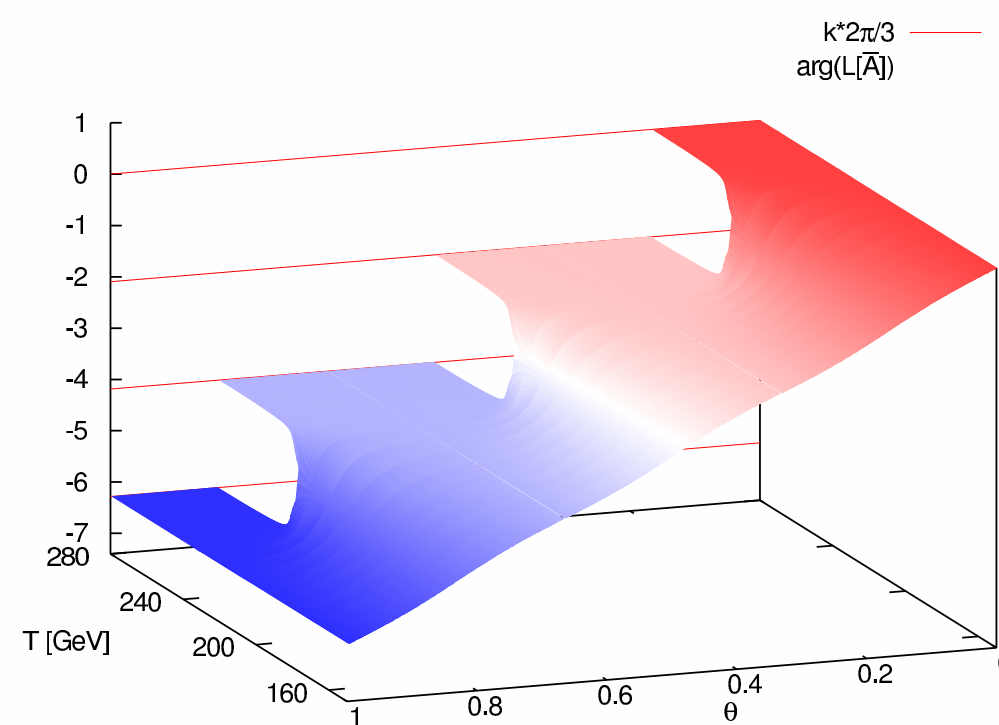
Polyakov loop at finite density



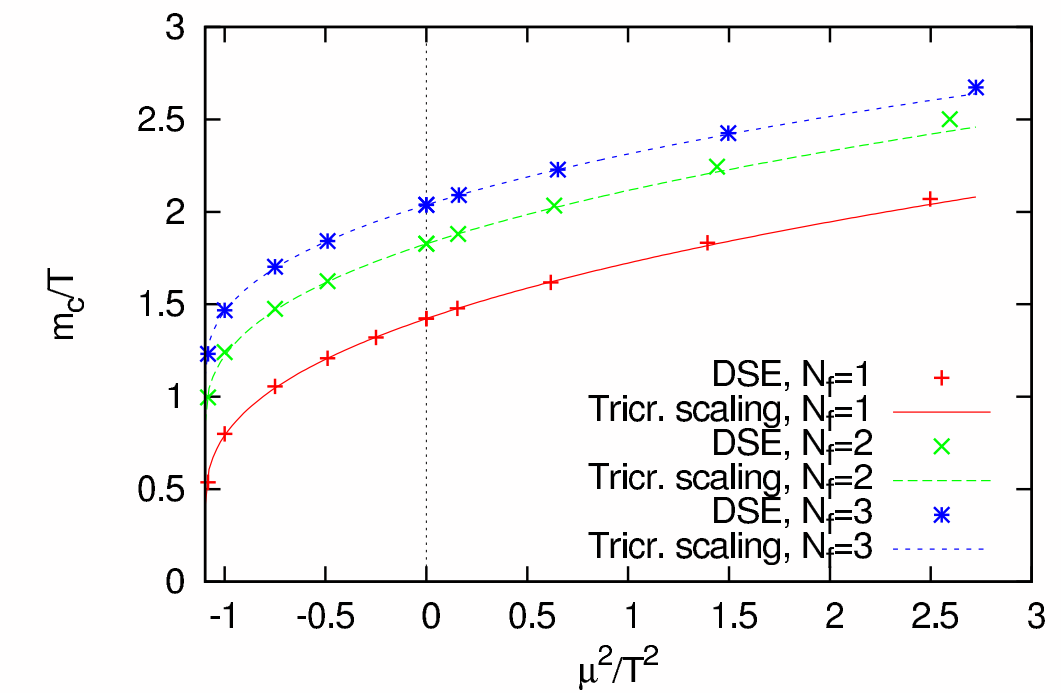
Critical surface at large masses



$k^* 2\pi/3$ —————
 $\arg(L[\bar{A}])$



Tricritical scaling



Outline

- **Vacuum QCD & the hadron spectrum**

- **Phase structure of QCD**

- **Spectral Functions & Transport Coefficients**

Part II

- **Outlook**

... and now for something completely different ...

Gauge dynamics far from equilibrium

Gasenzer, McLerran, JMP, Sexty, Nucl.Phys. A930 (2014) 163

see also talks of J. Berges, A. Dumitru, S. Schlichting

Abelian Higgs model in 2+1 dimensions

Classical action:

$$S[A_\mu, \phi] = - \int_x \left[\frac{1}{4} F_{\mu\nu} F^{\mu\nu} + (D_\mu \phi)^* D^\mu \phi + V(\phi) \right]$$

ϕ **Higgs**

phase
$$\frac{\phi}{|\phi|} = e^{i\varphi}$$

Abelian Higgs model in 2+1 dimensions

Classical action:

$$S[A_\mu, \phi] = - \int_x \left[\frac{1}{4} F_{\mu\nu} F^{\mu\nu} + (D_\mu \phi)^* D^\mu \phi + V(\phi) \right]$$

ϕ **Higgs**

phase
$$\frac{\phi}{|\phi|} = e^{i\varphi}$$

Classical action of Yang-Mills theory in diagonalisation gauges:

$$S_{\text{YM}} \simeq \frac{1}{2} \int_x \text{tr} F_{\bar{\mu}\bar{\nu}}^2 + \frac{1}{2} \int_x \text{tr} (D_{\bar{\mu}} A_2)^2$$

$$A_2 = A_2^c(x_0, x_1)$$

Wilson loop

$$\mathcal{W}_2 = \mathcal{P} \exp \left\{ i \int_0^{L_2} dx_2 A_2(x) \right\} = \exp \{ i \phi \}$$

Vortex winding

$$n(\mathcal{S}) = \frac{1}{16\pi i} \oint_{\mathcal{S}} d^2x \epsilon_{ij} \text{tr} \hat{\phi} \partial_i \hat{\phi} \partial_j \hat{\phi}$$

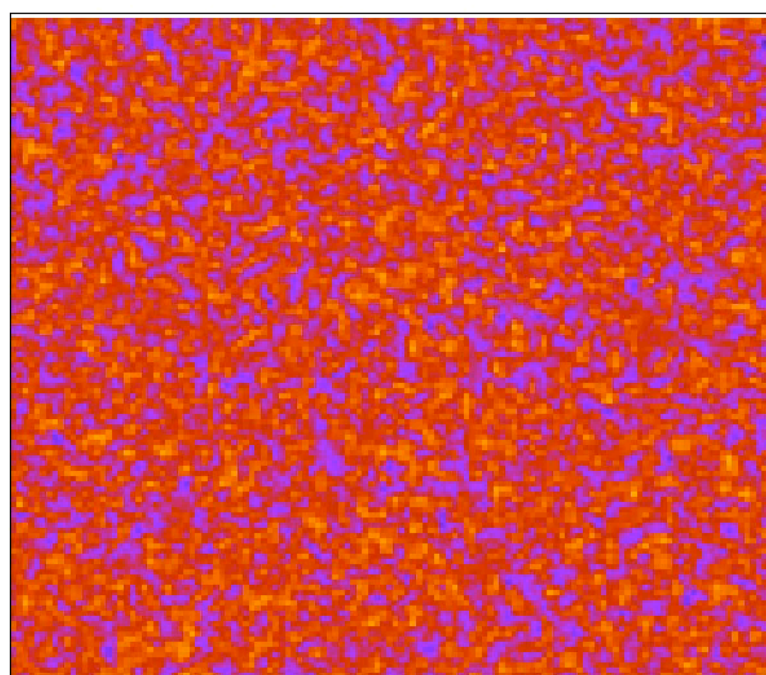
phase

$$\hat{\phi} = \frac{\phi}{\|\phi\|}$$

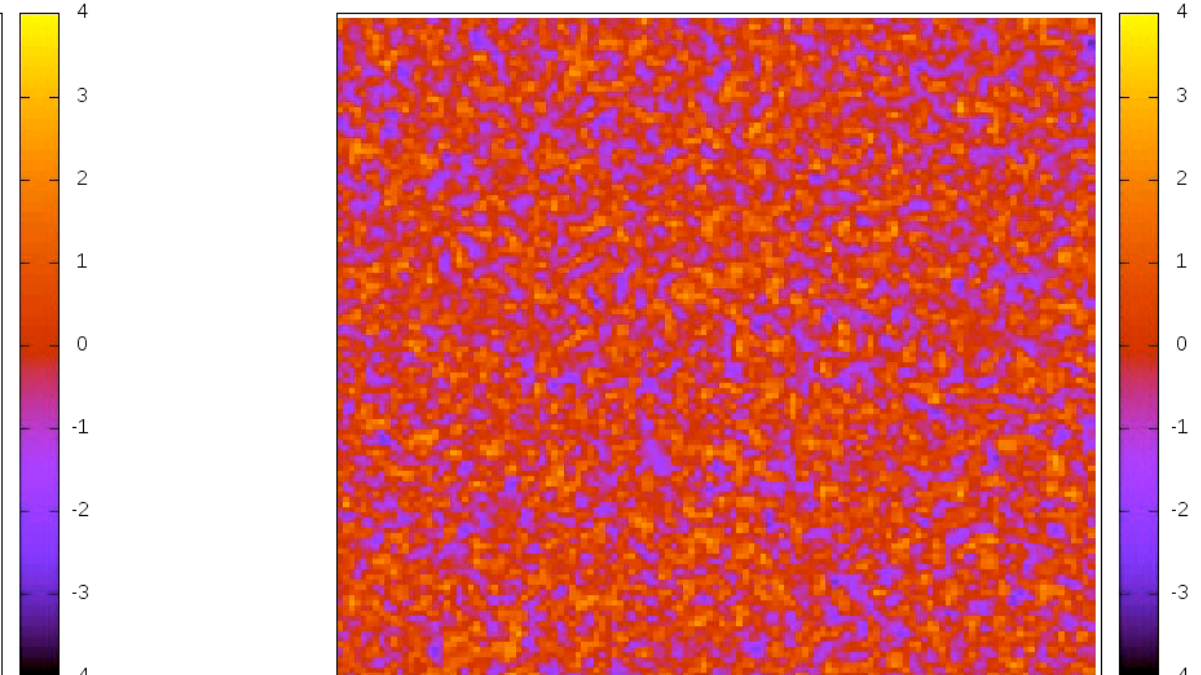
Quiz

Complex scalar vs Abelian Higgs

phase φ of scalar field



$mt=000000$



$mt=000000$

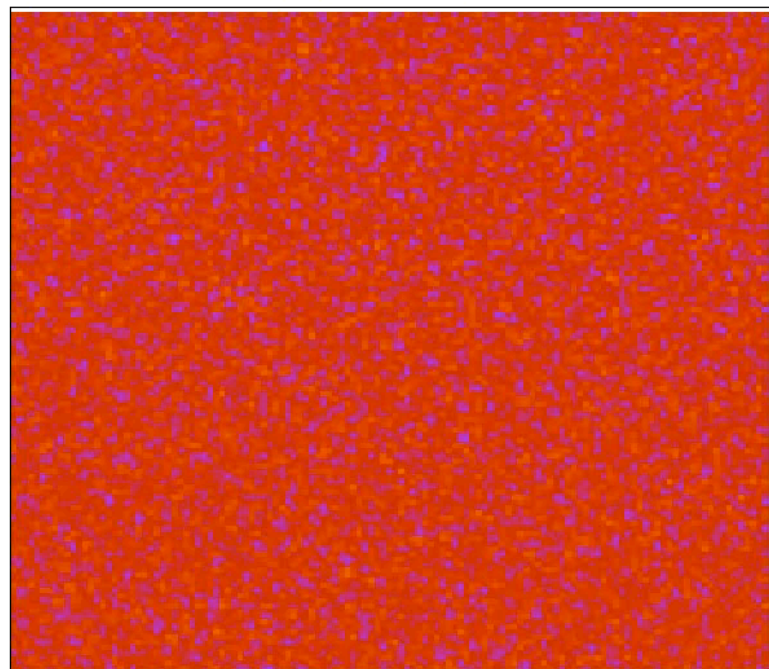
'tachyonic' initial conditions

classical statistical lattice simulations

Which is which?

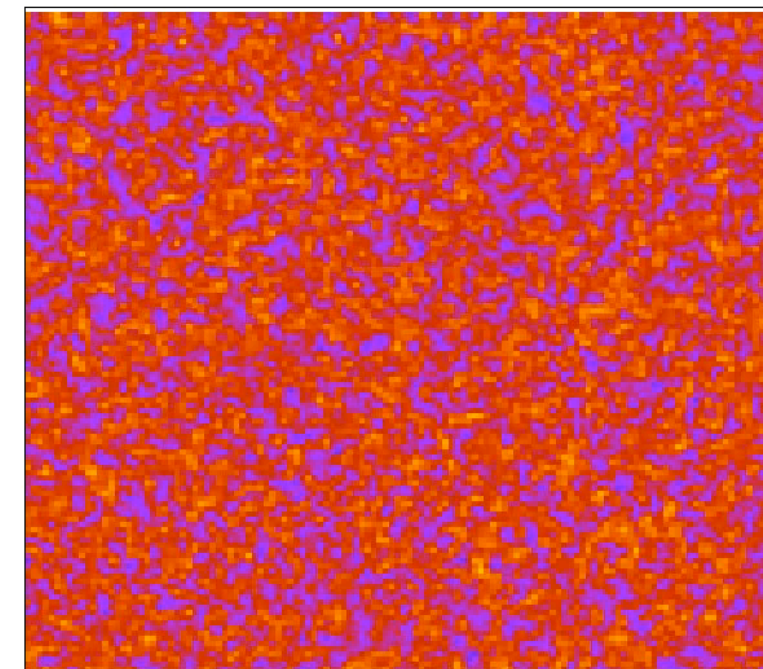
Vortex dynamics

magnetic field



mt=000000

phase of Higgs



mt=000000

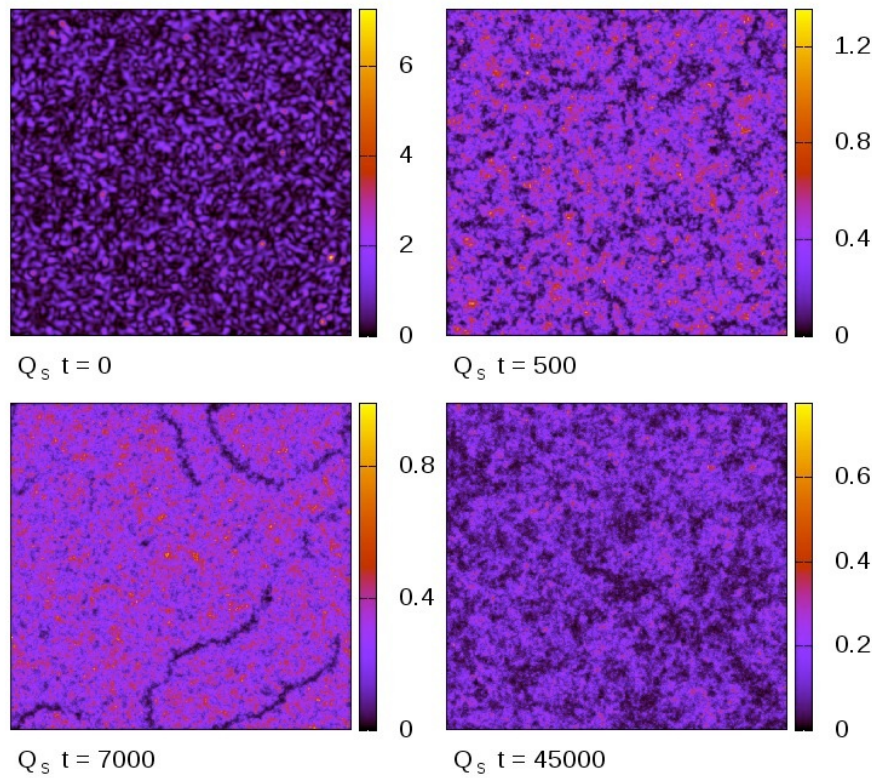
'tachyonic' initial conditions

classical statistical lattice simulations

Charge

'overpopulation' initial conditions

modulus of Higgs

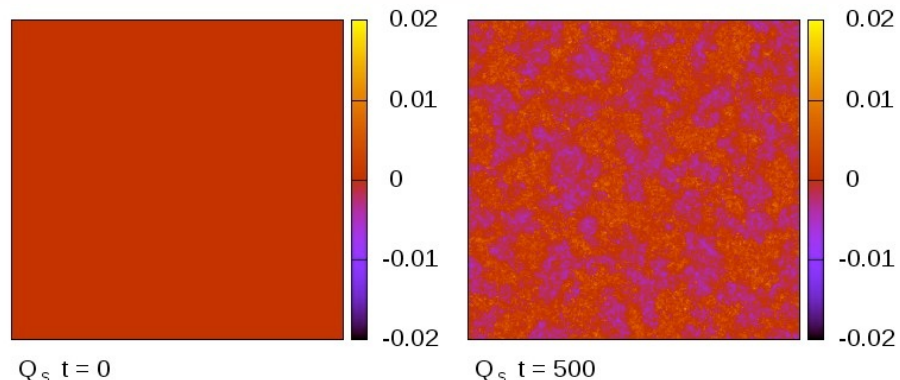
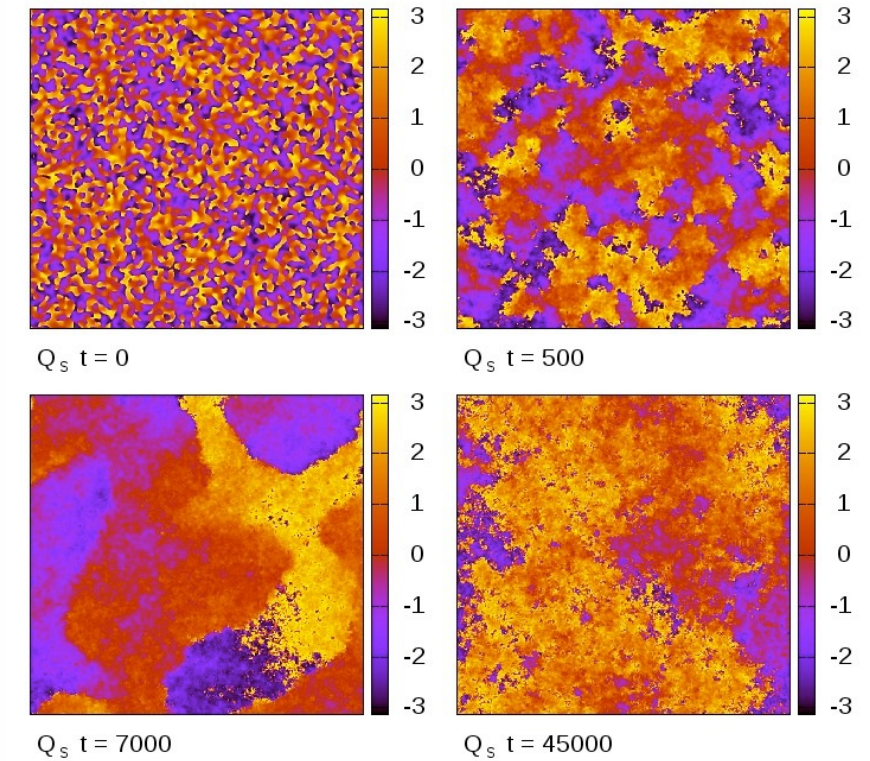


$$\xi = 0.025$$

coupling

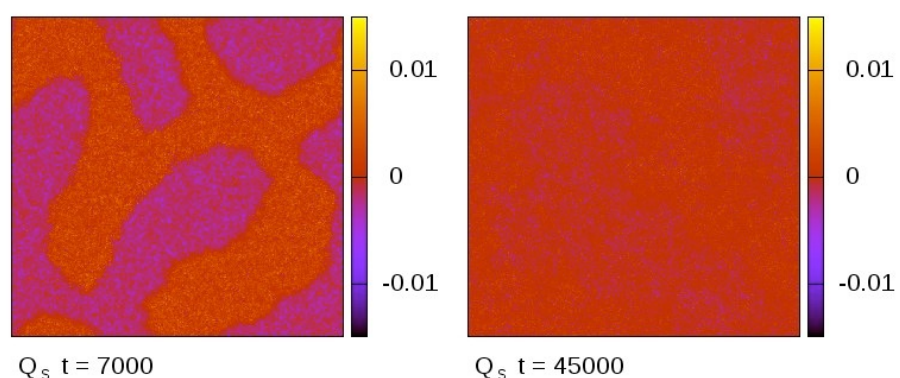
$$\xi = \frac{6e^2}{\lambda}$$

relative phase



$$\varphi^U(\vec{x}, t) = \arg(G^U(\vec{0}, \vec{x}, t))$$

relative phase



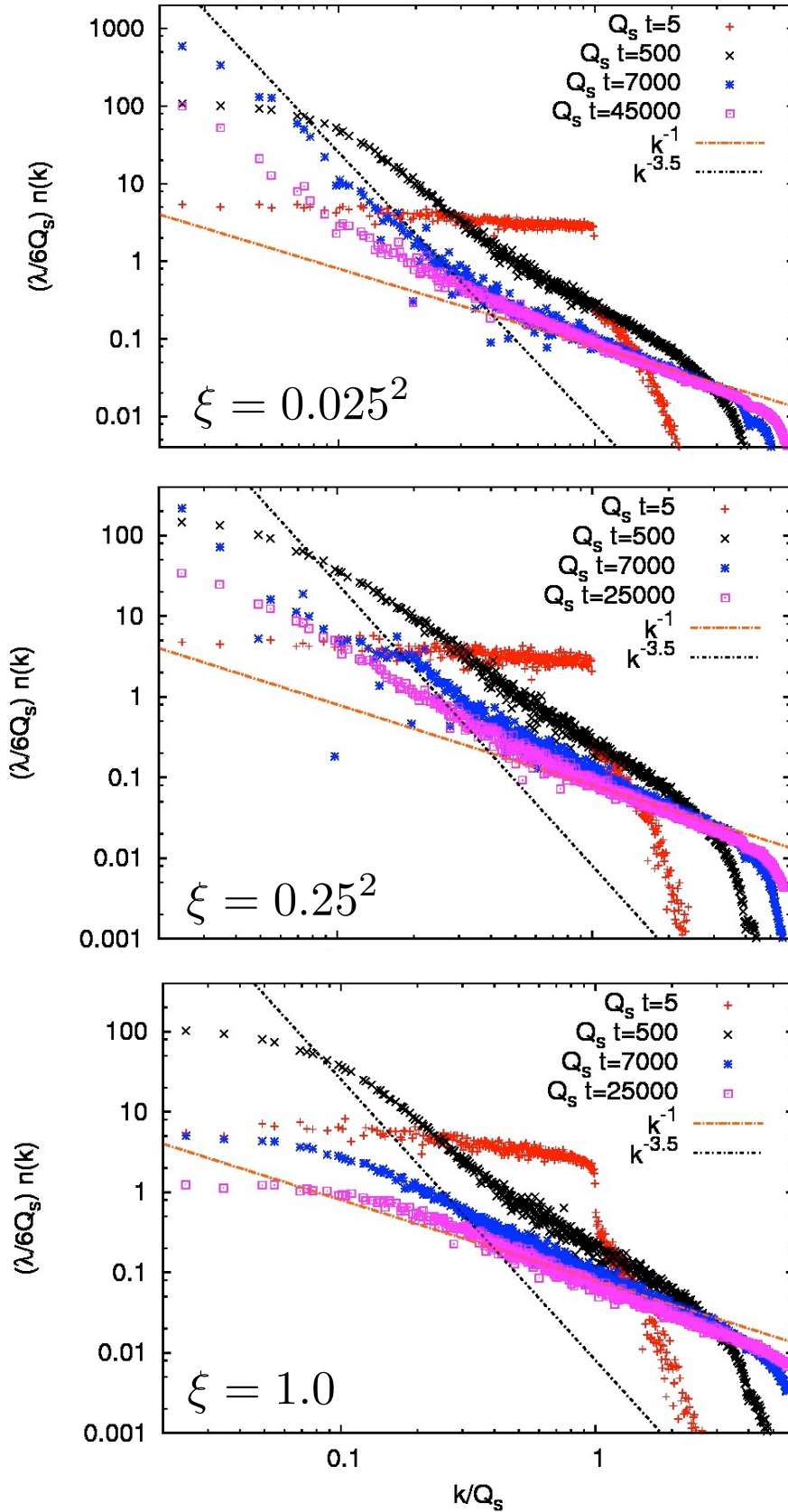
charge

$$G^U(\vec{x}, \vec{y}, t) = \langle \phi(\vec{x}, t) U(\vec{x}, \vec{y}, t) \phi(\vec{y}, t)^* \rangle_{\text{cl}}$$

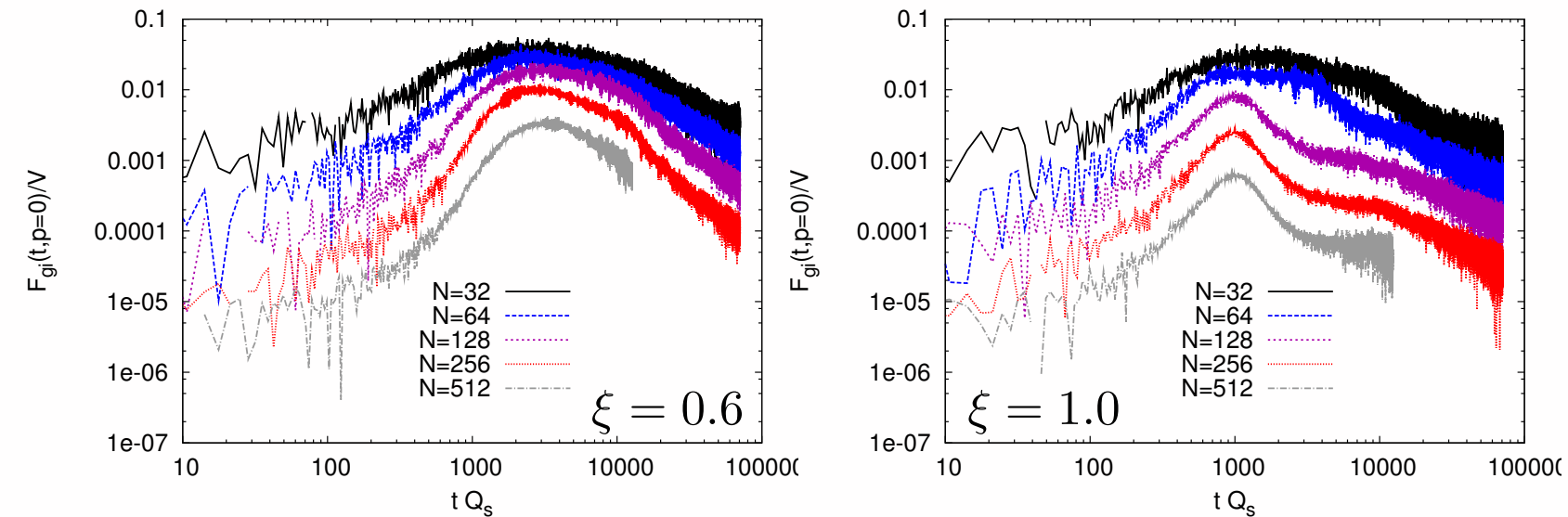
parallel transport U

Occupation number & 'condensate'

'overpopulation' initial conditions

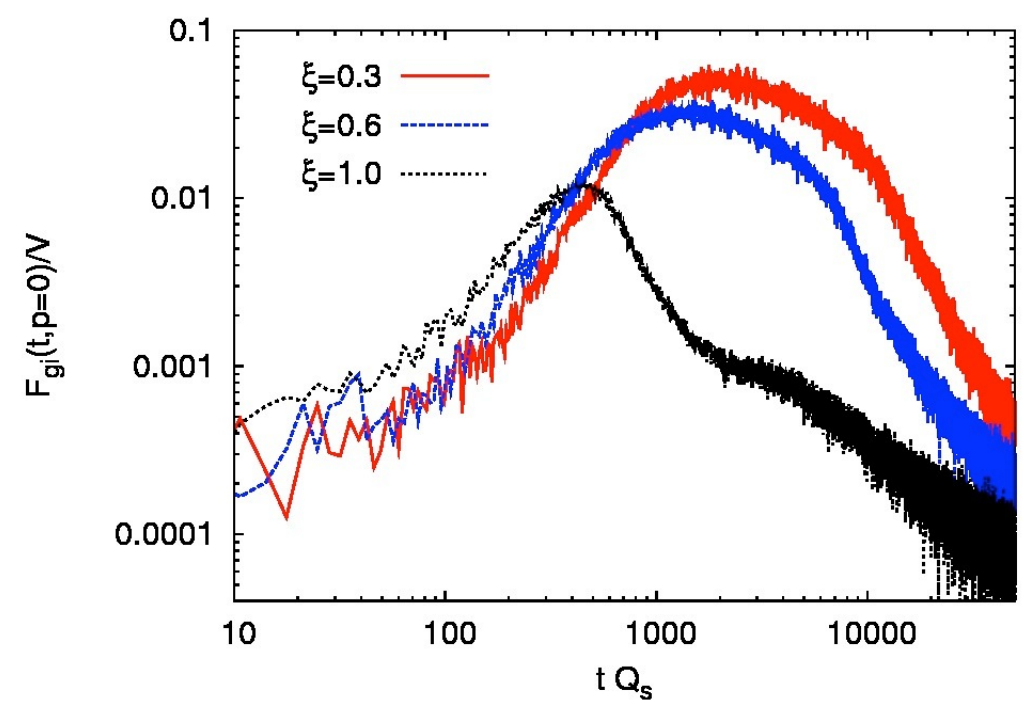


$$\frac{F_{gi}(p=0)}{V} = \frac{1}{V^2} \int dx dy \phi^*(x) U(x, y) \phi(y)$$



coupling

$$\xi = \frac{6e^2}{\lambda}$$

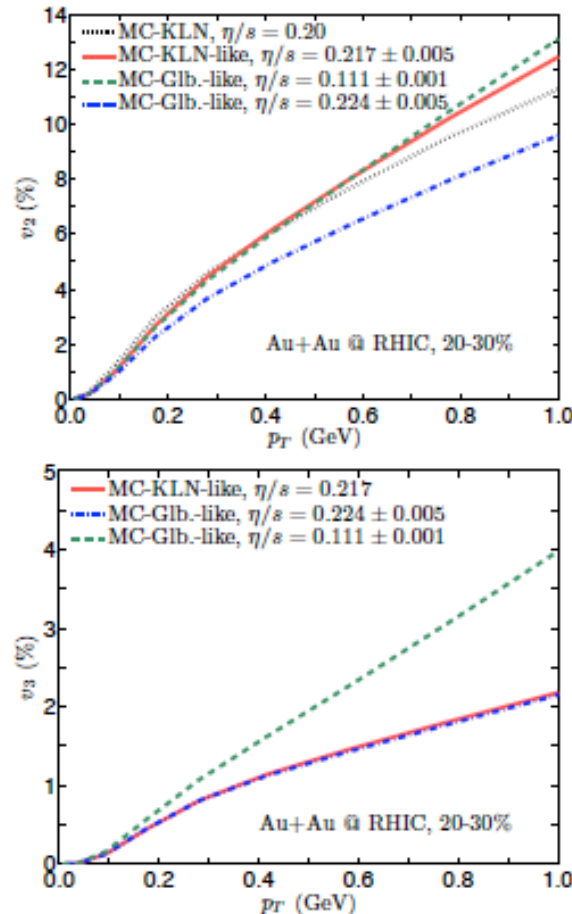


Dynamics

Shooting the elephant

Proof of principle calculation:

Zhi Qiu and U. Heinz, to be published



- Take ensemble of sum of deformed Gaussian profiles,
 $s(\mathbf{r}_\perp) = s_2(\mathbf{r}_\perp; \tilde{\epsilon}_2, \psi_2) + s_3(\mathbf{r}_\perp; \tilde{\epsilon}_3, \psi_3)$, with
 1. equal Gaussian radii $R_2^2 = R_3^2 = 8 \text{ fm}^2$ to reproduce $\langle r_\perp^2 \rangle$ of MC-KLN source for 20-30% AuAu
 2. $\tilde{\epsilon}_2$ and $\tilde{\epsilon}_3$ adjusted such that
 - $\bar{\epsilon}_{2,3} = \langle \epsilon_{2,3} \rangle_{\text{KLN}}^{20-30\%}$ ("MC-KLN-like")
 - $\bar{\epsilon}_{2,3} = \langle \epsilon_{2,3} \rangle_{\text{GI}}^{20-30\%}$ ("MC-Glauber-like")
 3. $\psi_2 = 0$, ψ_3 (direction of triangularity) distributed randomly
- Use $v_2^\pi(p_T)$ from VISH2+1 for $\eta/s = 0.20$ with MC-KLN initial conditions for 20-30% AuAu as "mock data"
- Fit mock $v_2^\pi(p_T)$ data with VISH2+1 for "MC-Glauber-like" or "MC-KLN-like" Gaussian initial conditions with both elliptic and triangular deformations by adjusting η/s
 $\Rightarrow (\eta/s)_{\text{KLN}} = 0.217 \pm 0.005$ for "MC-KLN-like",
 $(\eta/s)_{\text{GI}} = 0.111 \pm 0.001$ for "MC-Glauber-like"
- Compute $v_3^\pi(p_T)$ for "MC-KLN-like" fit with $(\eta/s)_{\text{GI}} = 0.217$ and reproduce it with "MC-Glauber-like" initial condition by readjusting η/s
 $\Rightarrow (\eta/s)_{\text{GI}}^{v_3} = 0.224 \pm 0.005$ for "MC-Glauber-like"
- Compute $v_2^\pi(p_T)$ for "MC-Glauber-like" initial profiles with readjusted $(\eta/s)_{\text{GI}}^{v_3} = 0.224$ and compare with "MC-Glauber-like" fit to original mock data \Rightarrow clearly visible (and measurable) difference!

This exercise proves: (i) Fitting $v_3(p_T)$ data with MC-Glauber and MC-KLN initial conditions yields the same η/s (within narrow error band); (ii) The corresponding $v_2(p_T)$ fits are quite different, and only one (more precisely: at most one!) of the models will fit the corresponding $v_2(p_T)$ data.

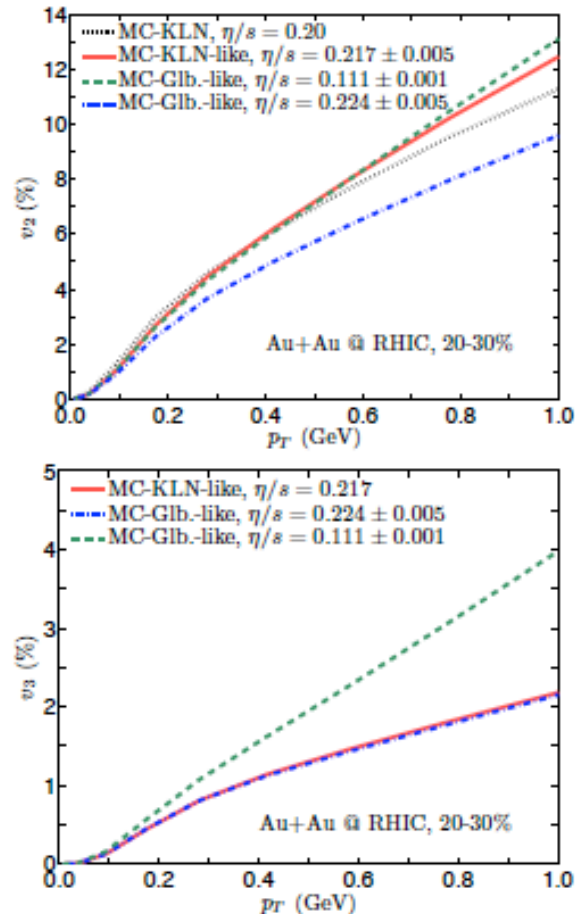
U. Heinz, talk at RETUNE '12

Dynamics

Computing the elephant

Proof of principle calculation:

Zhi Qiu and U. Heinz, to be published



- Take ensemble of sum of deformed Gaussian profiles,
 $s(\mathbf{r}_\perp) = s_2(\mathbf{r}_\perp; \tilde{\epsilon}_2, \psi_2) + s_3(\mathbf{r}_\perp; \tilde{\epsilon}_3, \psi_3)$, with
 - equal Gaussian radii $R_2^2 = R_3^2 = 8 \text{ fm}^2$ to reproduce $\langle r_\perp^2 \rangle$ of MC-KLN source for 20-30% AuAu
 - $\tilde{\epsilon}_2$ and $\tilde{\epsilon}_3$ adjusted such that
 - $\bar{\epsilon}_{2,3} = \langle \epsilon_{2,3} \rangle_{\text{KLN}}^{20-30\%}$ ("MC-KLN-like")
 - $\bar{\epsilon}_{2,3} = \langle \epsilon_{2,3} \rangle_{\text{GI}}^{20-30\%}$ ("MC-Glauber-like")
 - $\psi_2 = 0$, ψ_3 (direction of triangularity) distributed randomly
- Use $v_2^\pi(p_T)$ from VISH2+1 for $\eta/s = 0.20$ with MC-KLN initial conditions for 20-30% AuAu as "mock data"
- Fit mock $v_2^\pi(p_T)$ data with VISH2+1 for "MC-Glauber-like" or "MC-KLN-like" Gaussian initial conditions with both elliptic and triangular deformations by adjusting η/s
 $\Rightarrow (\eta/s)_{\text{KLN}} = 0.217 \pm 0.005$ for "MC-KLN-like",
 $(\eta/s)_{\text{GI}} = 0.111 \pm 0.001$ for "MC-Glauber-like"
- Compute $v_3^\pi(p_T)$ for "MC-KLN-like" fit with $(\eta/s)_{\text{GI}} = 0.217$ and reproduce it with "MC-Glauber-like" initial condition by readjusting η/s
 $\Rightarrow (\eta/s)_{\text{GI}}^{v_3} = 0.224 \pm 0.005$ for "MC-Glauber-like"
- Compute $v_2^\pi(p_T)$ for "MC-Glauber-like" initial profiles with readjusted $(\eta/s)_{\text{GI}}^{v_3} = 0.224$ and compare with "MC-Glauber-like" fit to original mock data
 \Rightarrow clearly visible (and measurable) difference!

This exercise proves: (i) Fitting $v_3(p_T)$ data with MC-Glauber and MC-KLN initial conditions yields the same η/s (within narrow error band); (ii) The corresponding $v_2(p_T)$ fits are quite different, and only one (more precisely: at most one!) of the models will fit the corresponding $v_2(p_T)$ data.

computing transport coefficients

Correlations of the energy-momentum tensor

Flow

$$\partial_t \text{---} \square = -\frac{1}{2} \text{---} \square + \text{---} \square + \text{---} \square - \frac{1}{2} \text{---} \square$$

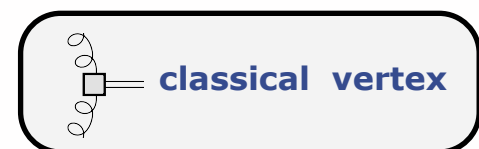
$\rho_{\pi\pi}$



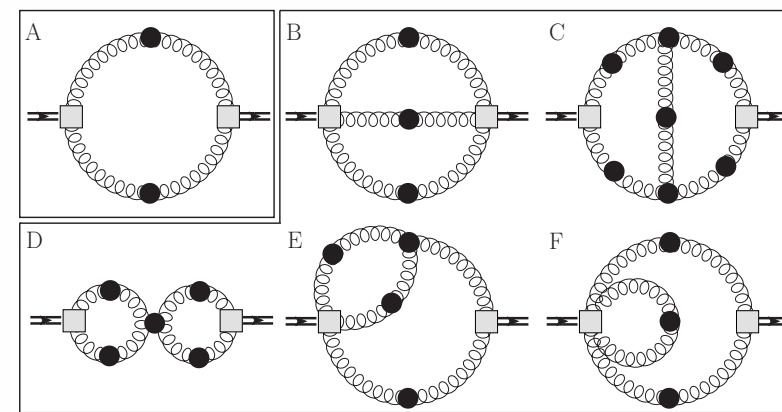
Diagrammatic representation

$$\rho_{\pi\pi} = \text{---} \square + \text{---} \square + \text{---} \square + \dots$$

closed form



Complete 2-loop corrections



Haas, Fister, JMP, PRD 90 (2014) 9, 091501

Christiansen, Haas, JMP, Strodthoff, arXiv:1411.7986

Correlations of the energy-momentum tensor

Flow

$$\partial_t \square = -\frac{1}{2} \square + \square + \square - \frac{1}{2} \square$$



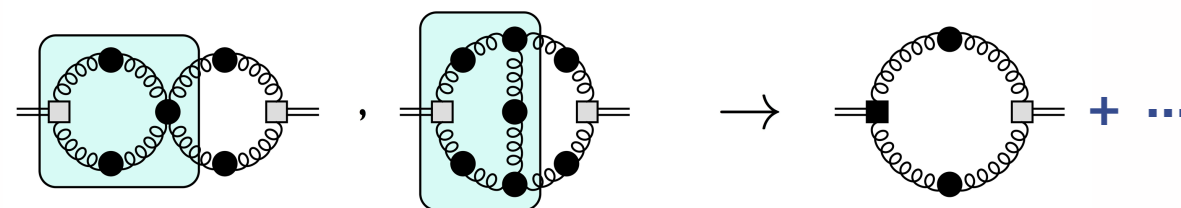
Diagrammatic representation

$$\rho_{\pi\pi} = \square + \square + \square + \dots$$

closed form



Vertex corrections



Haas, Fister, JMP, PRD 90 (2014) 9, 091501

Christiansen, Haas, JMP, Strodthoff, arXiv:1411.7986

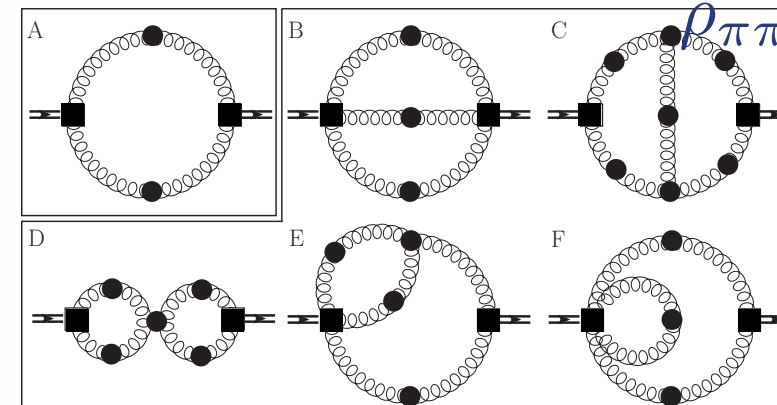
Correlations of the energy-momentum tensor

Flow

$$\partial_t \text{[square]} = -\frac{1}{2} \text{[loop with cross]} + \text{[loop with cross]} + \text{[loop with cross]} - \frac{1}{2} \text{[loop with cross]}$$

Current approximation

$$\rho_{\pi\pi} =$$



with optimised RG-scheme from
Haas, Fister, JMP 'Phys.Rev. D88 (2013) 045010

$\rho_{T/L}$ with MEM



full vertex

Haas, Fister, JMP, PRD 90 (2014) 9, 091501

Christiansen, Haas, JMP, Strodthoff, arXiv:1411.7986

Transport coefficients

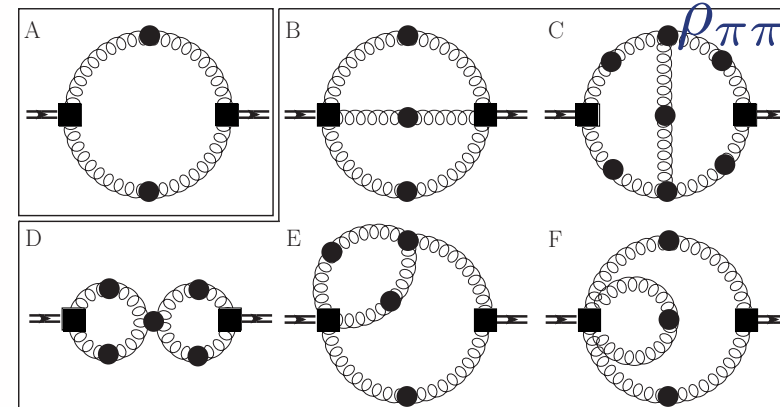
Shear viscosity

$$\eta = \frac{1}{20} \left. \frac{d}{d\omega} \right|_{\omega=0} \rho_{\pi\pi}(\omega, 0)$$

Kubo relation

Current approximation

$$\rho_{\pi\pi} =$$



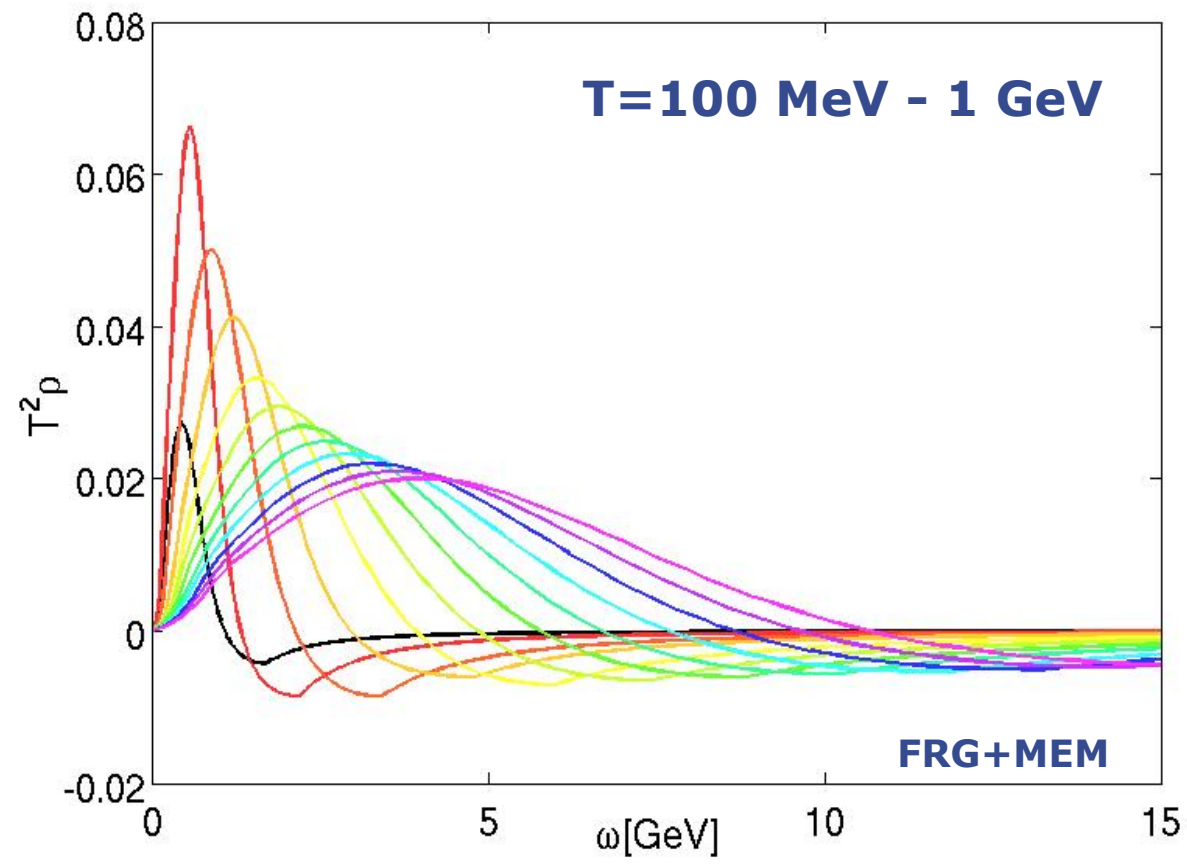
$\rho_{T/L}$ with MEM

$$\rho_{\pi\pi}(p) = \frac{2d_A}{3} \int \frac{d^4 k}{(2\pi)^4} [n(k^0) - n(k^0 + p_0)] (V_{TT}\rho_T(k)\rho_T(k+p) + V_{TL}\rho_T(k)\rho_L(k+p) + V_{LL}\rho_L(k)\rho_L(k+p)) + \dots$$

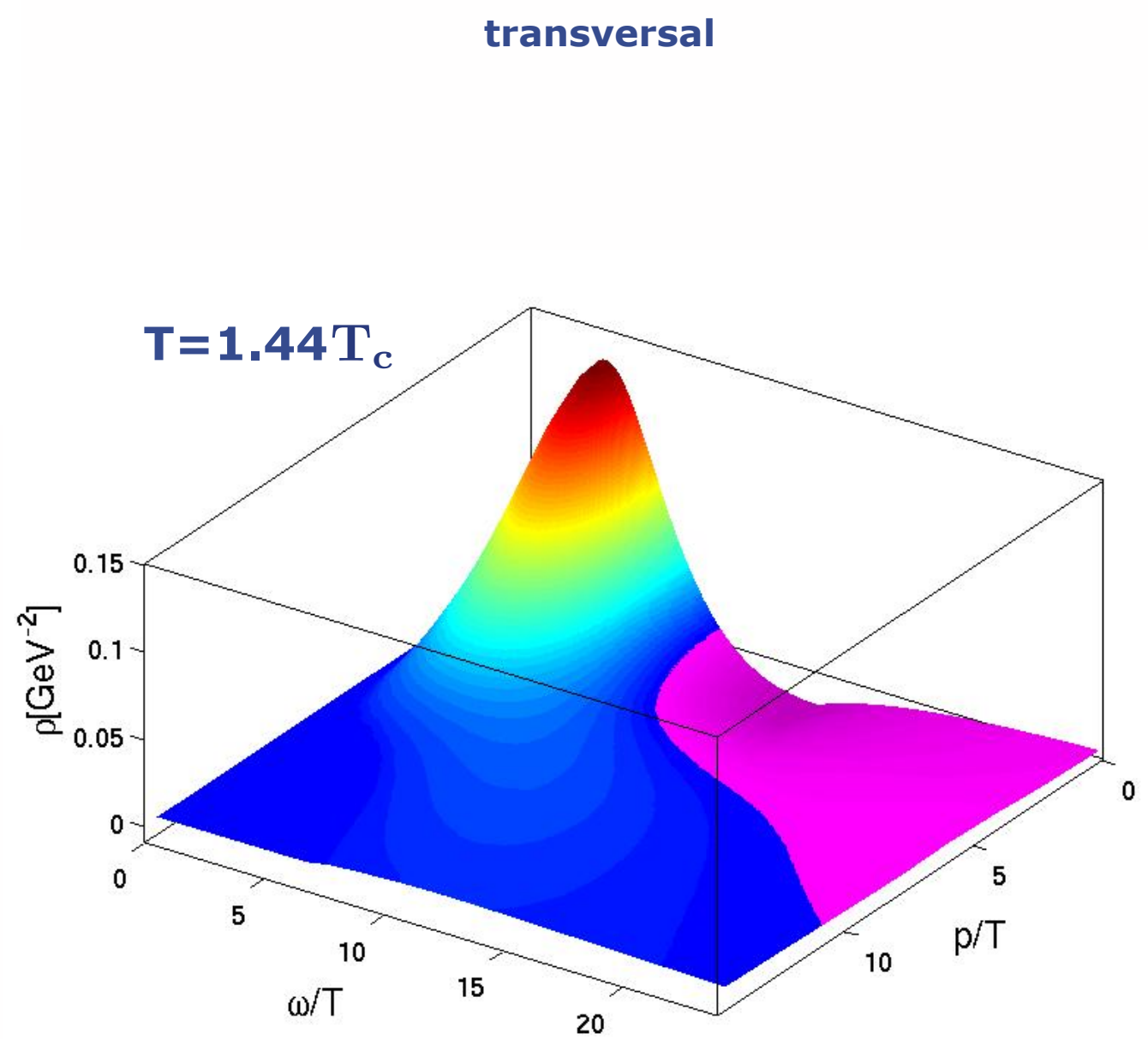
Haas, Fister, JMP, PRD 90 (2014) 9, 091501

Christiansen, Haas, JMP, Strodthoff, arXiv:1411.7986

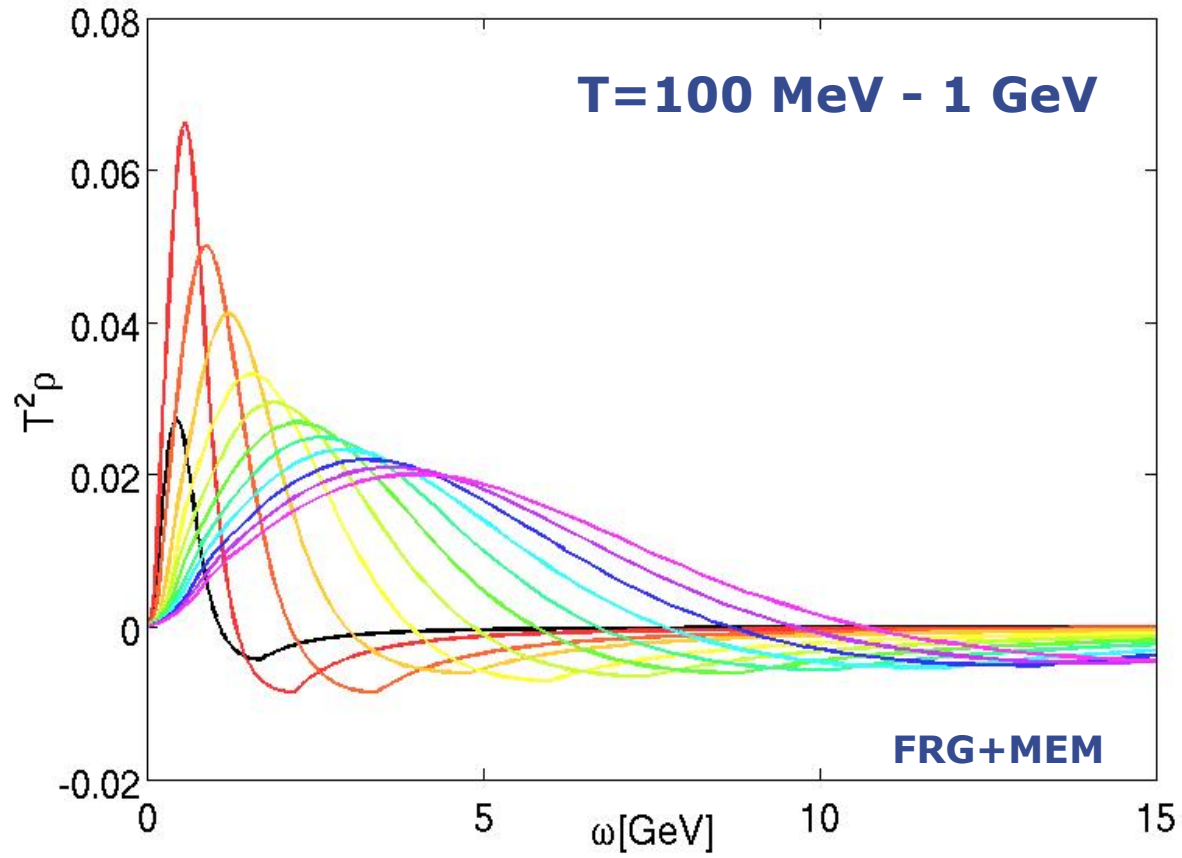
Gluon spectral function at finite T



MEM

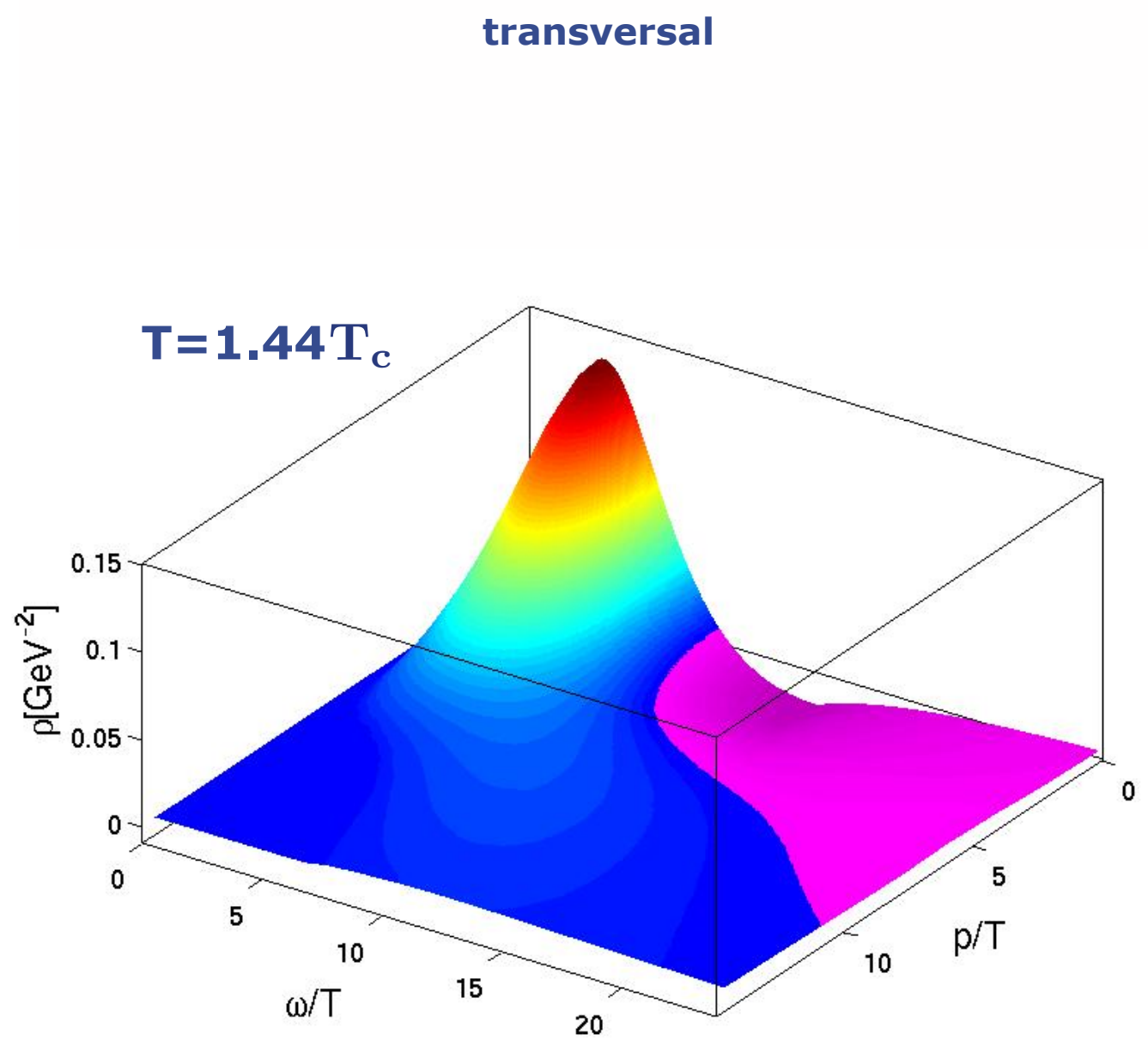


Gluon spectral function at finite T



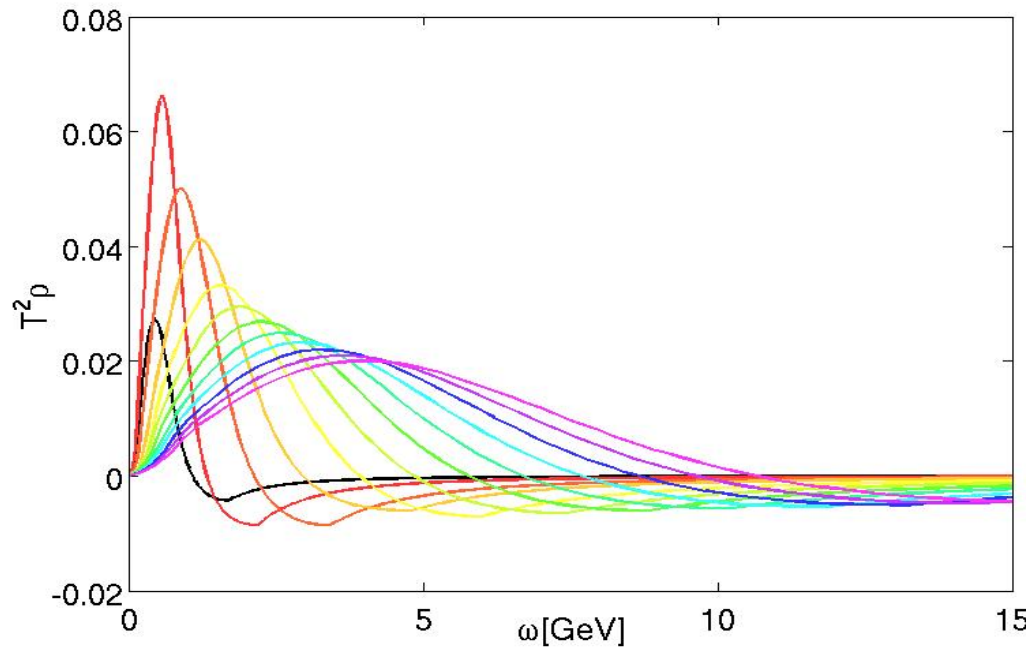
'Those are my methods (principles), and if you don't like them...well, I have others'
direct computation

Groucho Marx

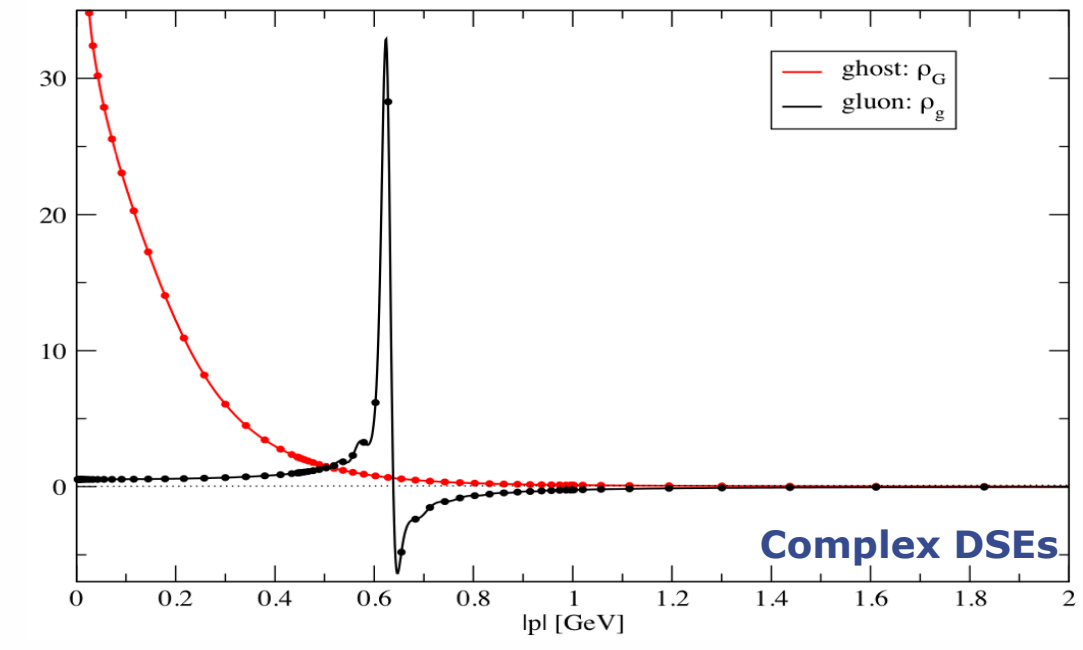


Dynamics

gluon spectral functions

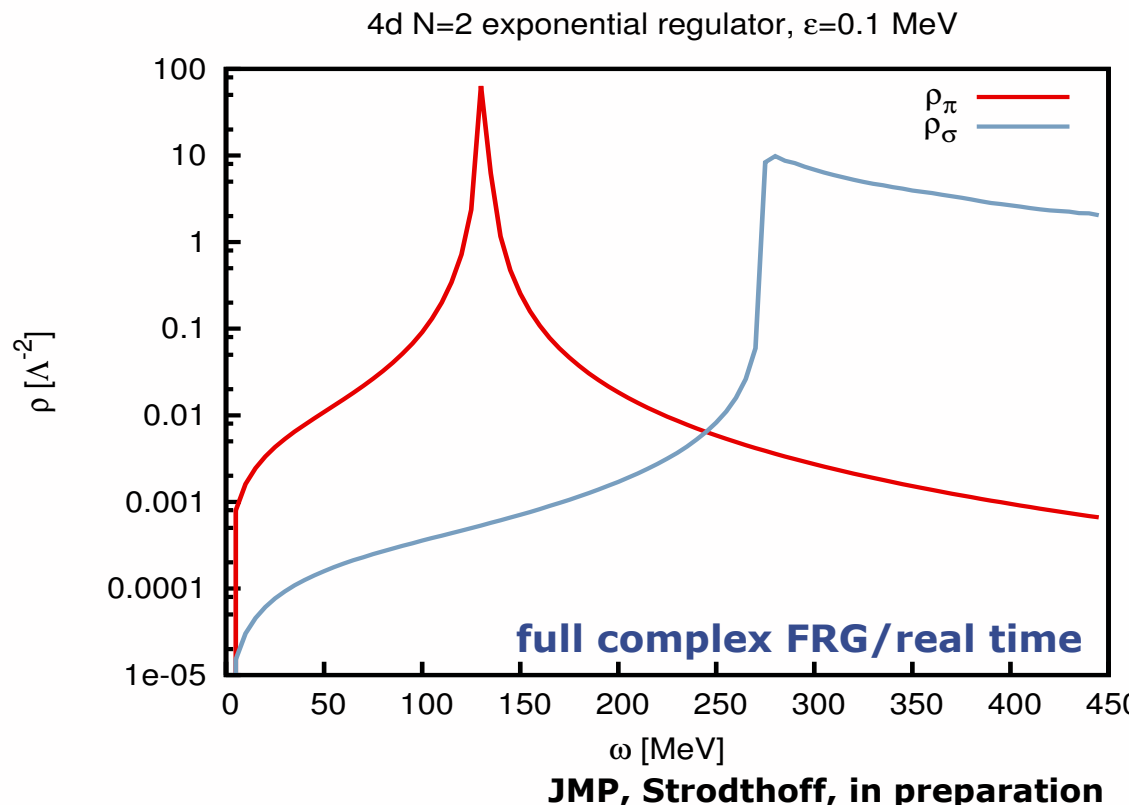


Haas, Fister, JMP, PRD 90 (2014) 9, 091501

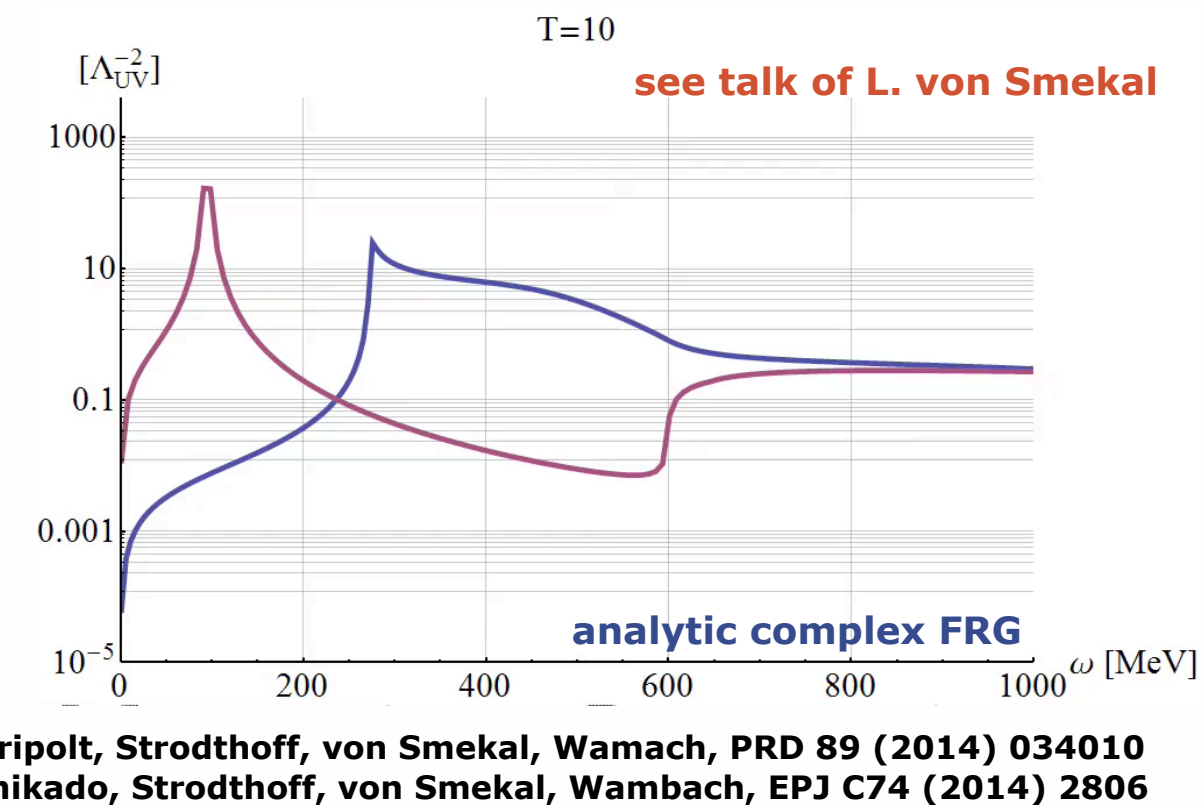


Strauss, Fischer, Kellermann, PRL 109 (2012) 252001

pion and sigma spectral functions



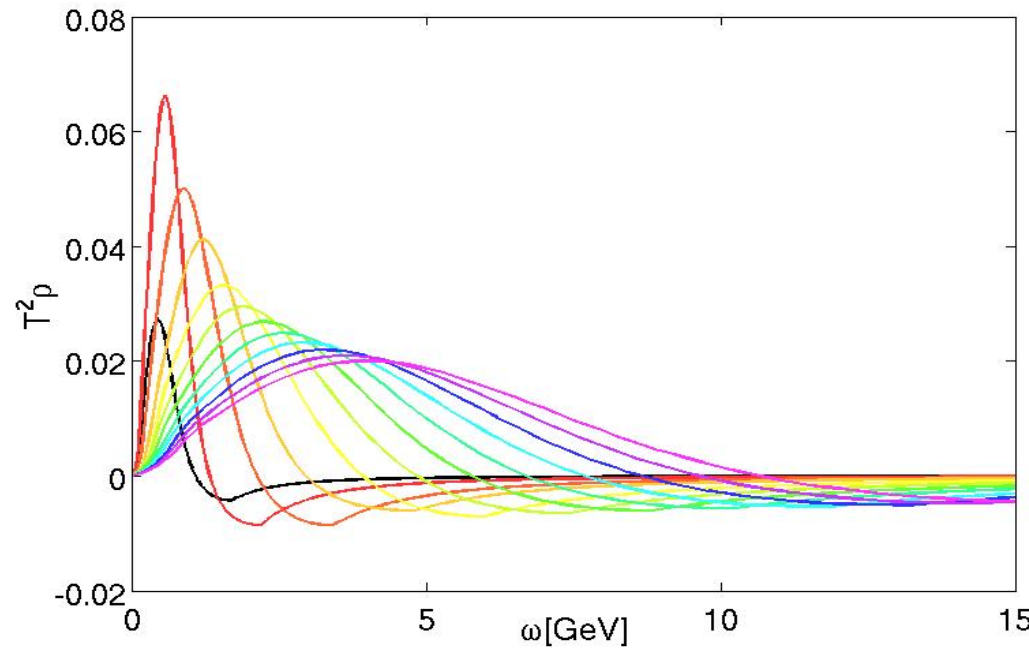
full complex FRG/real time
JMP, Strodthoff, in preparation



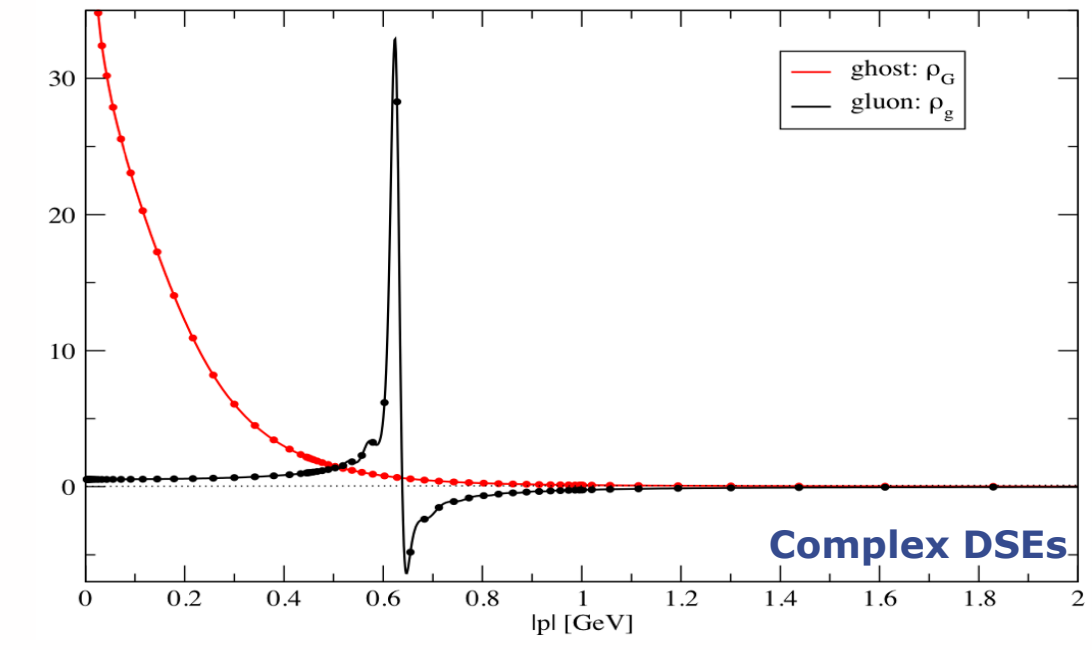
T=10
analytic complex FRG
Tripolt, Strodthoff, von Smekal, Wamach, PRD 89 (2014) 034010
Kamikado, Strodthoff, von Smekal, Wambach, EPJ C74 (2014) 2806

Dynamics

gluon spectral functions



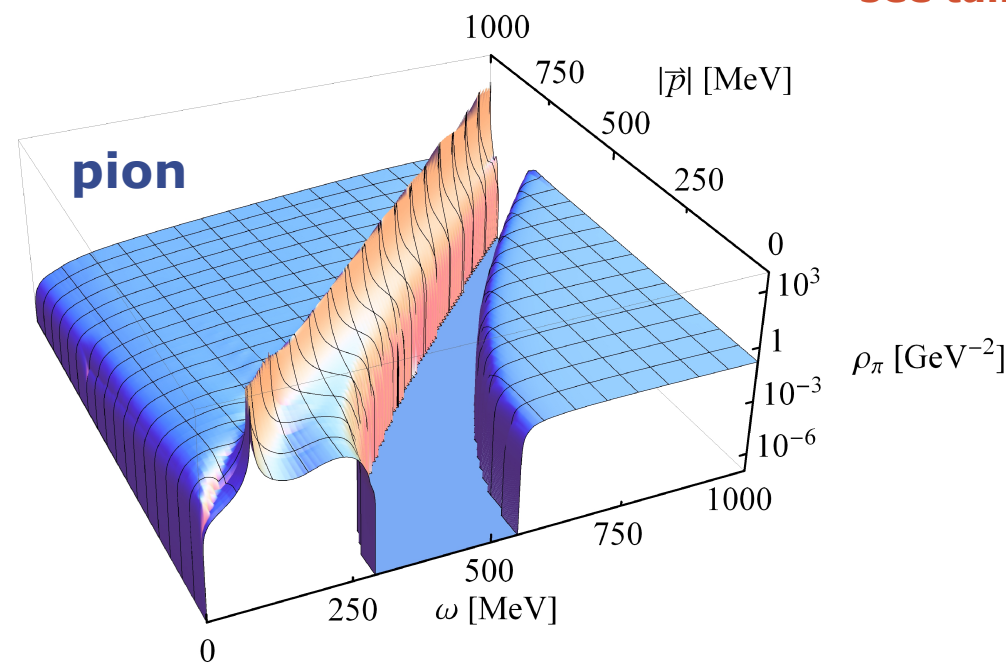
Haas, Fister, JMP, PRD 90 (2014) 9, 091501



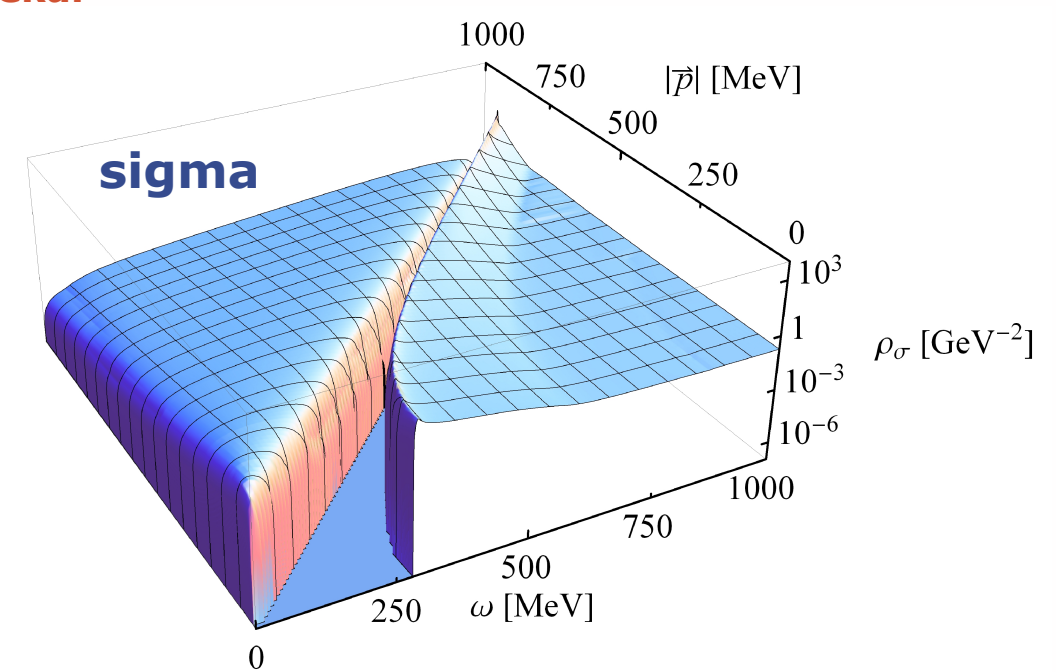
Strauss, Fischer, Kellermann, PRL 109 (2012) 252001

pion and sigma spectral functions

see talk of L. von Smekal



Tripolt, von Smekal, Wambach, Phys.Rev. D90 (2014) 7, 074031
Tripolt, PhD-thesis

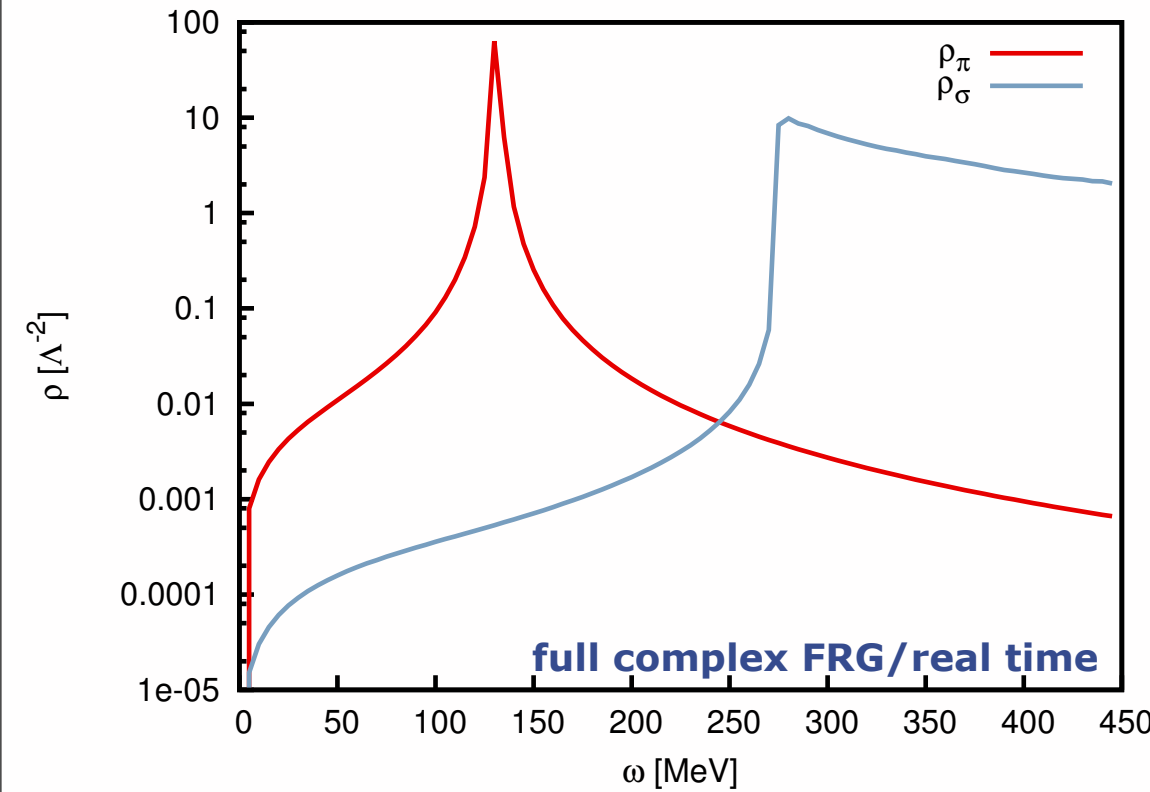


Viscosity in pure glue

spectral functions

pion and sigma spectral functions

4d N=2 exponential regulator, $\epsilon=0.1$ MeV



JMP, Strodthoff, in preparation

O(N)-model

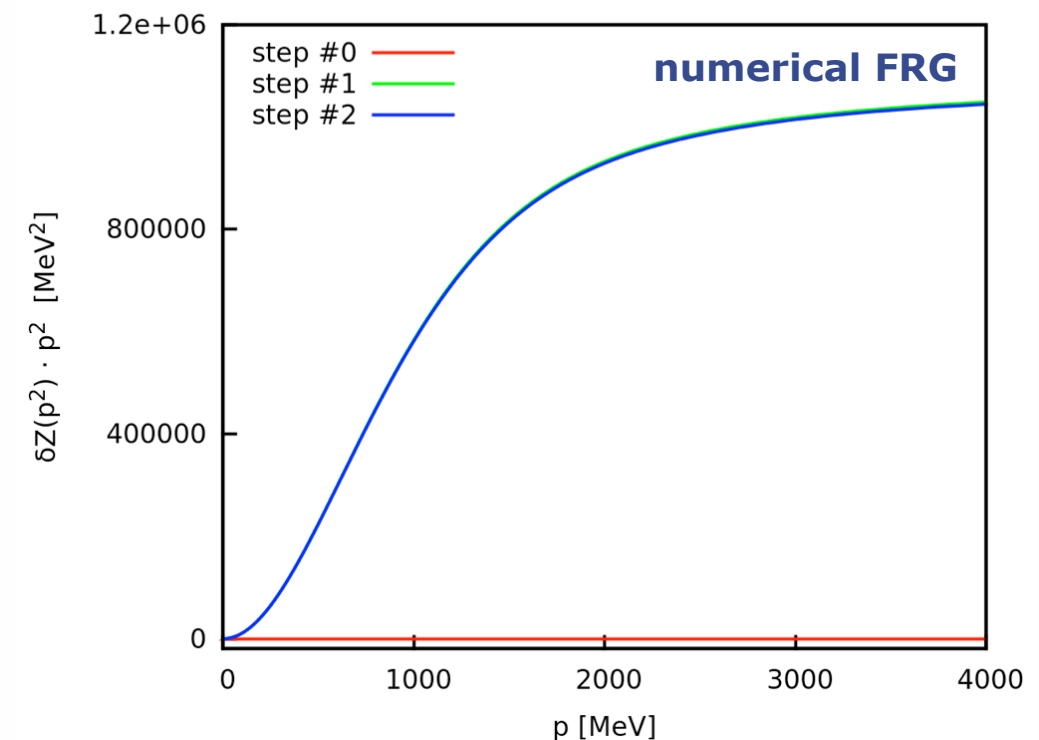
iteration step	σ_0 [MeV]	δ_ρ [%]	m_{pole} [MeV]	m_{cur} [MeV]	δ_m [%]
0	93.55	0.0043	130.3113	136.7593	4.9
1	100.05	0.0028	126.6390	126.4590	0.14
5	99.38	0.0043	127.0347	127.0110	0.019

iteration step	σ_0 [MeV]	δ_ρ [%]	m_{pole} [MeV]	m_{cur} [MeV]	δ_m [%]
0	96.25	0.0052	91.4911	134.8281	47
1	99.56	0.0044	90.8841	91.1611	0.30
5	99.56	0.0073	90.9244	91.1551	0.25

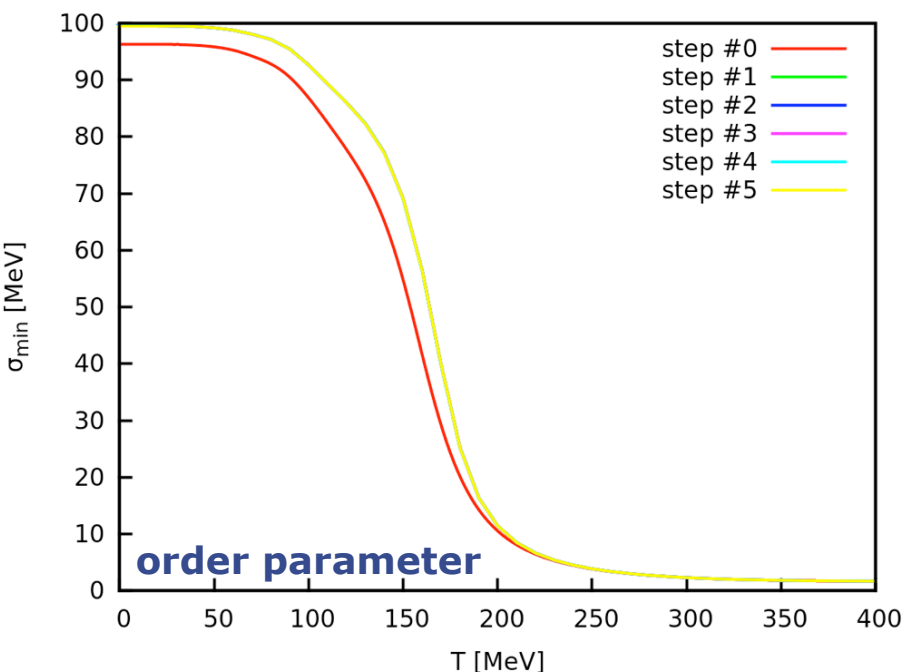
QM-model

QM-model

inverse pion propagator in the linear QM-model

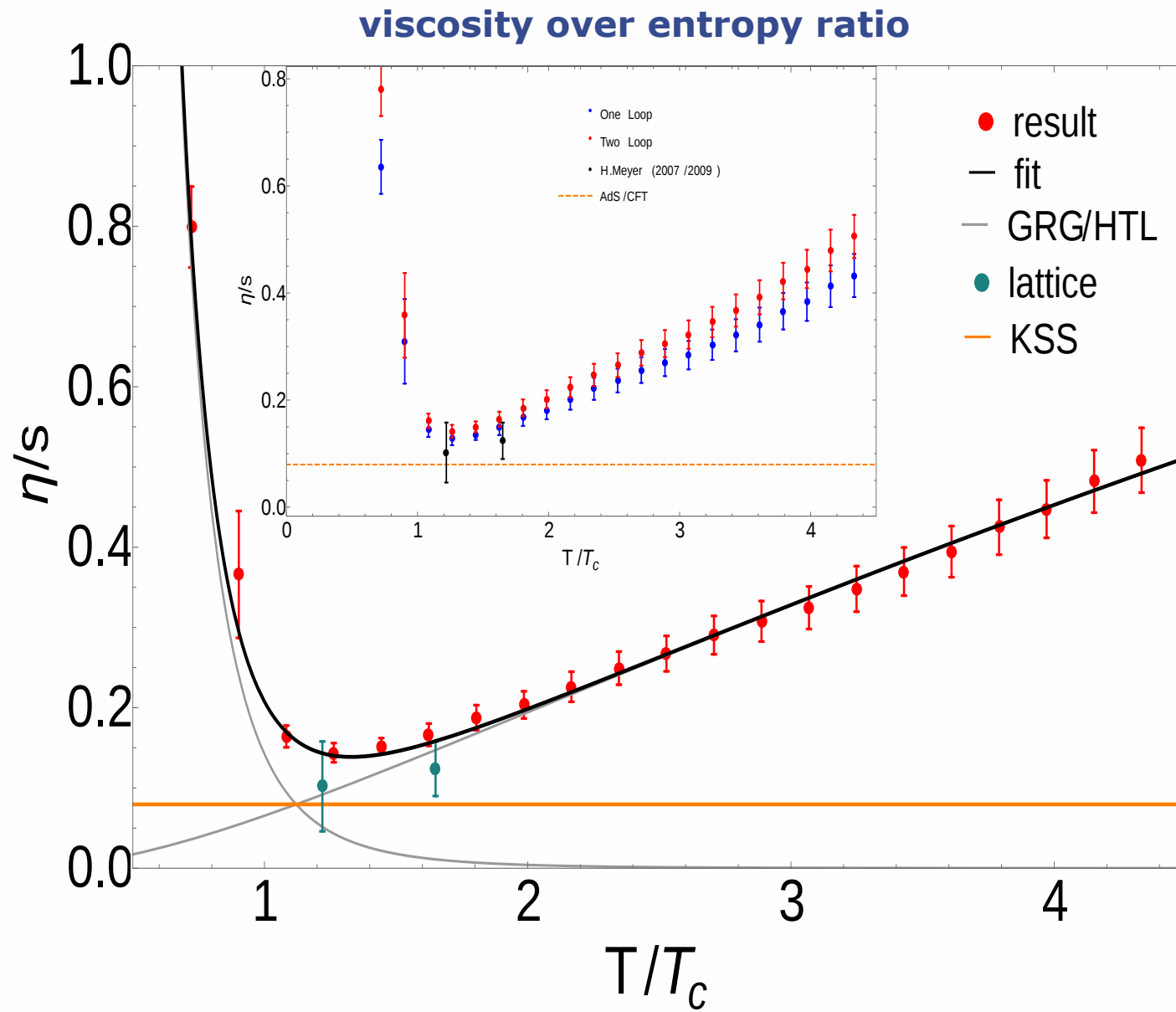


order parameter σ_{\min} as a function of T in the linear QM-model



Dynamics

transport coefficients

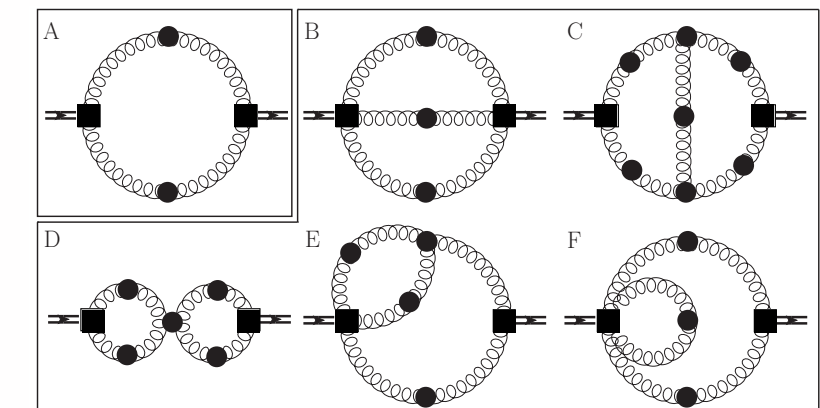


Kubo relation

$$\eta = \frac{1}{20} \left. \frac{d}{d\omega} \right|_{\omega=0} \rho_{\pi\pi}(\omega, 0)$$

'3-loop' exact functional relation for $\rho_{\pi\pi}$

1 & 2-loop terms

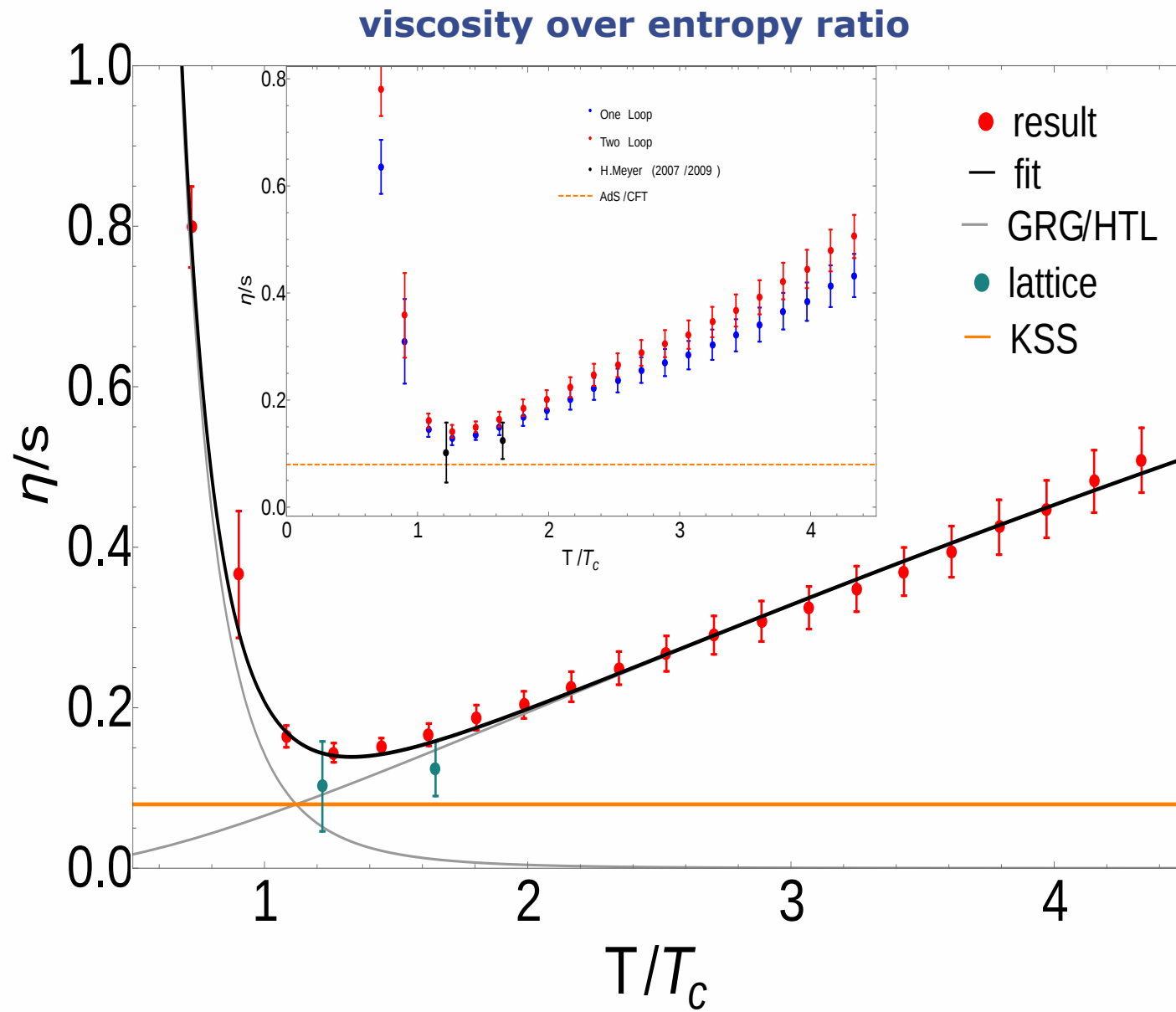


Haas, Fister, JMP, PRD 90 (2014) 9, 091501

Christiansen, Haas, JMP, Strodthoff, arXiv:1411.7986

Dynamics

QCD - estimate for viscosity over entropy ratio



$$\gamma_{\text{grg}} \approx 5$$

$$\gamma_{\text{qgp}} \approx 1.6$$

pure glue

$$a_{\text{qgp}} \approx 0.15$$

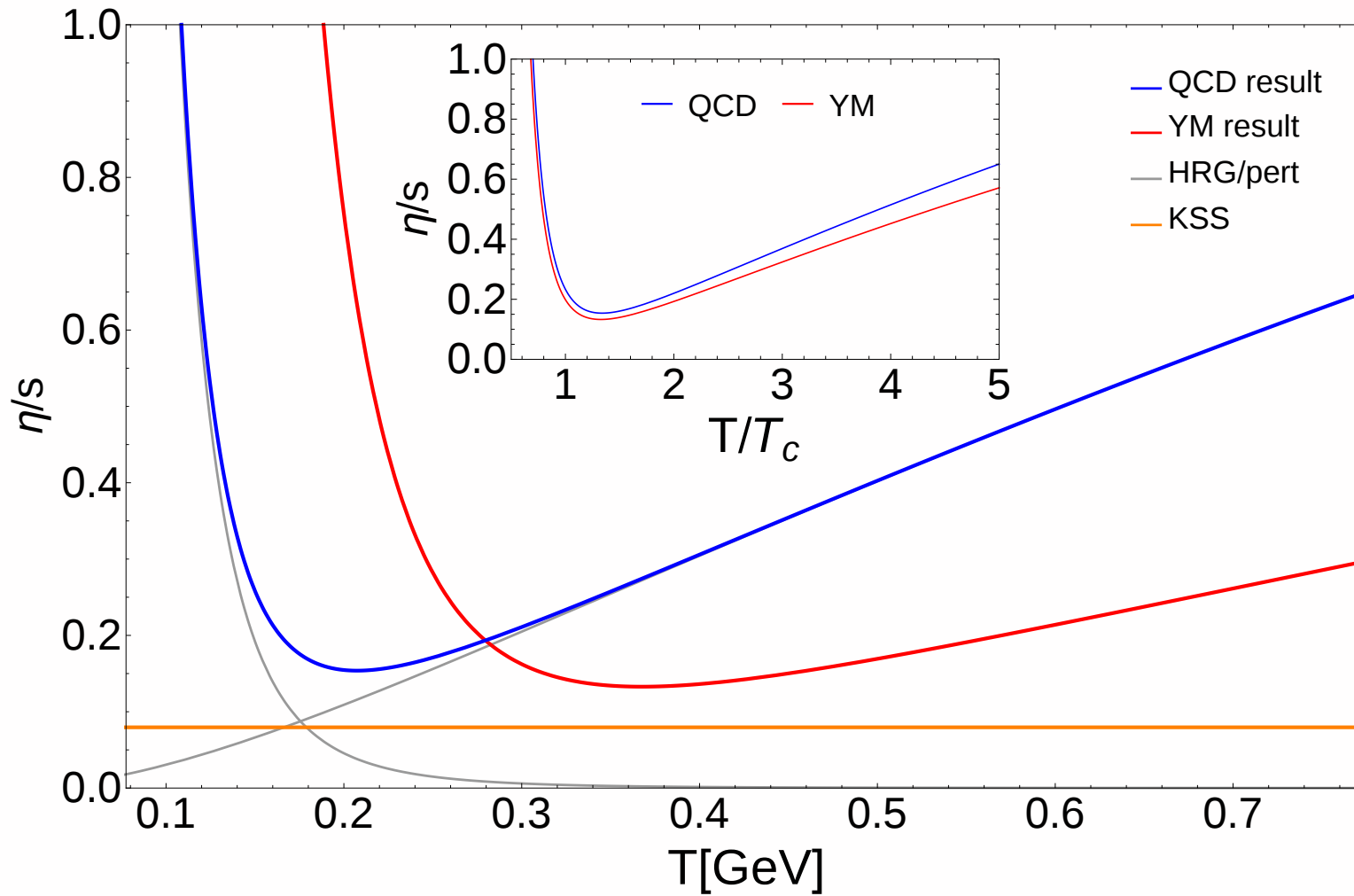
$$a_{\text{hrg}} \approx 0.14$$

$$c \approx 0.66$$

$$\frac{\eta}{s}(T) = \frac{a_{\text{qgp}}}{\alpha_s^{\gamma_{\text{qgp}}}(c T/T_c)} + \frac{a_{\text{grg}}}{(T/T_c)^{\gamma_{\text{grg}}}}$$

Dynamics

QCD - estimate for viscosity over entropy ratio



$$a_{\text{qgp}} \approx 0.2$$

$$a_{\text{hrg}} \approx 0.16$$

$$c \approx 0.79$$

QCD

$$\gamma_{\text{grg}} \approx 5$$

$$\gamma_{\text{qgp}} \approx 1.6$$

pure glue

$$a_{\text{qgp}} \approx 0.15$$

$$a_{\text{hrg}} \approx 0.14$$

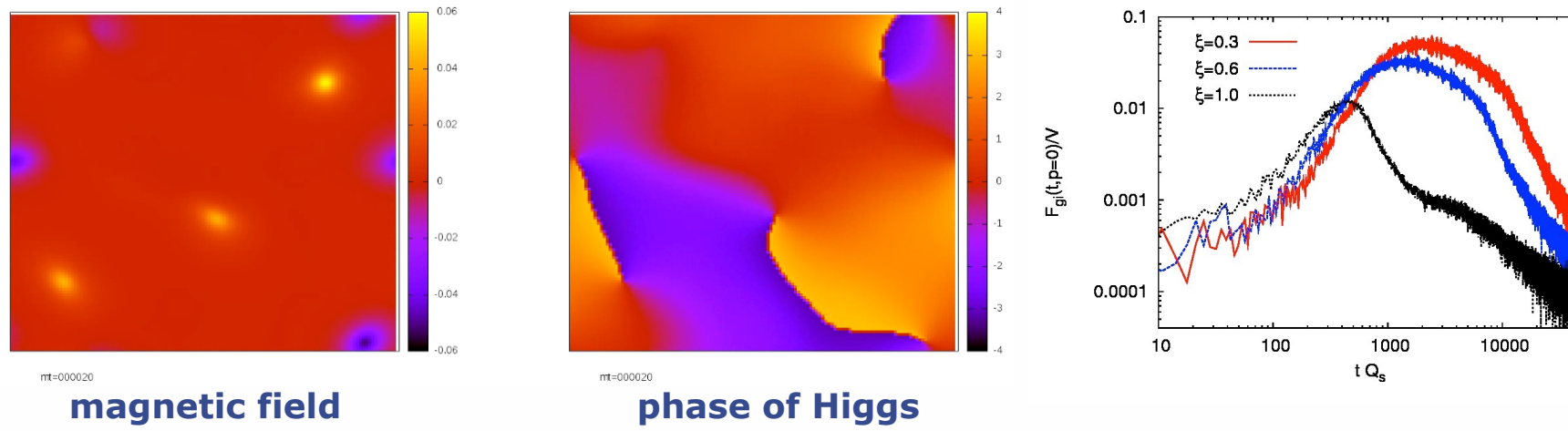
$$c \approx 0.66$$

$$\frac{\eta}{s}(T) = \frac{a_{\text{qgp}}}{\alpha_s^{\gamma_{\text{qgp}}}(c T/T_c)} + \frac{a_{\text{grg}}}{(T/T_c)^{\gamma_{\text{grg}}}}$$

Summary

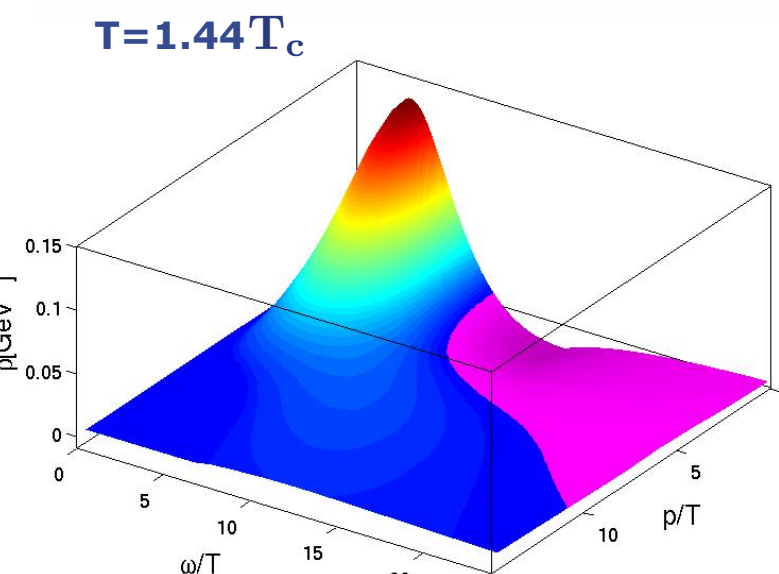
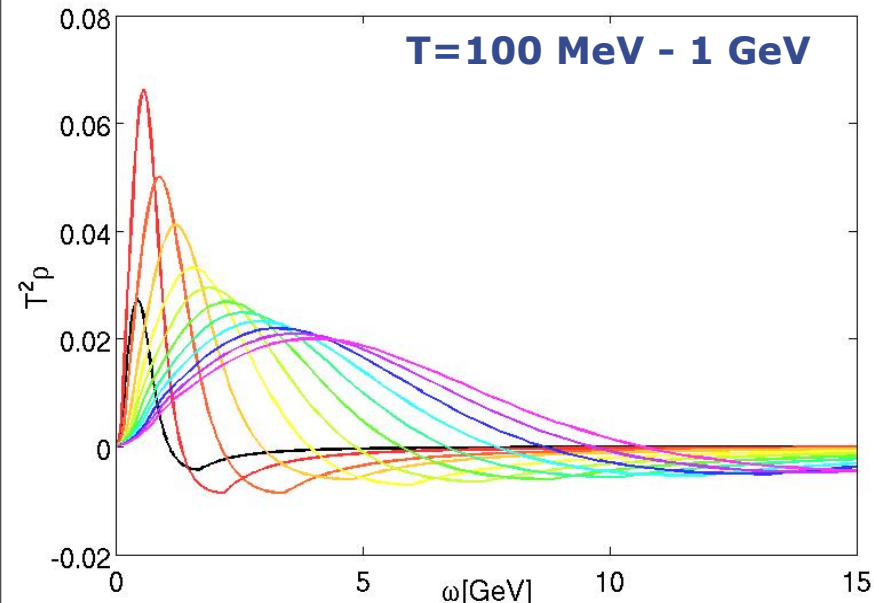
- **Gauge dynamics far from equilibrium**

Abelian Higgs

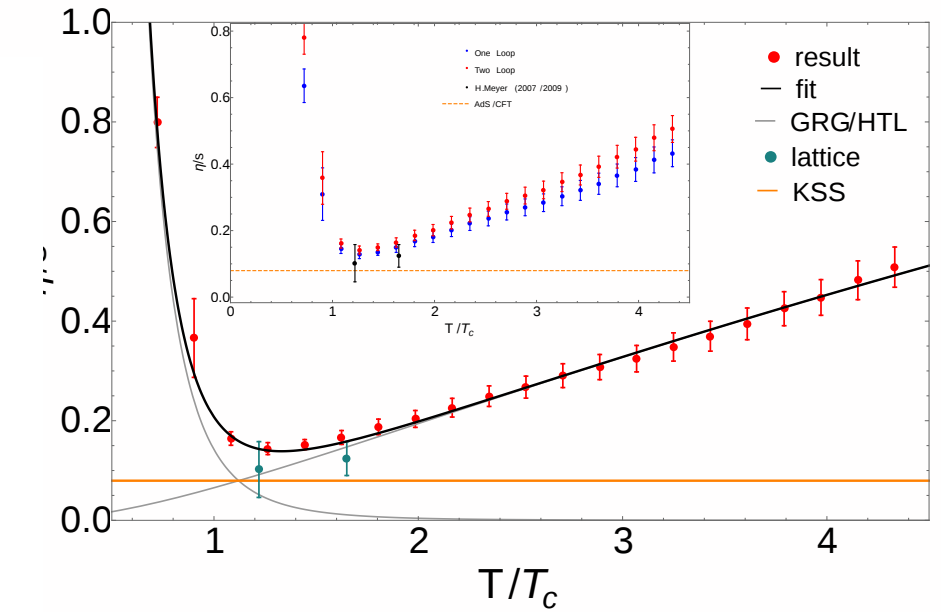


- **Spectral functions and transport coefficients**

spectral functions



viscosity over entropy ratio

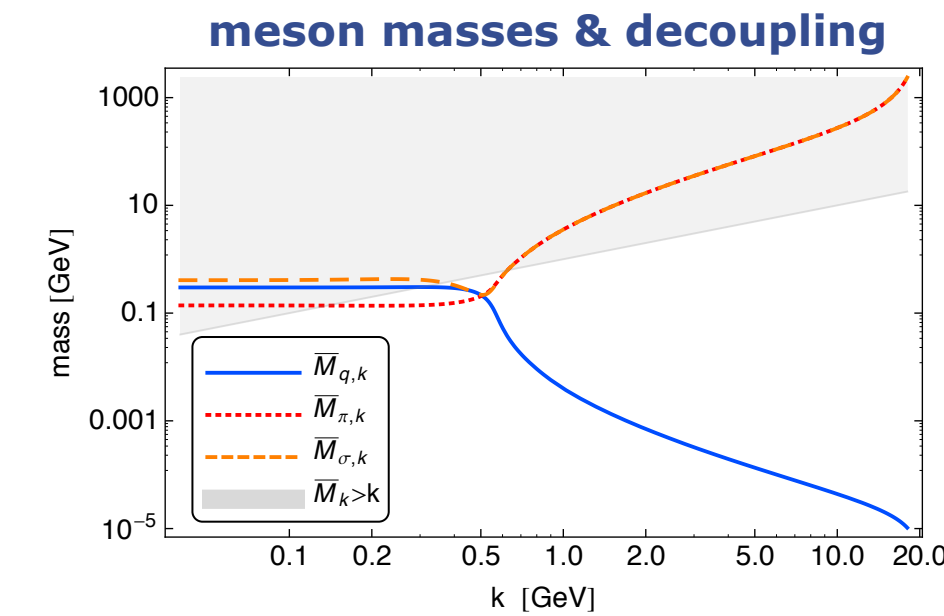
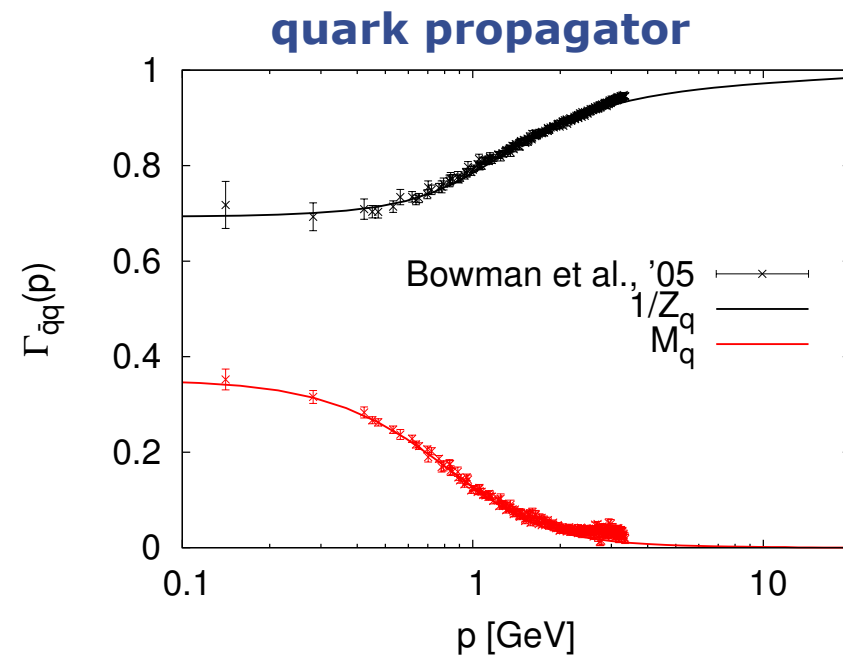


Summary & Outlook

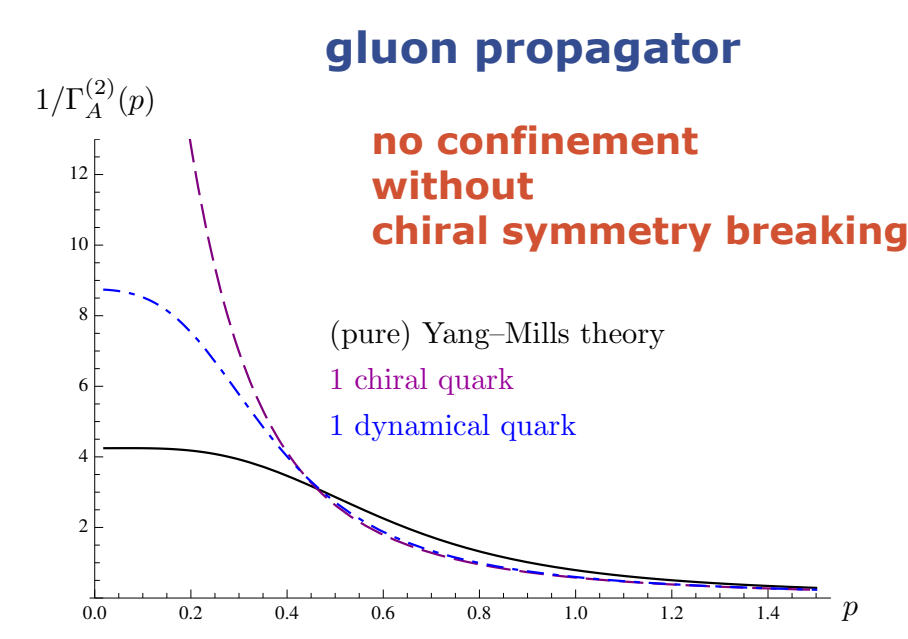
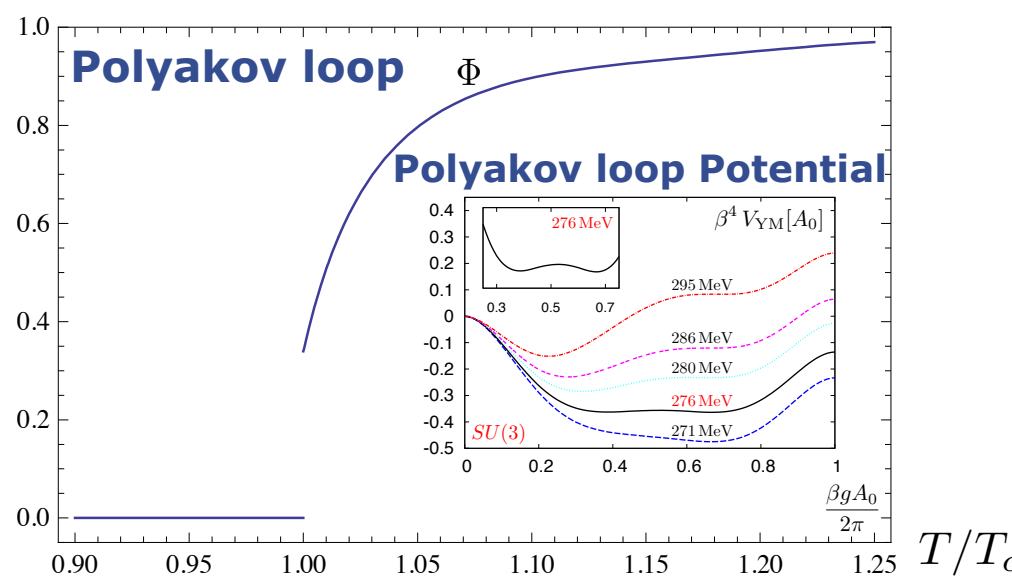
Summary & Outlook

Chiral Symmetry Breaking and Confinement

$$\frac{f_{\pi, \text{FRG}}}{f_{\pi, \text{lattice}}} = 0.99$$

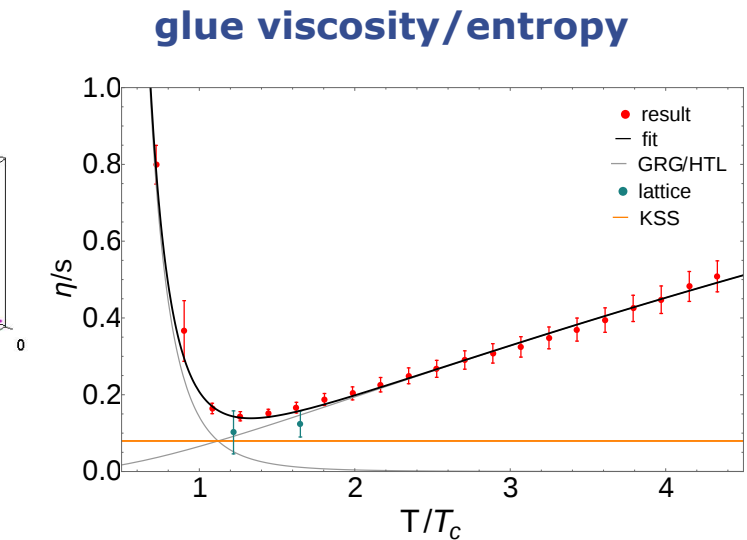
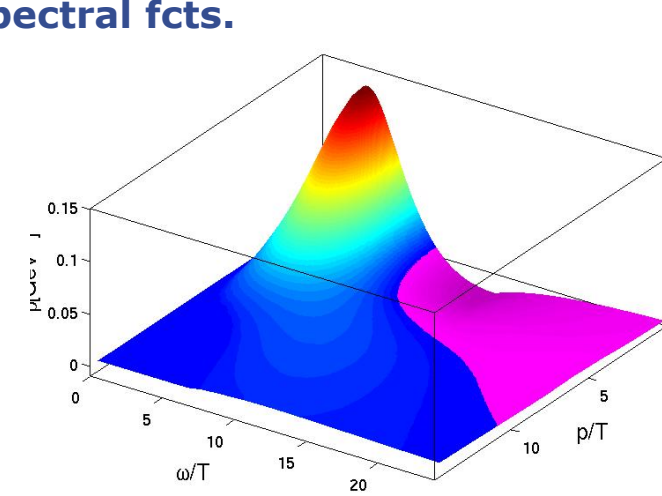
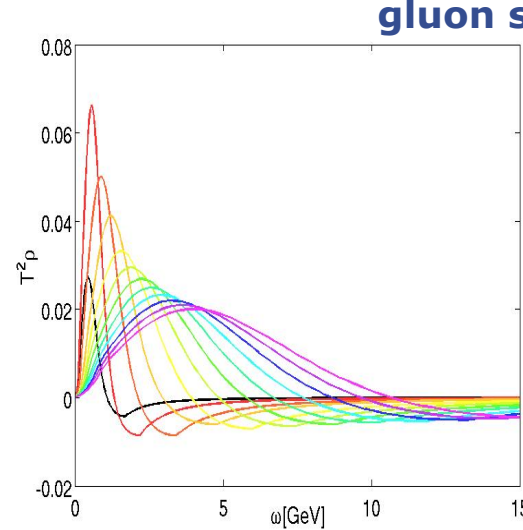
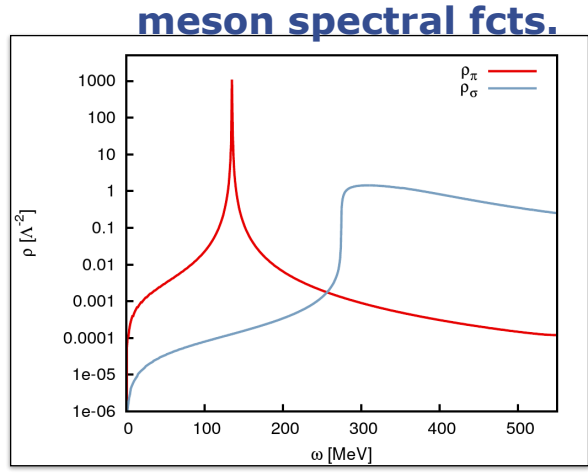
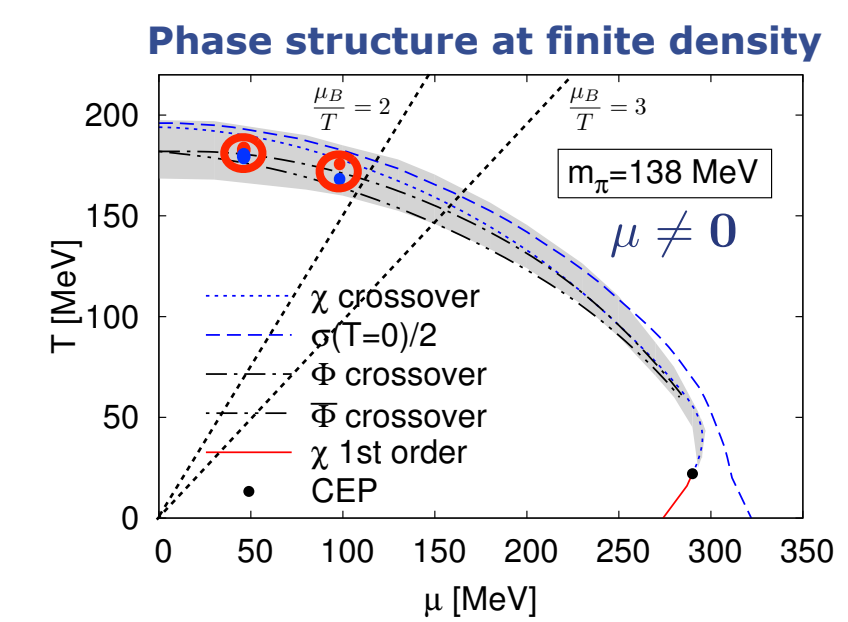
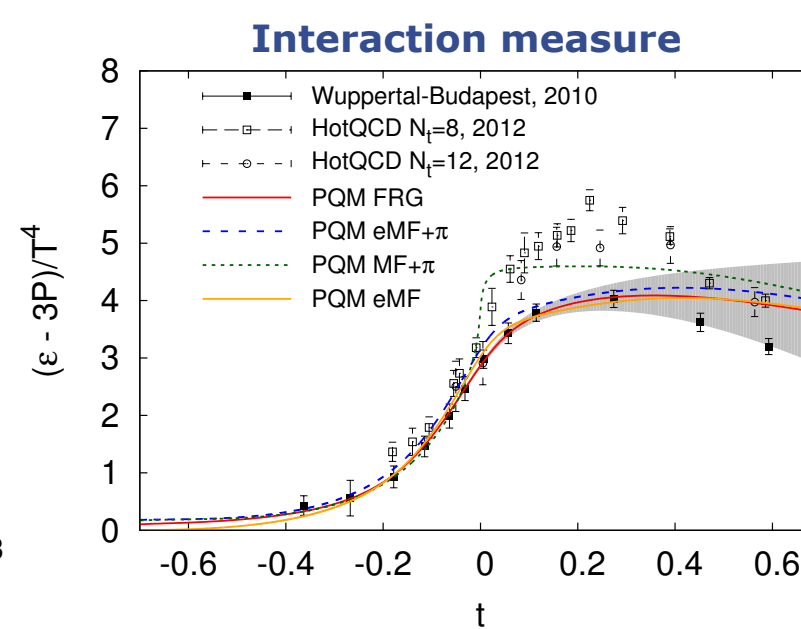
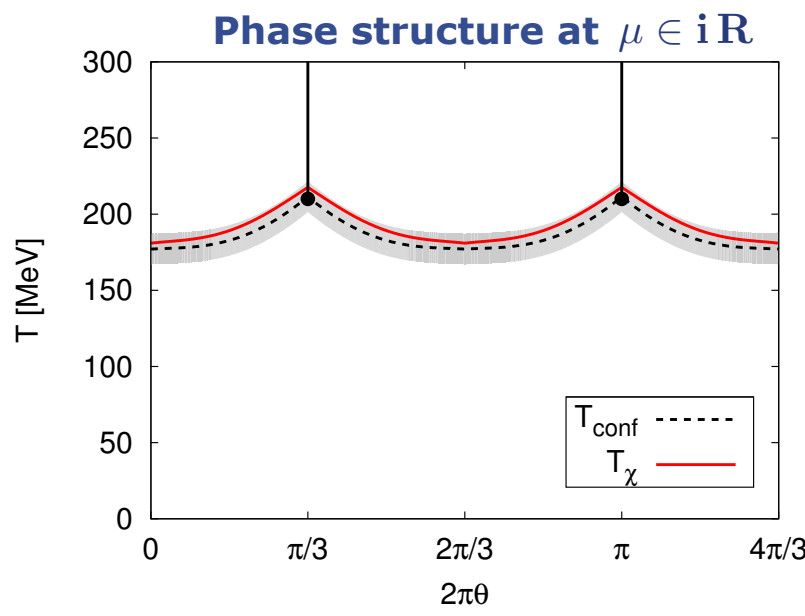


fQCD



Summary & Outlook

▪ Phase structure and Transport



Summary & Outlook

- **Chiral Symmetry Breaking and Confinement**
- **Phase Structure and Transport**
- **Towards quantitative precision**
- **Baryons, high density regime & CEP, dynamics**
- **Hadronic properties**
 - **hadron spectrum & in medium modifications**
 - **low energy constants**